

DISSERTATION

submitted to the
Combined Faculties for the Natural Sciences and for Mathematics of the
Ruperto-Carola University of Heidelberg, Germany

for the degree of
Doctor of Natural Sciences

presented by
Thomas Plum, Master of Science
born in: Aachen, Germany

Oral-examination: 21.09.2017

Identification of lineage-specific markers for therapeutic targeting of mast cells

Referees: Prof. Dr. Hans-Reimer Rodewald
Prof. Dr. Marc Freichel

Table of Content

1. INTRODUCTION	8
1.1. DISCOVERY OF MAST CELLS	8
1.2. PHYLOGENY AND LINEAGE DEVELOPMENT	8
1.3. MAST CELLS IN HEALTH AND DISEASE	10
1.4. CURRENT TREATMENT OF MAST CELL DEPENDENT DISEASES.....	16
1.5. ANTIBODY-BASED MECHANISMS OF CELL ABLATION	19
1.6. AIMS OF THE STUDY	21
2. MATERIALS AND METHODS	23
2.1. MATERIALS.....	23
2.1.1. <i>Chemicals</i>	23
2.1.2. <i>Kits</i>	23
2.1.3. <i>Enzymes</i>	23
2.1.4. <i>Anti-mouse Antibodies</i>	23
2.1.5. <i>Anti-human Antibodies</i>	24
2.1.6. <i>Media and supplements for cell culture</i>	25
2.1.7. <i>Buffers and solutions</i>	26
2.1.8. <i>Cells and animals</i>	26
2.1.8.1. Cell lines	26
2.1.8.2. Primary human mast cells	27
2.1.8.3. Mouse strains	27
2.1.9. <i>Equipment</i>	28
2.1.10. <i>Software</i>	28
2.2. METHODS.....	28
2.2.1. <i>Cell Biology</i>	28
2.2.1.1. Preparation of cells from murine organs.....	28
2.2.1.1.1. Recovery of peritoneal exudate cells (PEC)	28
2.2.1.1.2. Digestion of skin, tongue, trachea and fat for analysis of mast cells	28
2.2.1.1.3. Isolation of intra-epithelial leukocytes from the stomach.....	29
2.2.1.2. Preparation of cells from human organs.....	29
2.2.1.2.1. Digestion of skin, lung and fat for analysis of mast cells.....	29
2.2.2. <i>Flow Cytometry</i>	30
2.2.2.1. Antibody staining	30
2.2.2.2. Exclusion of dead cells	30
2.2.2.3. Magnetic enrichment of Kit ⁺ cells.....	30
2.2.2.4. Measurement on BD Fortessa	31
2.2.2.5. Murine cell sorting on BD Aria	31
2.2.2.6. Human cell sorting on BD Fusion	31
2.2.2.7. Cytospins & Toluidine blue staining.....	31
2.2.3. <i>Procedures of animal experimentation</i>	32
2.2.3.1. Antibody injections	32
2.2.3.2. Passive systemic anaphylaxis assay.....	32
2.2.4. <i>Cell culture</i>	32
2.2.4.1. General cell culture methods.....	32
2.2.4.2. Determination of the cell number.....	32
2.2.4.3. Generation of bone marrow-derived mast cells (BMMC).....	33
2.2.4.4. Generation of peritoneal cell-derived mast cells (PMC)	33
2.2.4.5. Antibody internalisation assay	33
2.2.4.6. In-vitro mast cell killing assay	34
2.2.5. <i>Molecular Biology</i>	34
2.2.5.1. Sample preparation for mass spectrometry.....	34
2.2.5.2. Liquid chromatography–electrospray ionization–tandem mass spectrometry	34
2.2.5.3. Bioinformatic analysis of proteomic data	35
2.2.5.4. Antibody clean-up and labelling.....	36
2.2.5.5. Biotin quantitation	36
3. RESULTS	37
3.1. ANTI-HCD4-MEDIATED MAST CELL ABLATION	37
3.1.1. <i>Characterisation of Cpa3^{hCD4}</i>	37
3.1.2. <i>Characterisation of TNX355 (anti-hCD4) antibody</i>	40

3.1.3.	<i>In vivo ablation of hCD4⁺ mast cells</i>	41
3.1.4.	<i>Bio-distribution of TNX355 in vivo</i>	45
3.1.5.	<i>Passive systemic anaphylaxis assay</i>	47
3.2.	MAST CELL PROTEOMICS	48
3.2.1.	<i>Mouse peritoneal mast cell proteomics</i>	48
3.2.2.	<i>Gene ontology analysis of the mouse mast cell proteome</i>	52
3.2.3.	<i>The most abundant proteins of murine mast cells</i>	54
3.2.4.	<i>Verification of the most enriched mouse mast cell markers</i>	58
3.2.5.	<i>Human mast cell proteomics</i>	60
3.2.6.	<i>Gene ontology analysis of the human mast cell proteome</i>	64
3.2.7.	<i>Human mast cell enriched proteins</i>	66
3.2.8.	<i>Verification of novel human mast cell markers</i>	68
3.2.9.	<i>Mapping of skin MC RNA-sequencing data to skin MC proteome</i>	71
3.2.10.	<i>Human – mouse mast cell comparison</i>	73
3.3.	IN VIVO DEPLETION OF MAST CELLS VIA TARGETING OF THE ENDOGENOUS MARKER CD63 75	
3.3.1.	<i>ADCC-dependent depletion mechanism</i>	75
3.3.2.	<i>Fluorimetric measurement of anti-CD63 internalization</i>	76
3.3.3.	<i>CD63 targeting by antibody-drug-conjugate</i>	77
4.	DISCUSSION	81
4.1.	MOUSE MAST CELL PROTEOMICS	81
4.2.	HUMAN MAST CELL PROTEOMICS	84
4.3.	EVOLUTIONARY CONSERVED MAST CELL PROTEOME	86
4.4.	ANTI-HCD4-MEDIATED MAST CELL ABLATION	87
4.5.	FUNCTIONAL ASSESSMENT OF MAST CELL DEPLETION	90
4.6.	CD63 AS PHYSIOLOGICAL TARGET FOR MAST CELL ABLATION	91
4.7.	SUMMARY AND OUTLOOK	92
5.	REFERENCES	95

Abstract

The number of people in the modern world being affected by allergic diseases and asthma has reached epidemic proportions. With over 1 out of three people requiring some sort of treatment for allergic disease, the burden placed onto industrialized nations healthcare systems is increasing. Mild forms of allergic diseases, such as allergic rhinitis, can be treated with anti-histamines or immunological desensitization. However, more severe forms of disease, such as asthma and atopic dermatitis, require a reduction of systemic inflammation by administration of broad acting systemic immunosuppressants, to effectively alleviate symptoms. However, systemic immunosuppression often results in susceptibility to infection.

Mast cells, which are evidently involved in numerous allergic pathologies, have not been adequately targeted by conventional therapeutics. Specific removal of mast cells, by means of antibody-dependent depletion, would interrupt the allergic cascade and might yield significant benefit for patients. In order to develop such a mAb-mediated mast cell ablation approach we sought to establish proof of principle in a well-controlled system with our newly developed transgenic mouse model. The *Cpa3^{hCD4}* mouse model expresses a truncated human CD4 receptor from a knockin into the mast cell specific *Cpa3* locus. With this model system, employing an artificial mast cell marker cell surface protein, we could show that several tissue-resident mast cell compartments can be safely and efficiently depleted after intravenous α -hCD4 administration. To identify a physiologically relevant target on the surface of mast cells, we underwent extensive mass spectrometry-assisted proteomic profiling of primary mouse and human mast cells. Analysis of the data revealed a cross-species conserved mast cell protein signature, among which we found several drugable receptors. Quantitative analysis, paired with flow cytometry-based verification of the cell surface expressed mast cell proteins allowed us to identify several highly expressed mast cell specific cell surface markers. Targeting of one of these receptors with an α -CD63-Immunotoxin resulted in the efficient depletion of mast cells *in vitro*. *In vivo* however, efficacy of mast cell depletion was limited by excessive on-target toxicities. Along these lines, we are currently evaluating the herein identified physiological mast cell targets for cellular depletion by different antibody-mediated mechanisms.

Zusammenfassung

In den Industrienationen nimmt die Anzahl der Menschen, die von allergischen Erkrankungen und Asthma betroffen sind, stetig zu und hat vielerorts bereits epidemische Ausmaße erreicht. Milde Formen von allergischen Erkrankungen, wie allergische Rhinitis, können mit Anti-Histaminika oder immunologischer Desensibilisierung behandelt werden. Ernsthaftere Krankheitsformen, wie z.B. Asthma oder atopische Dermatitis, erfordern allerdings die Verabreichung von breit wirkenden Immunsuppressiva, um die Symptome wirksam zu lindern. Solche systemisch verabreichten Immunsuppressiva führen oftmals zu pleiotropen Wirkungen wie z.B. erhöhter Infektionsanfälligkeit.

Mastzellen, die erwiesenermaßen in zahlreichen allergischen Krankheiten eine zentrale Rolle spielen, werden durch konventionelle Therapeutika nicht adäquat adressiert. Die spezifische Entfernung von Mastzellen, mittels Antikörper-abhängiger Zell ablation, würde die allergische Kaskade unterbrechen und für Patienten signifikante Vorteile bringen. Um einen solchen Mastzell-Ablationsansatz zu entwickeln, haben wir ein transgenes Mausmodell entwickelt, welches auf der ektopen Expression eines human-CD4-Rezeptors aus dem Mastzell-spezifischen Gen *Cpa3* basiert. Mit diesem Modellsystem, und dem artifiziellen Mastzell Oberflächenprotein, konnten wir zeigen, dass nach intravenöser Verabreichung von α -hCD4 Antikörpern mehrere Gewebs-ständige Mastzell Populationen effizient und gefahrlos ablatiert werden können. Um ein physiologisch relevantes Oberflächenprotein auf Mastzellen zu identifizieren, haben wir umfangreiche massenspektrometrisch-gestützte Proteom Untersuchungen von primären murinen- und menschlichen Mastzellen durchgeführt. Basierend auf den Daten konnten wir nicht nur mehrere Mastzell-spezifische Oberflächenziele identifizieren, sondern auch eine evolutionär erhaltene Mastzell-Protein Signatur entdecken.

Die Behandlung von Mastzellen, mit einem α -CD63-Immunotoxin, führte zu einer effizienten Ablation von Mastzellen in vitro. In vivo wurde jedoch die Wirksamkeit der Mastzellablation durch die auftretenden Nebenwirkungen limitiert. Zurzeit, evaluieren wir die hier identifizierten physiologischen Mastzell-Zielantigene für die zelluläre Ablation mit Hilfe verschiedener Antikörper-vermittelter Ablationsmechanismen.

List of Abbreviations

A647	Alexa647
AD	Atopic dermatitis
ADC	Antibody-drug-conjugate
ADCC	Antibody-dependent cell-mediated cytotoxicity
AHR	Airway hyper-reactivity
AOPI	Acridine-Orange Propidium-Iodide
BAL	Broncho-alveolar lavage
BMMC	Bone marrow-derived mast cells
Cpa3	Carboxypeptidase A3
CTMC	Connective tissue mast cell
CysLTR	Cysteinyl-leukotriene receptor
DMEM	Dulbeccos modified eagle medium
EDTA	Ethylenediaminetetraacetic acid
ESI-MS/MS	Electrospray ionization tandem mass spectrometry
Facs	Fluorescence-activated cell sorting
Fc	Fragment crystallizable
Fc ϵ RI	High affinity Immunoglobulin E receptor
FcR	Fc receptor
FDR	False discovery rate
GO	Gene Ontology
HBSS	Hanks buffered salt solution
HPLC	High-performance liquid chromatography
i.p.	intraperitoneal
i.v.	intravenous
IgE	Immunoglobulin E
Il-4	Interleukin-4
kDa	Kilodalton
Kit	Stem cell factor receptor (CD117)
mAb	Monoclonal antibody
MC	Mast cell
MCP	Mast cell progenitor
MC _T	Human mast cell containing tryptase only
MC _{TC}	Human mast cell containing tryptase and chymase
MMC	Mucosal mast cell
NK cells	Natural killer cells
PBMC	Peripheral blood mononuclear cells
PBS	Phosphate buffered Saline
PDE	Phosphodiesterase inhibitor
PEC	Peritoneal exudate cells
PMC	Peritoneal cell-derived mast cells
SCF	Stem cell factor
SIT	Specific immunotherapy
SPF	Specific pathogen free
T _{H2}	T helper type 2 cell
TLR	Toll-like receptor
T _{reg}	Regulatory T cell

List of figures

Figure 1: Functional and phenotypic differences between mast cell populations	9
Figure 2.: Sensitization to allergens in the airways	12
Figure 3: Non-humoral antibody-mediated cell targeting (tumour cell example)	20
Figure 4: Absolute number of mast cells in <i>Cpa3^{hCD4/+}</i> knockin mice	38
Figure 5: Mast cell specific cell surface expression of hCD4 in <i>Cpa3^{hCD4/+}</i> knockin mice	39
Figure 6: Receptor cleavage by collagenase treatment	40
Figure 7: TNX355 binds hCD4 expressing mast cells in <i>Cpa3^{hCD4/+}</i> knockin mice	41
Figure 8: Mast cell depletion with a single dose of TNX355 treatment	42
Figure 9: Mast cell depletion with multi-dose TNX355 treatment	43
Figure 10: Mast cell depletion with maximal dose escalation	44
Figure 11: Mast cell depletion by treatment with afucosylated TNX355	45
Figure 12: In situ labelling of mast cells by fluorescent coupled TNX355	46
Figure 13: Passive systemic anaphylaxis in mast cell-depleted mice	47
Figure 14: Isolation, enrichment and purification of mast cells for proteome analysis	49
Figure 15: Mouse mast cell proteomics and peptide mapping	50
Figure 16: Depiction of differential protein expression of mouse mast cells versus peritoneal cells	51
Figure 17: Proteome analysis based on mouse Gene Ontology (GO) analysis for the term 'Cellular Component'	53
Figure 18: Proteome analysis based on mouse GO analysis for the term 'Biological Process'	54
Figure 19: Flow cytometry of the 10 most enriched mast cell receptors	59
Figure 20: Purification of Human mast cells	61
Figure 21: Human mast cell proteomics and peptide mapping	62
Figure 22: Depiction of differential protein expression of human mast cells and PBMC	63
Figure 23: Proteome analysis based on human GO analysis for the term 'Cellular Component'	64
Figure 24: Proteome analysis based on human GO analysis for the term 'Biological Process'	65
Figure 25: Flow cytometry of the 10 most enriched human mast cell surface proteins	70
Figure 26: Comparison of RNA-sequencing to proteomics	72
Figure 27: Cross-species conserved mast cell protein signature	74
Figure 28: Anti-CD63 mediated mast cell ablation	76
Figure 29: Anti-CD63 is internalized into primary human skin mast cells	77
Figure 30: In vitro mast cell killing with CD63-Saporin	78
Figure 31: In vivo depletion of wild type mast cells with a CD63-Saporin conjugate	79

List of tables

Table 1: Mediators released from activated mast cells	13
Table 2: Number of proteins differentially expressed in mouse mast cells compared to peritoneal exudate cells	51
Table 3: Top 20 proteins (sorted mast cell vs. <i>Cpa3</i>^{Cre/+} PEC)	55
Table 4: Top 20 mouse mast cell specific cell surface proteins	56
Table 5: Number of proteins differentially expressed in human mast cells compared to peripheral blood mononuclear cells	62
Table 6: Top 20 proteins enriched in fat mast cells	66
Table 7: Top 20 cell surface proteins enriched in fat mast cells	67

1. Introduction

1.1. Discovery of mast cells

Paul Ehrlich first described mast cells in the late 19th century. When he stained connective tissue sections with aniline dyes, he observed granulated cells that exhibited metachromatic staining properties. The basic dyes he used (e.g. toluidine blue) stain the cells blue, however the acidic glycosaminoglycan residues within the mast cell granules react with the dye resulting in a characteristic colour change from blue to purple (metachromasia). The metachromatic staining properties of mast cells allowed the specific detection of the cells in tissues (Ehrlich, 1878). Due to their vast amount of intracellular granules he thought that the cells had a nourishing function to the surrounding tissue, and thus termed them “Mastzelle” which derives from the German word for “mästen” (fattening).

1.2. Phylogeny and lineage development

Mast cell-like cells are evolutionary ancient and have been described in the haemolymph of the ascidian *Styela plicata*, which belongs to the group of invertebrate chordates (urochordates), that first appeared over 500 million years ago (Cavalcante et al., 2002; de Barros et al., 2007). The so-called “test-cells”, that are associated with the ascidians’ oocytes, possess intracellular heparin positive granules and release histamine and tryptases after exposure to compound 48/80, a potent liberating compound of mammalian mast cells. The authors proposed that test cells protect the oocyte against microbial infections (Cavalcante et al., 2002). In osteichthyes that first appeared 420 million years ago, a primitive form of an activating Fc receptor (FcR) and the tyrosine receptor kinase Kit (CD117) could be identified on mast cells. However, the expression of the high-affinity receptor for IgE (FcεRI) and other activating FcRs on mast cells was not acquired until the evolution of mammals 225 million years ago (Voehringer, 2013).

Mast cells belong to the hematopoietic system and, like the other immune cells in mice and humans, they develop from hematopoietic stem cells residing in the bone marrow (Kitamura et al., 1977). Mature mast cells are only found in peripheral tissues mainly at the bodies’ interface to the environment, not in bone marrow or blood. The

fate and interrelationship of intermediary progenitors of the mast cell lineage are still under debate. Common consensus however is, that immature mast cell-committed progenitors (MCP) travel via the blood stream and migrate into tissues where they complete their tissue specific maturation (Gurish and Austen, 2012; Yojiro Arinobu, 2005). During embryonic development the earliest committed progenitor for mast cells was identified in murine foetal blood at day 15.5 of gestation (Rodewald et al., 1996). The occurrence of committed MCP declines with age, and in adult mice the frequency of MCPs is approximately 0.0045% of blood mononuclear cells (Dahlin et al., 2013). Such a low frequency suggests either self-renewing capacity or rapid migration of progenitors into the tissues; the degree of each would depend on the resident MC turnover rates.

An increase of the progenitor population is observed under specific inflammatory conditions, such as nematode infection or allergic lung inflammation. Under these conditions a sequential increase of MCPs first in the bone marrow, then in the blood and finally in the intestine or lung could be observed (Bankova et al., 2015; Pennock and Grecis, 2004).

Mature mast cells are categorized into two subtypes according to their tissue localization and their granule content: mucosal mast cells (MMC), and connective tissue resident mast cells (CTMC).

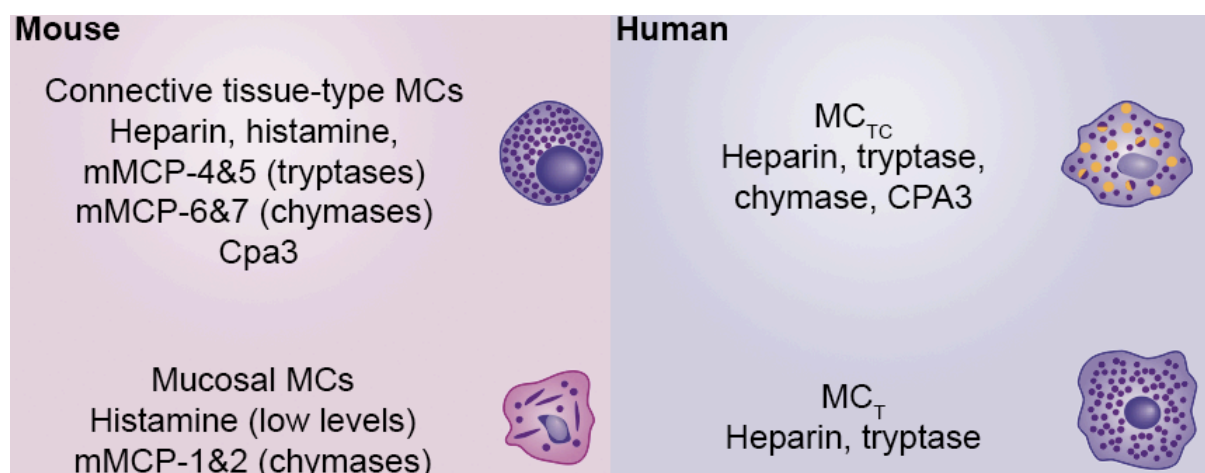


Figure 1: Functional and phenotypic differences between mast cell populations

Murine and human MC can be categorized into populations defined by anatomical location and/or granule content (proteoglycans (heparin or chondroitin sulfates) and proteases (tryptases, chymases or Cpa3). Figure was adapted from (Galli et al., 2011).

MMC differ from their CTMC counterparts in terms of anatomical location, staining characteristics, radiation sensitivity and T cell dependence for development (Fig. 1) (Galli et al., 2011; Gurish and Austen, 2012). CTMCs are predominantly located in the subepithelial layers of the skin and within the peritoneal cavity, as well as within the submucosal layers of the intestine. Their granules are storage compartments for different kind of mediators and proteases, most typical chymase, tryptases and mast cell carboxypeptidase A (*Cpa3*). These enzymes are complexed to proteoglycans. The glycosaminoglycan (GAG) side chains most characteristic for CTMC are heparin. In contrast, MMCs, predominantly locate to epithelial layers in the intestinal and respiratory tract. They are smaller in size than CTMC and contain fewer granules. The granules of MMC preferentially contain chondroitin sulphate GAG side chains. They contain chymase, but no tryptase (Metcalf et al., 1997). In contrast to the pool of CTMCs which are constitutively present, MMC are T cell dependent and mainly expand during inflammatory conditions from bone marrow derived MCPs (Gurish and Austen, 2012). Within three weeks after resolution of inflammation, MMC decrease again by number, suggesting a relatively short life span. CTMC on the contrary, have been postulated to have an extraordinary long life span of more than one year in mice (Kitamura, 1989).

Human MCs may also be classified into two subsets, based on their content of serine proteases within their granules. MCs that harbour tryptase-only granules are designated as MC_T whereas MC_{TC} are positive for tryptase and chymase (Moon et al., 2009). MC_T resemble the murine MMC whereas MC_{TC} are the counterparts to CTMC. While human lungs and intestinal mucosa mostly contain MC_T, MC_{TC} are the predominant subtype found in connective tissues such as skin and fat. However, it has been reported that under chronic inflammation, such as asthma, human lung mast cells can acquire a MC_{TC} phenotype (Erjefalt, 2014).

1.3. Mast cells in health and disease

Roughly 30 years after Paul Ehrlich discovered the mast cells, Clemens von Pirquet described patients who showed signs of hypersensitivity reaction to secondary immunization with smallpox. Based on these observations he proposed the concept of allergy as an immunological hypersensitivity reaction (Pirquet, 1906). In 1937 a link between mast cells and heparin was suggested upon observing that tissues

containing high mast cell numbers were enriched in heparin (Holmgren and Wilander, 1937). In 1947 it was shown that during anaphylactic shock histamine and heparin were liberated and subsequently it was formally shown that mast cells not only contain heparin but also histamine (Riley and West, 1953; Rocha e Silva and Scroggie, 1947), and may be activated by the polymeric basic secretagogue compound 48/80 to induce anaphylaxis (Mota and Vugman, 1956; Riley and West, 1955). However, not until the discovery of IgE in 1966, the molecular resolution of the complete FcεRI (1989) and its expression on mast cells, a clear cellular and molecular link between MC, allergen and type 1 hypersensitivity reactions could be drawn (Blank et al., 1989; Ishizaka and Ishizaka, 1966).

In order for mast cells to elicit a hypersensitivity reaction, allergen sensitization must occur prior to exposure. Allergen sensitization may take place at body surfaces that provide barriers to the environment e.g. lung, skin or intestine. Whether an individual becomes sensitized to a certain allergen depends on genetic and environmental factors (Tsai et al., 2008), and remains incompletely understood.

In case of the allergen sensitization in the lung, innocuous allergens are inhaled and deposited in the airway lumen. Activated dendritic cells sample the allergen and migrate to the draining lymph nodes where they encounter allergen-specific naïve T cells. With signalling downstream of IL-4, the T cells differentiate along the T_H2 pathway. Allergen-specific T_H2 cells then provide help to B cells in the germinal centers of draining lymph nodes to induce antibody generation and class switching to IgE. Allergen specific IgE antibodies are produced, bind to mast cells and preactivate them (sensitization). Upon re-exposure to allergen mast cells become activated and degranulate for immediate mediator release.

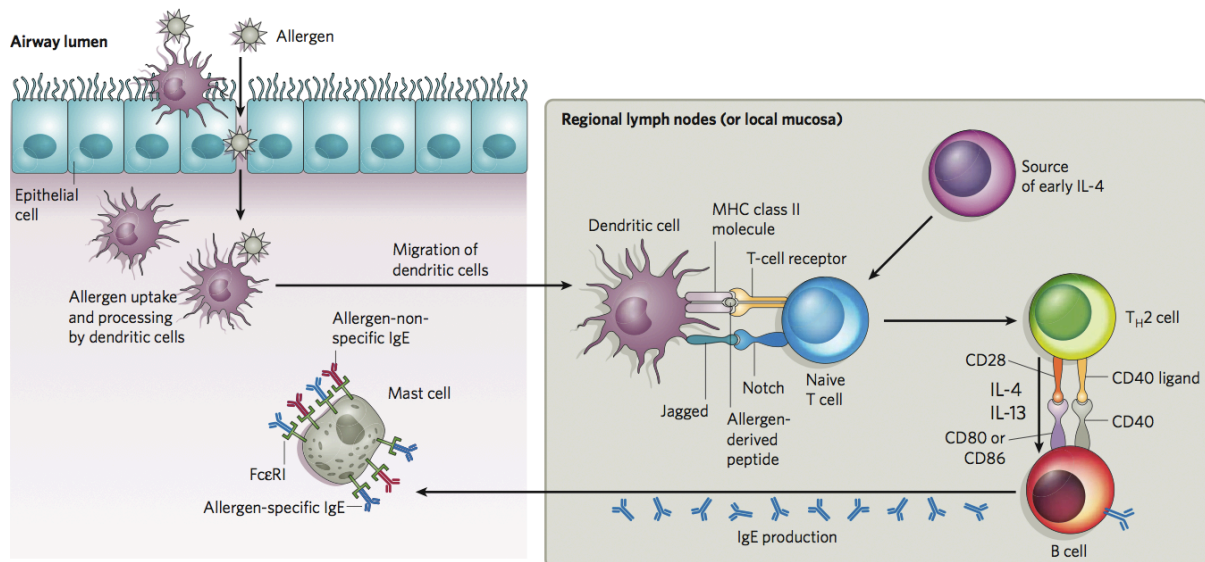


Figure 2.: Sensitization to allergens in the airways

Allergen inhalation results in activation of the immune system and generation of allergen specific IgE antibodies that may arm and subsequently activate mast cells. Adapted from (Tsai et al., 2008).

Apart from histamine and heparin, mast cell activation may result in the release of a wide array of bioactive substances (Wernersson and Pejler, 2014). Depending on the nature of stimulus three distinct classes of mediators are released: preformed mediators, stored in secretory granules; lipid mediators, derived from arachidonic acid; and newly synthesized mediators, which are produced following transcriptional activation (Marshall, 2004). An overview of mast cell derived mediators is presented in table 1.

	Mediators	Example of function
Granular	Histamine and 5-Hydroxytryptamine (Serotonin)	Promotes DC migration, suppresses T cell mediated adaptive immune responses, causes vasodilation, promotes angiogenesis, induces pain and itch
	Heparin and chondroitin sulphate peptidoglycans	Enhance chemokine and/or cytokine function and angiogenesis
	Tryptase, chymase, Cpa3 and other proteases	Tissue remodelling and recruitment of effector cells
	TNF- α , VEGF and FGF2	Recruit effector cells and enhance angiogenesis
Lipid-derived	LTC ₄ , LTB ₄ , PGD ₂ and PGE ₂	Recruit effector cells, regulate immune responses and promote angiogenesis, oedema and bronchoconstriction
	Platelet-activating factor	Activates effector cells, enhances angiogenesis and induces physiological inflammation
Cytokines	TNF- α , IL-1 α/β , IL-6	Promotes recruitment of innate immune cells (i.e. neutrophils), enhances protective antigen-specific antibody dependent immune response
	IL-4, IL-5, IL-13	Promotes T _H 2 immune response
	IL-12, IFN- γ	Promotes T _H 1 immune response
	IL-10, TGF- β	Suppresses adaptive immunity, promotes peripheral tolerance to skin allograft, suppresses innate immune response to chronic UVB radiation exposure
	VEGF and FGF2	Angiogenesis
Growth factors	SCF, GM-CSF, GnRH-1, b-FGF, NGF, VEGF	Promote mast cell development, differentiation, maturation and proliferation
Chemokines	CCL2, CCL3, CCL4, CCL5, CCL11 and CCL20	Recruit effector immune cells (i.e. neutrophils, monocytes and dendritic cells)
	CXCL1, CXCL2, CXCL8, CXCL9, CXCL10 and CXCL11	Recruit immune cells and regulate immune response
Other	Nitric oxide and superoxide anions	Bactericidal
	Antimicrobial peptides	Bactericidal

Table 1: Mediators released from activated mast cells

CCL, CC-chemokine ligand; CXCL, CXC-chemokine ligand; FGF2, fibroblast growth factor 2; GM-CSF, granulocyte/macrophage colony-stimulating factor; IFN, interferon; IL, interleukin; LIF, leukaemia inhibitory factor; LT, leukotriene; PG, prostaglandin; TGF- β , transforming growth factor- β ; TNF, tumour-necrosis factor; VEGF, vascular endothelial growth factor (Kumar and Sharma, 2010; Marshall, 2004).

Mast cells are strategically located in tissues facing the environment and in close proximity to blood vessels, lymphatic vessels and nerve fibres (Krystel-Whittemore et al., 2015; Kumar and Sharma, 2010). Their location within sites of frequent microbial exposure suggests a sentinel function of mast cells in host defence. In that regard, mast cells can release potent vasodilators such as histamine and serotonin and are able to recruit immune cells by secretion of chemokines and cytokines (Table 1) (Marshall, 2004). Consistent with this idea, mast cells have been shown to express a wide array of cell surface receptors that allow for recognition and detection of noxious substances and pathogens (Kumar and Sharma, 2010). Among these are toll-like receptors (TLRs), of which functional expression of TLR1, TLR2, TLR3, TLR4, TLR6,

TLR7 and TLR9 has been described for murine mast cells (Sandig and Bulfone-Paus, 2012). However, almost all of these studies were performed with in-vitro differentiated mast cells from various sources and thus have to be confirmed on primary mast cells before conclusions about potential functions may be drawn. Similarly, TLR mRNA expression in human primary mast cells has been described, however verification of TLR protein is still missing (Sandig and Bulfone-Paus, 2012). Receptors other than TLRs that can be found on mast cells are Fcγ-receptors (Tkaczyk et al., 2004), complement receptors (Johnson et al., 1975), cytokine and chemokine receptors (Marshall, 2004). The latter might sense local inflammation and induce mast cell activation independent of IgE.

Functional studies on TLR activation in cultured mast cells revealed selective production of inflammatory cytokines and chemokines (Matsushima et al., 2004; Supajatura et al., 2002). A potential function that is largely overlapping with other tissue resident immune cells, such as macrophages and dendritic cells (Galli et al., 2011).

In order to test in vivo mast cell functions researchers have traditionally relied on *Kit* mutant mice. *Kit*^{W^W} mice carry a spontaneous loss-of-function mutation in both *Kit* alleles and were the first *Kit* mutant strain described to be mast cell deficient (Kitamura et al., 1978). Because Kit expression is not restricted to mast cells and SCF signalling is crucial for various other cell types within and outside of the hematopoietic system, these mice carry many abnormalities apart from their mast cell deficiency (Nigrovic et al., 2008; Rodewald and Feyerabend, 2012).

Based on experiments performed with these mouse strains, mast cells have been erroneously regarded as masters of the immune system with a widespread spectrum of functions in innate and adaptive immunity, autoimmunity, immune metabolic diseases, and other areas. Unexpectedly, of all these proposed functions, experiments in *Kit*-independent mast cell deficient mouse strains could only recapitulate the unique functions of mast cells in IgE-mediated processes such as allergies, anaphylaxis and protection against helminths (Dudeck et al., 2011; Feyerabend et al., 2011; Rodewald and Feyerabend, 2012; Sawaguchi et al., 2012).

In humans IgE-dependent processes contribute to diverse pathologies such as anaphylaxis, allergic asthma, and hypersensitivity disorders of the skin.

Systemic anaphylaxis is the most severe and potentially fatal form of allergy, which can occur in response to insect venoms, drugs, and food allergens (Simons, 2010). The term allergy describing hypersensitivity reactions was postulated in 1906, Paul Portier and Charles Richet already described anaphylaxis in 1902, when they observed that dogs immunized against a toxin from the jellyfish *Physalia* did not induce protective immunity but instead died after a second injection of the toxin (Portier and Richet, 1902). In the USA, anaphylactic shock is responsible for an estimate of 1500 deaths annually (Matasar and Neugut, 2003). Anaphylaxis is caused by crosslinking of IgE on the surface of mast cells resulting rapidly in degranulation. In particular histamine that is systemically release from mast cells causes the symptoms of anaphylaxis such as oedema and reduced blood pressure (Simons, 2010).

Allergic asthma is a disease affecting the airways and is characterized by airway hyper-reactivity (AHR), mucus production, eosinophilia and fibrosis in the lungs. Clinical parameters such as mast cell infiltration into the airways correlate with bronchial hyper responsiveness (Wardlaw et al., 1988), and increased concentrations of histamine (Casale et al., 1987) and tryptase (Zhang and Timmerman, 1997) in bronchoalveolar lavage (BAL).

Clinical studies provide strong evidence for a crucial role of IgE and Fc ϵ RI in human asthma, as demonstrated by use of the anti-IgE mAb Omalizumab which was shown to decrease serum IgE levels and allergen-induced bronchoconstriction (Vichyanond, 2011).

The contribution of mast cells to chronic disease is difficult to assess. In order to shed light on the specific contribution of mast cells to asthma, animal models may provide crucial information on underlying mechanisms. However, animal models of asthma are suffering from inherent drawbacks that are mainly due to structural and cellular composition of the airways (under physiological conditions murine lungs do not contain mast cells), and non-physiological sensitization protocols (mostly very rapid sensitization) (Kumar, 2012; Voehringer, 2013).

Clinically observed hypersensitivity reactions of the skin, such as atopic dermatitis (AD), urticaria and IgE-mediated chronic allergic inflammation, have been linked to elevated IgE levels and mast cell infiltration into sites of inflammation. As a consequence, it is generally assumed that mast cells contribute to the inflammatory response. However, to date only few studies have shown to what degree and by

which mechanism mast cells contribute to hypersensitivity reactions such as AD. Available studies were performed with *Kit*-dependent mast cell deficiency models (Kawakami et al., 2009) and require independent verification.

1.4. Current treatment of mast cell dependent diseases

The three pillars of treatment of allergic disease are allergen avoidance, allergen-specific immunotherapy (SIT), and pharmacological intervention.

Allergen avoidance in children, to circumvent sensitization, has been explored. However, the results of such primary prophylaxis have been disappointing as most children became sensitized due to accidental intake minute quantities of antigen, which were sufficient for sensitization (Holgate and Polosa, 2008).

SIT is a therapy that modulates the immune response to allergens. This type of therapy is recommended for the treatment of allergic rhinitis, venom hypersensitivity, certain drug reactions and mild bronchial asthma. The mechanism of action is based on the induction of tolerance by allergen-specific IgG4 antibodies and regulatory T cells (T_{Reg}). T_{Reg} produce large amounts of IL-10 and TGF- β , which attenuates allergen-specific T_H2 in favor of a T_H1 immune response (Wu et al., 2007).

Pharmacological interventions mainly focus on four classes of substances: Corticosteroids, receptor agonists, receptor antagonists and biologics. Corticosteroids, suppress inflammation of the asthmatic airways by inhibition of the two major pro-inflammatory transcription factors nuclear factor- κ B and activator protein 1 (Barnes and Adcock, 1998). α/β -adrenoreceptor agonists are bronchodilators that bind to their cognate receptors, which triggers a signaling cascade that results in smooth muscle relaxation. H1-antihistamines, leukotriene modifiers (e.g. CysLTR1 antagonists), and cAMP phosphodiesterase inhibitors (PDE) belong to the third category of available pharmacological drugs to treat allergic disease. While H1- and CysLTR1 antagonists block the interaction of their respective mediator with their cognate receptor on structural cells of the airways, PDE suppresses the release of cytokines and other inflammatory signals in immune cells (Holgate and Polosa, 2008).

The fourth class of pharmacological interventions are biologics. Two biologics in use are directed against IgE, which is the most prominent indicator and mediator of allergic disease. Omalizumab (anti-IgE) was the first mAb to become approved in severe asthmatics and binds to soluble IgE (sIgE) at an epitope that overlaps with the

FcεRI binding site. As a consequence, binding of Omalizumab to sIgE blocks the IgE-FcεRI interaction and generates small immune complexes that are cleared from the body by a yet undescribed mechanism (Chang et al., 2007b). Apart from clearing sIgE, Omalizumab treatment results in the reduction of FcεRI on the surface of mast cells and basophils (Holgate, 2014). IgE-occupied FcεRI are structurally stable and are maintained on the cell surface, however FcεRI that are not bound by IgE are structurally unstable and are internalized for degradation (Kubo et al., 2001). Mast cells and basophils that have reduced levels of IgE-occupied FcεRI become refractory to antigen-mediated activation (Holgate, 2014). However, sIgE is continuously produced by memory B cells creating two major drawbacks for the treatment with Omalizumab. Firstly, patients rely on continuous treatment for maintaining the therapeutic efficacy, secondly lowering the cost-effectiveness (Hochhaus et al., 2003).

In order to target IgE-producing cells, a novel anti-IgE antibody has been developed: Quilizumab. It targets the 52 amino acid long M1' extracellular part of the segment of human membrane bound IgE, found on IgE producing B cells (Brightbill and Lin, 2014). IgE⁺ B cells are opsonized by the anti-M1' antibody, and thus can be depleted in an Fc-dependent manner. In preclinical models, administration of the anti-M1' antibody reduced de novo IgE production by more than 90%, which was found to be the result of depletion of IgE-positive memory B cells and plasmablasts (Brightbill et al., 2010). However, in humans Quilizumab was only able to reduce total IgE by 20-30% which suggests that 70-80% of IgE is produced by M1' negative cells, most likely plasma cells in the bone marrow (Gauvreau et al., 2014).

Mild forms of allergic diseases (allergic rhinitis) can be treated with anti-histamines, leukotriene antagonists or immunological desensitization. However, more severe forms of disease, such as asthma and atopic dermatitis, require a reduction of systemic inflammation by administration of broad acting immunosuppressive agents such as oral or intravenous corticosteroids to effectively alleviate symptoms (Leung and Bieber, 2003). However, systemic immunosuppressive therapies result in pleiotropic side effects such as susceptibility to infection (Nesbitt, 1995; Seale and Compton, 1986).

Particularly for severe asthmatics, defined by persisting symptoms despite treatment with high-dose inhaled steroids, novel therapeutic agents are urgently required (D

Amato et al., 2014). In addition, a subgroup of these patients may not be able to sufficiently control the disease, and thus have a particular high risk of morbidity and mortality, requiring frequent health-care services, such as emergency visits, hospitalizations and additional consumption of drugs for recurrent exacerbations (Pakhale et al., 2011; Serra-Batlles et al., 1998). Patients with severe/refractory asthma are a greater burden on industrialized nations healthcare systems than 90% of asthma patients with well controlled asthma (Holgate and Polosa, 2008). While steroids are the mainstay of treatment for severe asthma patients, Omalizumab has been reported to provide benefit for such patients by improving asthma symptoms, increasing disease control, reducing exacerbations and improving quality of life (D Amato et al., 2014).

Many of the current treatment strategies for allergic disease rely either on the neutralization of mast cell derived molecules (histamine and leukotriene), aim at reducing the activation of mast cells (corticosteroids, cromolyn sodium, and anti-IgE) or interfere with survival and proliferation of mast cells (Kit inhibitor) (Reber and Frossard, 2014). However, there is yet no therapeutic approach directed specifically against mast cells that would alleviate all mast cell-dependent symptoms and thereby reduce burden on the patients and on the healthcare providers.

Pharmaceutical companies are heavily investigating cell-directed therapies, using cell-depleting antibodies, due to their specific actions, reduction in side effects, and good safety profile. The key to cellular targeting (i.e. cellular depletion) of mast cells would be to find specific surface molecules that ensure safety and specificity. Experimentally, the therapeutic intervention directed specifically against mast cells has only scarcely been explored. Experimental studies on mice that used mAb directed against Fc ϵ RI or CD117 (Kit) have shown that mast cells, which express both Fc ϵ RI and Kit, can be targeted with cell-depleting antibodies (Brandt et al., 2003). Unfortunately, Kit is expressed in many cells beyond mast cells, thus the treatment of mice resulted in simultaneous depletion of cajal cells and hematopoietic progenitor cells (Daëron and Jönsson, 2012). Moreover, antibodies targeting the Fc ϵ RI pose high risk of activating mast cells, which could result in anaphylactic shock.

Apart from experimental work in mice, Siglec-8 has recently been identified as a human mast cell restricted receptor that may be suitable for the development of an antibody-dependent cytotoxic targeting approach (Kiwamoto et al., 2012).

1.5. Antibody-based mechanisms of cell ablation

Apart from discovering the mast cell, Paul Ehrlich also conceptualized the “magic bullet” hypothesis of specific recognition and elimination of malignant cells by antibodies. Since the discovery of hybridoma technology by Georges Köhler in 1975 the development of antibodies for therapeutic use has surged. Antibodies may target tumour cells by binding to cell surface antigens that are differentially expressed in cancer. One of the first antigens that were found to be suitable candidates in the clinics was CD20. The antibody rituximab targets CD20 in non-Hodgkin B cell lymphoma and was one of the most prominent antibody-based cytotoxic drugs to be approved for therapeutic use. Investigation of the killing mechanism revealed that three different pathways induce cell death. First, direct signalling of bound CD20 interferes with essential cellular functions. Secondly, antibody opsonisation initiates the complement cascade resulting in lysis by the membrane attack complex. And lastly, cell death may be induced by antibody-dependent cellular cytotoxicity (Weiner et al., 2010).

An overview of the anti-cancer mechanisms of mAbs with direct cytotoxic effect on target cells is depicted in Figure 3.

Fc-mediated effector engagement includes the cell-mediated killing of antibody opsonized tumour cells by Fc γ -expressing innate immune cells as well as complement dependent lysis by membrane attack complex. In antibody-dependent cellular phagocytosis, mononuclear phagocytes that express Fc γ R bind to the Fc-portion of the antibodies thereby inducing phagocytosis of the target cell. In antibody-dependent cell-mediated cytotoxicity (ADCC), NK cells bind to cell bound antibodies via their Fc γ R, and induce the release of cytotoxic granules containing perforin and granzymes that kill the target cell (Scott et al., 2012). During complement dependent lysis C1q molecules bind to Fc-portions of opsonising antibodies, thereby initiating the alternative complement cascade resulting in generation of the membrane attack complex (Weiner et al., 2012).

Direct cytotoxicity of mAbs may be induced by attachment of a cytotoxic conjugates (mostly toxins but also some radioactive or photoactivatable compounds) to the antibody. For cytotoxicity of such an antibody-drug conjugate (ADC), target:toxin complex internalisation is required. In contrast, ADCC requires cell surface exposition

for efficient killing (Trail, 2013). In addition, ligand binding itself has, in several instances, been identified to induce cell death (Rituximab).

Non-restricted activation of T cells comprises bispecific antibodies and antibody-derived recombinant proteins that possess more than one targeting domain. The mechanism of action is based on the simultaneous engagement of target cell and T cell to facilitate anti-tumour activity (Spiess et al., 2015).

The third major cell-directed antibody-mediated anti-tumour mechanism is based on blocking of inhibitory signals on naturally occurring cytotoxic lymphocytes within the tissues. A balance of activating and inhibitory signals tightly regulates the activation of NK cells. By engagement of the activating receptors on NK cells or blocking of inhibitory receptors on cytotoxic T cells the balance can be shifted towards cellular activation and tumour cell killing (Weiner et al., 2012).

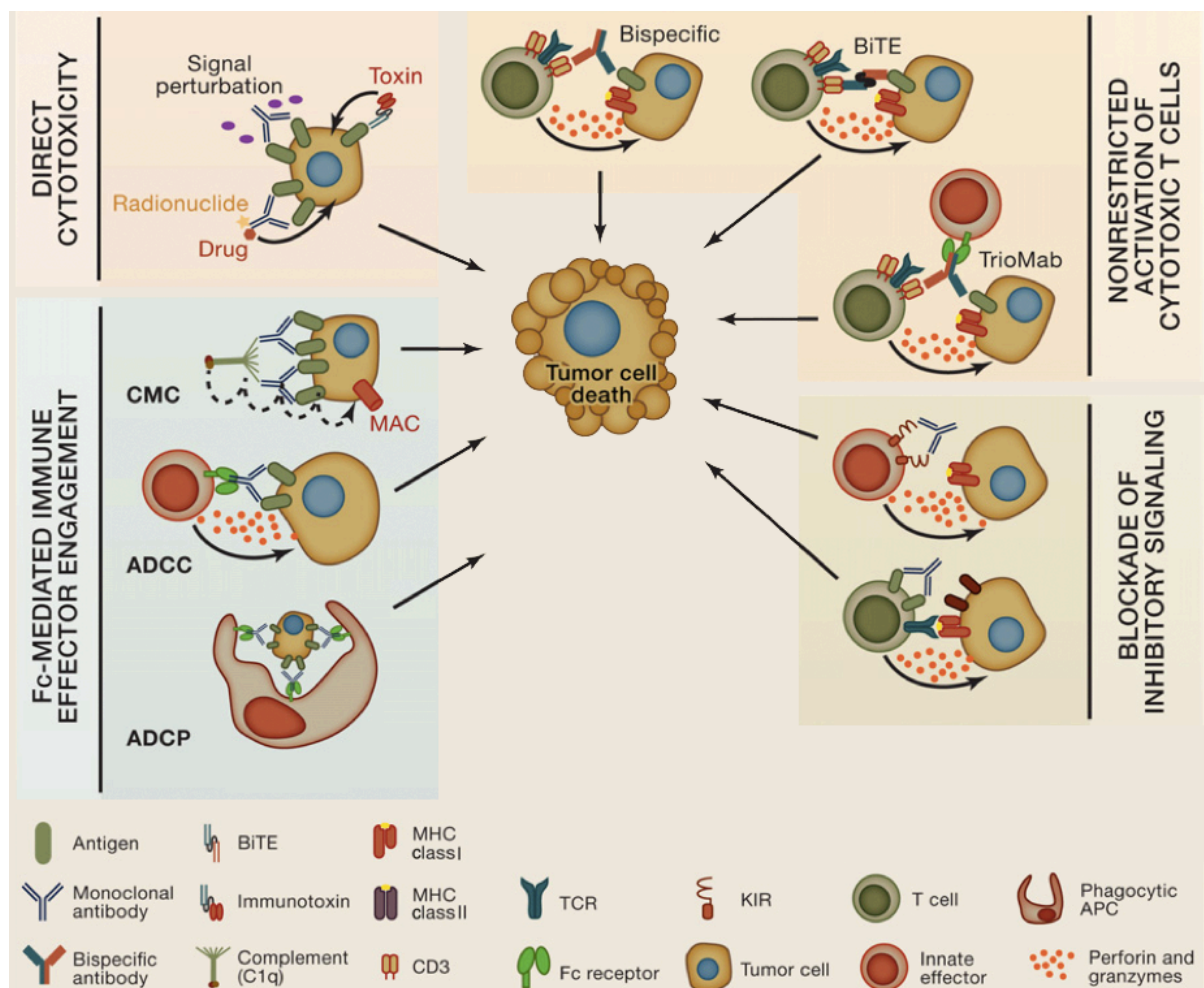


Figure 3: Non-humoral antibody-mediated cell targeting (tumour cell example)
Cell depletion mechanisms by monoclonal antibodies are versatile. Here, four groups of anti-cell mechanisms are depicted. Fc-mediated immune effector engagement, direct cytotoxic mechanisms, non-restricted activation of cytotoxic t cells, and

blockade of lymphocyte inhibitory signals. Figure was adapted from (Weiner et al., 2012).

During the last few decades' researchers have optimized the efficacy of mAbs for clinical utility. For example, structural engineering of the antibody sequence or glycosylation patterns has improved immunogenicity and immune effector cell engagement. In this regard it has been shown that removal of the core fucose within the antibody heavy chain glycosylation, increases the affinity for activating FcγRs expressed on myeloid cells and thereby increases the cell depleting activity (Nimmerjahn and Ravetch, 2011).

Mast cells, which are involved in numerous allergic pathologies, cannot be targeted by conventional therapeutics. Specific removal of mast cells by means of antibody targeting would interrupt the allergic cascade and is expected to offer significant benefit for patients. In order to develop such a mAb-mediated mast cell targeting approach I aim to establish proof of principle in a well-controlled system provided by our newly developed transgenic mouse model expressing an ectopic cell surface receptor selectively on MC. To transfer our findings towards the clinics I aim to identify novel mast cell specific cell surface markers by mass spectrometry and elucidate their mast cell targeting potential in mice.

1.6. Aims of the study

In principle any cell in the body may be the target of a cell-depleting antibody. Once a cell-type specific cell surface protein is recognized by a monoclonal antibody, immune cells can bind and eliminate the target cell. This strategy has been successfully adapted for several malignancies, such as B cell lymphoma, for which an Ab drug, Rituximab (anti-CD20), was developed. Due to their high degree of specificity mAb-based therapies are, in general, well tolerated. However, the efficacy mainly depends on the specificity of the target and the turnover of the target cell (Scott et al., 2012). Mast cells in particular, have been reported to exhibit extraordinary longevity in tissues, which would be highly advantageous for the efficacy of a mast cell ablation strategy (Dudeck et al., 2011; Julia Scholten, 2009).

With this study I aim to develop and test strategies to efficiently and safely ablate mast cells by monoclonal antibody-mediated mechanisms. The objectives are:

- 1.) Identification and verification of a suitable target molecule on the surface of mouse and human mast cells
- 2.) Exploration of different antibody-dependent mast cell ablation mechanisms for their efficacy
- 3.) Investigation on safety of mAb-dependent mast cell ablation in mice
- 4.) Functional test of mast cell ablation in a relevant animal model of human disease

2. Materials and Methods

2.1. Materials

2.1.1. Chemicals

All chemicals not listed below were either purchased from Merck and Fluka or Sigma-Aldrich.

Reagent	Company
DNP ₁₁ -OVA	BioCat
EDTA disodium salt	Gibco
SYTOX Blue Dead Cell Stain	Invitrogen
SYTOX Green Dead Cell Stain	Invitrogen
RBC lysis buffer (10x)	eBioscience

2.1.2. Kits

Kit	Company
Pierce™ Antibody Clean-up Kit	ThermoFisher Scientific
Alexa Fluor® 647 Antibody Labeling Kit	ThermoFisher Scientific
pHrodo™ Red, succinimidyl ester	ThermoFisher Scientific
EZ-Link™ NHS-PEG4-Biotin, No-Weigh™ Format	ThermoFisher Scientific
Pierce™ Fluorescence Biotin Quantitation Kit	ThermoFisher Scientific
CellTiter-Blue® Cell Viability Assay	Promega

2.1.3. Enzymes

Enzymes	Company
Collagenase Type VIII	Sigma-Aldrich
Collagenase Type IV	Sigma-Aldrich
Hyaluronidase	Sigma-Aldrich
DNase I	Sigma-Aldrich

2.1.4. Anti-mouse Antibodies

Fluorophore	Dilution	Supplier	Clone	Isotype
CD3e BV421	1:200	BioLegend	17A2	Rat IgG2b, κ
CD3e APC eF780	1:25	eBioscience	17A2	Rat IgG2b, κ
CD11b BV421	1:800	BioLegend	M1/70	Rat IgG2b, κ
CD11b PeCy7	1:400	eBioscience	M1/70	Rat IgG2b, κ
CD11b PerCP-Cy5.5	1:400	eBioscience	M1/70	Rat IgG2b, κ
CD11c BV421	1:100	BioLegend	N418	Armenian hamster IgG
CD13 BV421	1:100	BD	WM15	Mouse IgG1, κ
CD19 BV421	1:400	Biolegend	6D5	Rat IgG2a, κ
CD19 BV605	1:800	Biolegend	6D5	Rat IgG2a, κ
CD31 PE	1:100	BD	MEC13.3	Rat IgG2a, κ
CD34 FITC	1:25	eBioscience	RAM34	Rat IgG2a, κ
CD43 APC	1:100	BD	S7	Rat IgG2a, κ
CD45 APC eF780	1:400	eBioscience	30-F11	Rat IgG2b, κ
CD45 BV785	1:400	Biolegend	30-F11	Rat IgG2b, κ

CD45 Pe Cy7	1:400	eBioscience	30-F11	Rat IgG2b, κ
CD47 PE	1:100	Biolegend	miap301	Rat IgG2a, κ
CD49b APC	1:100	eBioscience	DX5	Rat IgM
CD49d FITC	1:100	BD	9C10(MFR4.B)	Rat IgG2a, κ
CD56 A647	1:100	R&D	#809220	Rat IgG2a, κ
CD63 PE	1:100	Biolegend	NVG-2	Rat IgG2a, κ
CD81 PE	1:100	eBioscience	Eat-2	Armenian hamster IgG
CD98 FITC	1:100	eBioscience	RL388	Rat IgG2a, κ
CD107a PE	1:100	Biolegend	1D4B	Rat IgG2a, κ
CD117 APC	1:800	BD	2B8	Rat IgG2b, κ
CD117 APC eF780	1:800	eBioscience	2B8	Rat IgG2b, κ
CD117 PE	1:800	eBioscience	2B8	Rat IgG2b, κ
CD147 PE	1:100	Biolegend	OX-144	Rat IgG1, κ
CD171 APC	1:100	R&D	FAB5674A	Rat IgG2a, κ
CD200r3 PE	1:100	Biolegend	Ba160	Rat IgG2a, κ
CD317 PE	1:200	eBioscience	ebio927	Rat IgG2b, κ
F4/80 BV605	1:100	Biolegend	BM8	Rat IgG2a, κ
F4/80 PE-Cy7	1:100	eBioscience	BM8	Rat IgG2a, κ
FcεRI PE	1:100	eBioscience	MAR-1	Armenian hamster IgG
Gr-1 BV421	1:800	Biolegend	RB6-8C5	Rat IgG2b, κ
IgE BV 786	1:200	BD	R35-72	Rat IgG1, κ
IgE FITC	1:200	BD	R35-72	Rat IgG1, κ
T1/ST2 eFluor710	1:400	eBioscience	RMST2-2	Rat IgG2a, κ
Integrin β7 PE	1:100	BD	M293	Rat IgG2a, κ
P2X7R A488	1:100	Biolegend	1F11	Rat IgG2b, κ
Isotype PE		eBioscience	eBR2a	Rat IgG2a, κ
Isotype PE		BD	A95-1	Rat IgG2b, κ
Isotype PE		eBioscience	eBio299Arm	Armenian hamster IgG
Isotype PE		Invitrogen	R104	Rat IgG1, κ
Isotype eFluor710		eBioscience	eBR2a	Rat IgG2a, κ
Isotype FITC		Biolegend	RTK2758	Rat IgG2a, κ
Isotype FITC		eBioscience	eB149/10HS	Rat IgG2b, κ
Isotype FITC		eBioscience	eBRG1	Rat IgG1, κ
Isotype APC		eBioscience	eBRM	Rat IgM
Isotype APC		Biolegend	RTK2758	Rat IgG2a, κ
Isotype A647		Biolegend	RTK2758	Rat IgG2a, κ
Isotype BV421		Biolegend	RTK2071	Rat IgG1, κ
MslgG2a eFluor710		eBioscience	m2a-15F8	Rat IgG1, κ

2.1.5. Anti-human Antibodies

Fluorophore	Dilution	Supplier	Clone	Isotype
CD3 BV421	1:100	Biolegend	OKT3	Mouse IgG2a,k
CD4 PE	1:100	Dako	MT 310	Mouse IgG1,k
CD4 Pe-Cy7	1:100	eBioscience	SK3	Mouse IgG1,k
CD14 BV605	1:100	Biolegend	M5E2	Mouse IgG2a,k
CD16 FITC	1:100	eBioscience	eBioCB16	Mouse IgG1,k
CD19 Alexa Fluor 700	1:100	Biolegend	HIB19	Mouse IgG1,k
CD26 PE	1:100	Biolegend	Ba5b	Mouse IgG2b,k
CD36 PE	1:100	Biolegend	5-271	Mouse IgG2a,k
CD44 PE	1:100	Biolegend	BJ18	Mouse IgG1,k
CD45 BV785	1:100	Biolegend	HI30	Mouse IgG1,k
CD51 PE	1:100	Biolegend	NKI-M9	Mouse IgG2a,k
CD54 PE	1:100	Biolegend	HA58	Mouse IgG1,k
CD59 PE	1:100	Biolegend	p282 (H19)	Mouse IgG2a,k
CD63 PE	1:100	Biolegend	H5C6	Mouse IgG1,k
CD82 PE	1:100	Biolegend	ASL-24	Mouse IgG1,k
CD92 APC	1:100	BD	VIM15	Mouse IgG1,k
CD107a PE	1:100	Biolegend	H4A3	Mouse IgG1,k
CD117 APC	1:100	eBioscience	YB5.B8	Mouse IgG1,k
CD117 PE	1:100	eBioscience	YB5.B8	Mouse IgG1,k

CD123 PerCP Cy5.5	1:100	eBioscience	6H6	Mouse IgG1,k
CD171 PE	1:100	eBioscience	eBio5G3	Mouse IgG2a,k
CD193 APC-Cy7	1:100	Biolegend	5E8	Mouse IgG2b,k
CD203c PE	1:100	eBioscience	NP4D6	Mouse IgG1,k
CD312 PE	1:100	Miltenyi	REA302	Human IgG1
FcεRIα APC	1:100	eBioscience	AER-37	Mouse IgG2b,k
FcεRIα PE	1:100	eBioscience	AER-37	Mouse IgG2b,k
IgE FITC	1:100	eBioscience	IgE21	Mouse IgG1,k
MRGPRX2	1:100	Biolegend	K125H4	Mouse IgG2b,k
Isotype APC		eBioscience	P3.6.2.8.1	Mouse IgG1,k
Isotype PE		Biolegend	MOPC-173	Mouse IgG2a,k
Isotype PE		BD	55617	Mouse IgG1,k
Isotype PE		eBioscience	eBMG2b	Mouse IgG2b,k

2.1.6. Media and supplements for cell culture

Media, buffers and supplement	Supplier
DMEM with GlutaMAX I	Gibco
FCS (fetal calf serum)	HyClone
HBSS (w/o CaCl ₂ , w/o MgCl ₂ , w/o phenol red)	Gibco
IMDM with GlutaMAX I	Gibco
MEM non-essential amino acids (100x)	Gibco
MEM sodium pyruvate (100mM = 100x)	Gibco
β-mercaptoethanol	Gibco
PBS (Dulbecco's w/o CaCl ₂ , w/o MgCl ₂)	Gibco
Penicillin-Streptomycin (100x, 10.000U penicillin/ml, 10.000 µg streptomycin/ml)	Peprotech Peprotech
Mouse Interleukin-3	Supernatant from an <i>IL-3/SCF</i> gene transfected cell line (Karasuyama and Melchers, 1988)
Mouse Stem cell factor (SCF)	
Recombinant human Interleukin 4 (rhIL-4)	
Recombinant human Stem cell factor (rhSCF)	

Medium for peritoneal- (PMC) and bonemarrow-derived mast cells (BMDC):

- IMDM
- 10 % FCS
- 100 µM MEM Non-essential amino acids
- 1 mM MEM Sodium pyruvate
- 100 U/ml Penicillin
- 100 U/ml Streptomycin
- 50 µM β-mercaptoethanol
- 1 % SCF conditioned medium
- 1 % IL-3 conditioned medium

Medium for human mast cell culture:

IMDM
10% FCS
20 ng/ml rhIL-4
100 mg/ml rhSCF
100 U/ml Penicillin
100 U/ml Streptomycin

2.1.7. Buffers and solutions

1x PBS 9.55 g/l of a D-PBS ready-to-use mixture (Gibco)
 8 g/l NaCl,
 0.2 g/l KCl
 1.15 g/l Na₂HPO₄
 0.2 g/l KH₂PO₄

Mota's fixative 4 g lead acetate (basic)
 30 ml 100% ethanol
 2-3 drops of glacial acetic acid

Acidic toluidine blue 0.5 g of toluidine blue
 50 ml 100% ethanol
 2-3 drops of glacial acetic acid

2.1.8. Cells and animals

2.1.8.1. Cell lines

CHO-SCF CHO cells transfected with mouse SCF cDNA to produce SCF,
 Genetics Institute, Boston

X63-IL3 X63 myeloma cell line transfected with a mouse IL-3 cDNA construct to
 secrete large quantities of the cytokine IL-3 (Karasuyama and
 Melchers, 1988).

H5C6 P3X653-Ag8 hybridoma cells expressing anti-hCD63 mouse IgG1, κ (clone H5C6). H5C6 was deposited to the DSHB by August, J.T. / Hildreth, J.E.K. (DSHB Hybridoma Product H5C6)

2.1.8.2. Primary human mast cells

Human mast cells were isolated from skin and fat tissue obtained from Proaesthetics.gmbh after written and oral consent of patients undergoing cosmetic surgery (Ethics approval no. S-377/2015). Human lung mast cells were isolated from bronchial biopsies obtained during lung surgery at the Thorax Clinics Heidelberg after written and oral consent (Ethics approval no. S-381/2014). Human colon mast cells were isolated from bowel biopsies obtained during bowel surgery at the University Hospital Heidelberg after written and oral consent approval.

2.1.8.3. Mouse strains

Inbred strains

The inbred mouse strains C57BL/6 and BALB/c were originally obtained from Charles River or Harlan and maintained in the mouse facilities of the DKFZ in Heidelberg under specific pathogen-free (SPF) conditions.

Cpa3^{Cre/+} mice

Cpa3^{Cre/+} mice were generated from targeted E14.1 ES-cells. ES cell clones bearing the *Cpa3*^{Cre/+} knock-in allele were injected into C57BL/6 blastocysts to produce chimeric mice (Feyerabend et al., 2011). Subsequent crossing to C57BL/6 transmitted the targeted allele through the germ line. Heterozygous offspring were then used to backcross the *Cpa3*^{Cre/+} allele onto C57BL/6 and BALB/c background. All strains were kept under specific pathogen-free (SPF) conditions at the animal facilities of the DKFZ in Heidelberg.

Cpa3^{hCD4/+} mice

Cpa3^{hCD4/+} mice were generated from targeted E14.1 ES-cell clones following blastocyst injection (Feyerabend, 2007). Homozygous *Cpa3*^{hCD4/hCD4} mice were derived from intercrosses of *Cpa3*^{hCD4/+} mice on the C57BL/6 background. All strains were kept under SPF conditions at the animal facilities of the DKFZ in Heidelberg.

2.1.9. Equipment

Laboratory equipment	Company
Cytospin4 (centrifuge)	Shandon
Digital thermometer Qtemp 200	VWR International
Heraeus Fresco 17 (benchtop centrifuge)	Thermo Scientific
Heraeus Megafuge 40R	Thermo Scientific
Inverse light microscope Primo Vert	Zeiss
Light microscope DM LB2	Leica
Light microscope Lab.A1	Zeiss
Light Microscope Axioplan	Zeiss
LSRFortessa (FACS analyzer)	BD Bioscience
Aria (Cell sorter)	BD Bioscience
Fusion (Cell sorter)	BD Bioscience
Cellometer Auto 2000	Nexcelem

2.1.10. Software

Flow cytometry data were acquired and analysed with FACS Diva software (BD Bioscience) or FlowJo software (Treestar). Microscopic images were acquired using ZEN 2011 lite software and further processed with Photoshop CS (Adobe).

Statistical analyses and graphs were generated with Prism 6 (Graphpad).

2.2. Methods

2.2.1. Cell Biology

2.2.1.1. Preparation of cells from murine organs

2.2.1.1.1. Recovery of peritoneal exudate cells (PEC)

Mice were euthanized by CO₂ asphyxiation. The peritoneum was opened by a small cut. The peritoneal cavity was flushed successively with a total of 10 ml 37°C pre-warmed FACS buffer and the recovered PEC were collected on ice.

2.2.1.1.2. Digestion of skin, tongue, trachea and fat for analysis of mast cells

Ear/back skin, tongue, trachea and fat were minced and re-suspended in 500 µl DMEM containing 0.025 mg/ml DNase I (Sigma-Aldrich) and 1mg/ml collagenase 4 (Sigma-Aldrich). The minced tissues were incubated at 37°C under shaking at 700 rpm for 20 min. The supernatant, containing liberated cells, was collected on ice and 2 mM EDTA and 5% FCS were added to inhibit remaining enzymatic activity. Undigested tissue clumps were subjected to further digestion rounds with fresh

digestion mix until the tissues were completely digested. Finally, the cells were pelleted, re-suspended in FACS buffer and analysed.,

2.2.1.1.3. Isolation of intra-epithelial leukocytes from the stomach

Stomach was removed from the mouse and cut open longitudinally. Washing with FACS buffer cleared undigested food away. Subsequently the stomach was minced and re-suspended in 1 ml $\text{Ca}^{2+}/\text{Mg}^{2+}$ free HBSS containing 4 mM EDTA. The minced stomach was then incubated at 37 °C under shaking at 700 rpm for 20 min. Tissue fragments were separated from intra-epithelial leukocytes by filtration through a 100 μm cell strainer. Finally, the cells were pelleted, re-suspended in FACS buffer and utilized for FACS.

2.2.1.2. Preparation of cells from human organs

2.2.1.2.1. Digestion of skin, lung and fat for analysis of mast cells

Skin was obtained from either cosmetic abdominoplasty, labioplasty, blepharoplasty or breast reduction surgery. Specimens were minced with scissors or scalpels and resuspended in 10 ml of PBS with 0.2 mg/ml Collagenase 8 (Sigma), 0.025 mg/ml DNase I (Sigma-Aldrich) and 0.1 mg/ml Hyluronidase (Sigma) per gram tissue. The minced tissues were incubated at 37°C under shaking at 150 rpm for 120 min. Undigested tissue fragments were filtered through gauze and centrifuged at 1200rpm for 5 min. Pellets were washed with PBS +5% FCS + 2 mM EDTA and filtered through 100 μm cell strainer. Filtered cells were used for antibody staining or magnetic enrichment.

Lung tissue was obtained from patients undergoing lobectomy surgery due lung cancer (mostly non-small-cell-lung-carcinoma). Colon tissue was obtained from patients undergoing partial bowel resection due to bowel cancer. In either case, patients did not receive chemotherapeutic treatment before surgery. Specimens were minced with scissors or scalpels and resuspended in 10 ml of PBS with 0.2 mg/ml Collagenase 8 (Sigma) and 0.025 mg/ml DNase I (Sigma-Aldrich) per gram tissue. The minced tissues were incubated at 37°C under shaking at 150 rpm for 40 min. The supernatant, containing liberated cells, was collected on ice and 2 mM EDTA and 5% FCS were added to inhibit remaining enzymatic activity. Undigested tissue clumps were subjected to further digestion rounds with fresh digestion mix until the

tissues were completely digested. Finally, the cells were pelleted, re-suspended in FACS buffer and analysed by flow cytometry.

2.2.2. Flow Cytometry

2.2.2.1. Antibody staining

Cells were stained in 96-well V-bottom plates or in 1.5-ml tubes. Up to 5×10^6 cells were incubated in 50 μ l FACS buffer. Prior to antibody staining, cells were incubated for 20 min with 0.28 mg/ml mouse IgG (Jackson ImmunoResearch Laboratories) to block Fc γ -receptors. The cells were then centrifuged and resuspended in FACS buffer containing the diluted fluorochrome-coupled antibodies. Cells were incubated for 30 min on ice protected from light. After staining, cells were washed once with 1ml FACS buffer in 1.5-ml tubes, or with 200 μ l FACS buffer in 96-well plates. If necessary, cells were incubated for another 20 min with a secondary antibody and washed accordingly. The optimal working concentration for each antibody was determined by separate titration experiments and is listed under table 1.

Finally, cells were re-suspended in FACS buffer and analysed on a LSRFortessa (BD Bioscience). Data are displayed as dot plots or histograms using FlowJo software (Treestar).

Flow cytometry data was normalized across experiments by calculating the staining index ($\frac{MFI\ marker - MFI\ isotype\ control}{2 \times SD\ MFI\ isotype\ control}$) (Maecker et al., 2004).

2.2.2.2. Exclusion of dead cells

To exclude dead cells from FACS analysis, 1 μ M SYTOX Blue or Green Dead Cell Stain (Invitrogen) was added to the cell samples 5 min before analysis.

2.2.2.3. Magnetic enrichment of Kit⁺ cells

Peritoneal cavity cells were incubated with CD117 specific magnetic micro beads for 20 min at 4°C. Cells were then spun down and washed with FACS buffer. A single MACS LS column was placed into the magnet and equilibrated with cold FACS buffer. Magnetically labelled cells were applied to the column and unlabelled cells are not retained in the magnetic field. After washing, CD117⁺ cells could be eluted from the column by removing it from the magnet and flushing the cells with cold FACS buffer from the column. Cells were then pelleted and counted and prepared for subsequent analysis or further purification on the cell sorter.

2.2.2.4. Measurement on BD Fortessa

Antibody stained cells were measured on a BD LSR Fortessa equipped with a violet (405 nm), green (488 nm), yellow (560 nm), and red laser (633 nm). Cells were first gated based on their forward / sideward scatter characteristics, followed by gating on single cells and live cells (Sytox negative). Cells were further characterised depending on the antibodies used within the individual experiments.

2.2.2.5. Murine cell sorting on BD Aria

Antibody stained peritoneal cavity cells or CD117⁺ selected peritoneal cells were sorted on a BD Aria cell sorter using a 100 µm nozzle at 20 PSI. Cells were sorted into pure PBS. For proteomics experiments, the sorted cells were immediately centrifuged at 2000 rpm for 5 minutes and shock frozen in liquid nitrogen. Cells were stored at -80°C.

2.2.2.6. Human cell sorting on BD Fusion

Antibody stained CD117⁺ selected cells from skin or fat tissue were sorted on a BD FUSION cell sorter using a 100 µm nozzle at 20 PSI. Cells were sorted into pure PBS.

2.2.2.7. Cytospins & Toluidine blue staining

Sorted human mast cells were resuspended at 10.000 cells per 200 µl in PBS. The cell suspension was added to the cytospin slides. The cytospin slides were inserted into a Cytospin™ 4 Cytocentrifuge and centrifuged at 700 rpm for 5 min. with acceleration set to medium.

Cytospun human mast cells were fixed by adding several drops Mota's fixative directly onto the cells. Cells were incubated for 10 min and fixative was replenished twice to prevent drying of the cells. The slides were then rinsed with water to remove the fixative. Two to three drops of acidic toluidine blue were added directly onto the cells and slides were incubated for 20 min at room temperature. Afterwards they were rinsed with water and blotted dry. The cells were then embedded in Permount and enclosed by a coverslip. Images were taken on a Zeiss Axioplan upright microscope with a 40x objective using the ZEN 2011 lite software suite.

2.2.3. Procedures of animal experimentation

2.2.3.1. Antibody injections

Mice were injected intraperitoneally (i.p.) or intravenously (i.v.) with 30-90 mg/kg (0.3 – 2.7 mg) of TNX355 or afucosylated TNX355 antibody with varying numbers of injections and treatment intervals. In case of immunotoxin treatment, mice were injected i.v. with either 100 µg of 1:1 molar mixture of biotinylated CD63 antibody and streptavidin-saporin (SAP) (60 µg mAb + 40 µg SAP) or with 40 µg SAP alone. All injections were performed in 200 µl PBS.

2.2.3.2. Passive systemic anaphylaxis assay

Mice were first sensitized with IgE directed against dinitrophenol (DNP). DNP-specific IgE binds the high affinity IgE receptor (FcεRI) on the cell surface of mast cells and basophils. Upon challenge with antigen, mast cells and basophils become activated, which in mice results in hypothermia. Mice were sensitized by i.v. injection of 20 µg mouse anti-DNP-IgE (clone SPE-7, Sigma). 24 h later, the mice were challenged by i.v. injection of 20 µg DNP₁₁-OVA (Biocat). The anaphylactic response was monitored by change in core (rectal) body temperature every 10 min over a period of 3 h using the digital thermometer Qtemp 200 (VWR International, Germany)

2.2.4. Cell culture

2.2.4.1. General cell culture methods

Murine cells were kept at 37 °C, 95% humidity and 5% CO₂. Human cells were kept at 37 °C, 95% humidity and 10% CO₂. Unless otherwise indicated, standard handling of the cells during experiments was as follows: Cells were kept on ice, standard washing buffer was PBS containing 5% FBS and 2 mM EDTA (FACS buffer). Standard centrifugation was 5 min at 138 g (1200 rpm) in the Heraeus Fresco 17 centrifuge, or 5 min at 314 g (1200 rpm) in the Heraeus Megafuge 40R at 4 °C.

2.2.4.2. Determination of the cell number

An aliquot of cells was diluted in an appropriate volume of FACS buffer and 20 µl of the cell suspension mixed with the same volume of AOPI solution. 20 µl of this dilution were applied to a counting slide, which was subsequently inserted into a Nexcelem Cellometer Auto 2000 cell counter. Acridine Orange and

Propidium Iodide-negative cells (nucleated living cells) were used to calculate the cell number.

2.2.4.3. Generation of bone marrow-derived mast cells (BMMC)

Femurs of mice were crushed with a mortar and pestle, and cells were filtered through a 100 µm cell strainer. Whole bone marrow cells were pelleted, re-suspended in 1 ml BMMC medium and counted. Cells were adjusted to 1×10^6 cells/ml in BMMC medium and plated into 6-well plates (3 ml/well). One ml medium was replaced by fresh BMMC medium on a biweekly basis. After two weeks non-adherent cells were transferred into new 6-well plates. After four to five weeks of culture the purity of the differentiated mast cells (FcεRI⁺ and Kit⁺) was at least 95 % as analysed by flow cytometry. The optimal cell density is $0.5 - 1 \times 10^6$ cells/ml and BMMC were split accordingly.

2.2.4.4. Generation of peritoneal cell-derived mast cells (PMC)

Peritoneal cells were collected by lavage as described earlier. Cells were pelleted, re-suspended in 1 ml BMMC medium and counted. Cells were adjusted to 1×10^6 cells/ml in BMMC medium and plated into 6-well plates (3 ml/well). 1 ml medium was replaced by fresh BMMC medium on a weekly basis. After one week non-adherent cells were transferred into new 6-well plates. After two to three weeks of culture the purity of mast cells (FcεRI⁺ and Kit⁺) in the culture was at least 95% as analysed by flow cytometry.

2.2.4.5. Antibody internalisation assay

pHrodoRed coupled H5C6 or isotype control antibody (mIgG1) was incubated with primary human fat and skin mast cells at 10 µg/ml at 37 °C. After different time points cells were resuspended in 10x volume of FACS buffer and centrifuged at 1200 rpm for 5 minutes. Cells were then resuspended in FACS buffer and analysed by flow cytometry. The pHrodo™ red dye has excitation and emission maxima of approximately 560 nm and 585 nm. At neutral pH pHrodoRed does not emit fluorescence. Internalisation of the dye bound to the antibody, and entry into acidic (pH<7) compartments induces a conformational change in the dye resulting in fluorescence emission after excitation at 560 nm. Fluorescence at that wavelength as detected by flow cytometry, measured in the PE-channel.

2.2.4.6. In-vitro mast cell killing assay

10.000 peritoneal- and bone marrow-derived mast cells were incubated with different amounts of 1:1 molar mixed anti-CD63-biotin (clone NVG-2) and streptavidin-saporin in a 96 well plate in 100 µl growth medium. After 72 hours at 37 °C the amount of viable cells was assessed by the CellTiter-Blue viability assay. Briefly, 10 µl of reagent were added to 100 µl of cell suspension. The cells were then incubated for 2 hours at 37 °C. The metabolic conversion of the redox dye (resazurin) into a fluorescent end product (resorufin) was detected at 560Ex/590Em in a fluorescent plate reader. Cells treated with 10 µM Mefloquine, which has been reported to induce mast cell apoptosis in vitro, served as a positive control (Paivandy et al., 2014).

2.2.5. Molecular Biology

2.2.5.1. Sample preparation for mass spectrometry

Peritoneal cavity exudate cells of 6-8 week old C57BL/6J *Cpa3*^{+/+}, C57BL/6J *Cpa3*^{Cre/+} and FACS sorted peritoneal mast cells of C57BL/6J *Cpa3*^{+/+} mice were pelleted and frozen in liquid nitrogen. Cells were lysed in 0.1% RapiGest (Waters) and 50 mM (NH₄)HCO₃, extracted proteins were reduced and alkylated with 5 mM DTT and 10 mM iodoacetamide. Impurities were removed by precipitation with TCA and washing with acetone. Proteins were then digested overnight with sequencing-grade modified trypsin (Promega). Peptides were labelled differentially with stable isotope dimethyl labels on a column as described previously (Boersema et al., 2009). Labelled peptides were mixed 1:1:1 (i.e. from the three samples) according to cell number (50.000 cells) and separated by offline high pH reverse phase fractionation over a 90-minute gradient on a C18 column (Phenomenex) with an Agilent 1200 Infinity high-performance liquid chromatography (HPLC) system. Thirty-two fractions were collected and subsequently pooled into 10 fractions. Pooled fractions were dried under vacuum centrifugation, reconstituted in 4% acetonitrile/ 1% formic acid and then stored at -80 °C until LC-MS analysis.

2.2.5.2. Liquid chromatography–electrospray ionization–tandem mass spectrometry

Pooled peptide fractions were separated with the nanoACQUITY UPLC system (Waters) fitted with a trapping column (nanoAcquity Symmetry C18). Peptides were separated on a 120-minute gradient and were analyzed by electrospray ionization-

tandem mass spectrometry (ESI-MS/MS) on a linear trap quadrupole Orbitrap Velos Pro (Thermo Fisher Scientific). Full-scan spectra from a mass/charge ratio of 300 to 1,700 at a resolution of 30,000 full width at half maximum were acquired in the Orbitrap mass spectrometer. From each full-scan spectrum, the 15 ions with the highest intensity were selected for fragmentation in the ion trap. A lock-mass correction with a background ion (mass/charge ratio, 445.12003) was applied.

2.2.5.3. Bioinformatic analysis of proteomic data

MS raw data files were processed with Bioconductor using the packages: Biobase, BiocGenerics, and Parallel. Contaminants and reverse sequences were removed. The peptides were mapped to the Uniprot database. Using the protein identifier, the peptides were mapped to the associated ensembl genes as reported by Uniprot. For each ensembl gene id a generic protein was selected. Among all proteins that cover most peptides, the longest was selected. Peptides not mapping to the longest protein were not considered in the sequel analysis.

The samples were labelled as follows with a label swap between the two technical replicates. All biological replicates were labelled the same.

Mouse:

Technical replicate a		Technical replicate b	
Cpa3 ^{Cre/+} PEC	Heavy	Cpa3 ^{Cre/+}	Light
Cpa3 ^{+/+} sorted MC	Light	Cpa3 ^{+/+} sorted MC	Heavy
Cpa3 ^{+/+} PEC	Medium	Cpa3 ^{+/+} PEC	Medium

Human:

Technical replicate a		Technical replicate b	
Skin MC	Heavy	Skin MC	Light
Fat MC	Light	Fat MC	Heavy
PBMC	Medium	PBMC	Medium

Peptide intensities of 0 were interpreted as missing values and therefore replaced by NA. The expression data was normalized using the variance stabilising normalization (Huber et al., 2002). Computing the mean summarized the technical replicates. For statistical analysis of the comparisons (e.g. Skin MC/PBMC), the peptide intensities in the two conditions were subtracted from each other. The peptide log-ratios are averaged for each protein. The p-value was computed by a moderated t-test as implemented in the R/Bioconductor package limma (Lönstedt and Speed; Smyth,

2004). p-values were corrected for multiple testing by the method of Benjamini-Hochberg (Benjamini and Hochberg, 1995).

Enrichment of gene sets was analysed for all genes that were up- (down-) regulated in mast cells. Redundant mouse mast cell enriched gene sets were reduced and summarized using REVIGO (Supek et al., 2011).

2.2.5.4. Antibody clean-up and labelling

Commercially available antibodies often contain BSA for stabilization of low concentrated antibody solutions, which interferes with downstream antibody labelling. Anti-CD63 antibody (Clone NVG-2) was purchased from Biolegend. BSA was removed from the antibody solution using the Pierce™ Antibody Clean-up Kit according to the manufacturers instructions. AlexaFluor647, pHrodoRed, or Biotin was conjugated to hCD4 (TNX355), NVG-2 (mCD63), and H5C5 (hCD63). Briefly, amine reactive AlexaFluor647, pHrodoRed or Biotin was mixed with 100 ug of antibody (10X molar excess) in 0.1 M sodium bicarbonate buffer, and incubated for 60 minutes at RT in the dark. Subsequently unbound dye was removed by size exclusion using either the supplied purification resin or Zeba™ Spin desalting columns.

2.2.5.5. Biotin quantitation

The degree of biotin labelling was determined using the Pierce™ Fluorescence Biotin Quantitation Kit. Briefly, the Thermo Scientific DyLight Reporter (i.e., fluorescent avidin and HABA premix) was added to the biotinylated antibodies and diluted biocytin standards. HABA (4'-hydroxyazobenzene-2-carboxylic acid) binds weakly to the fluorescent avidin, thereby quenching the fluorescent signal. When the HABA is displaced by biotin in the test sample, fluorescence can be measured with a fluorescence plate reader (excitation 494 nm; emission 520 nm). The amount of fluorescence in the sample is determined by comparing the fluorescence to the standard curve. The antibody concentration was determined by measuring the absorbance of the antibody solution at 280 nm with a UV-VIS Spectrophotometer (NanoDrop2000). The molar concentration was calculated using an extinction coefficient of $230.000 \text{ M}^{-1} \text{ cm}^{-1}$ (Maity et al., 2015).

3. Results

3.1. Anti-hCD4-mediated mast cell ablation

The aim of this work was to label and eliminate mast cells by monoclonal antibodies. For this, I sought to establish an in vivo mast cell ablation strategy. To date, there is a lack of information on mast cell specific cell surface receptors that may be used for targeting of mast cells with mAbs. In order to avoid difficulties with unspecific mast cell markers we first sought to establish antibody-dependent mast cell ablation by using a model antigen. Thorsten Feyerabend, in the Rodewald laboratory, previously developed an animal that expresses an ectopic antigen specifically in mast cells. In this *Cpa3^{hCD4}* mouse model, a modified human CD4 receptor was introduced into the mast cell specific *Cpa3* locus by gene targeting (Feyerabend, 2007). This hCD4 molecule lacks intracellular signalling domains to exclude signalling dependent receptor internalization, and thus increase surface exposition of the receptor for enhanced sensitivity in flow cytometric analysis. hCD4 was chosen since a variety of commercially available antibodies specific for this receptor are available, yet its sequence is differential to any other mouse proteins, providing high specificity and low staining background.

This model system was used towards establishment of systemic mast cell ablation after anti-hCD4 antibody administration. Once established, we aim to transfer the ablation conditions to physiological mast cell antigens that I identified in parallel.

3.1.1. Characterisation of *Cpa3^{hCD4}*

Ear skin, tongue, fat, stomach and peritoneal cells were stained with antibodies specific F4/80, CD45, CD117 and IgE. Phenotypic mast cells ($F4/80^- CD45^+ CD117^+ IgE^+$) were found in all tissues. There is no difference in mast cell numbers between *Cpa3^{+/+}* and *Cpa3^{hCD4/+}* mice. It has been previously shown that homozygous knockin into the *Cpa3* locus, such as in *Cpa3^{hCD4/hCD4}* (*Cpa3* knockout) does not have an influence on the number of mast cells (Feyerabend et al., 2005).

In the C57BL/6 strain background more mast cells could be found in the skin, tongue, fat and peritoneal cavity, while BALB/c mice had slightly more mast cells in the stomach (Figure 4).

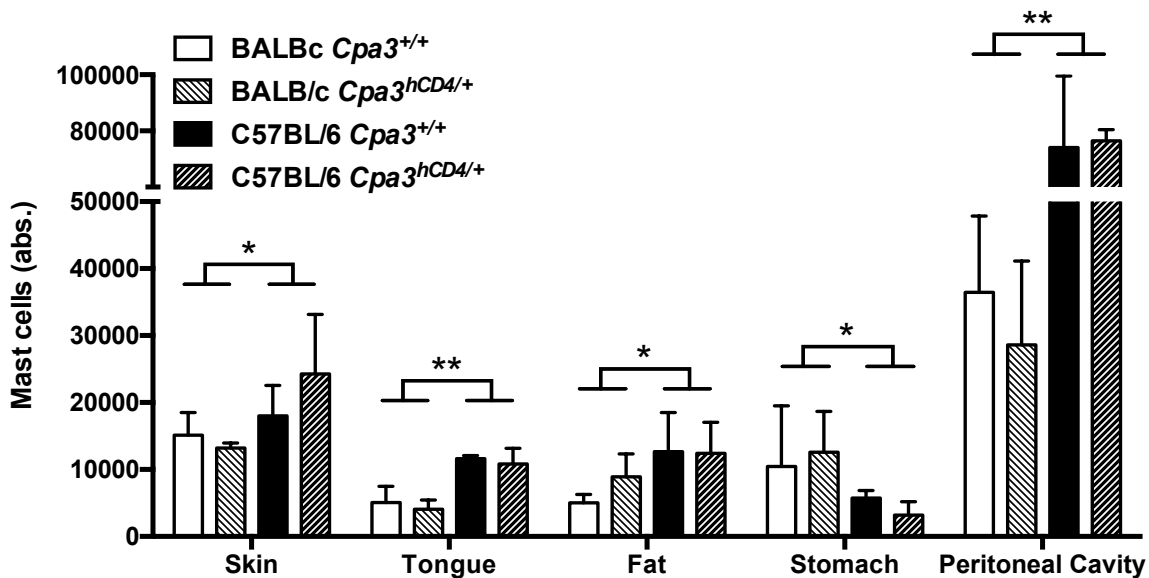


Figure 4: Absolute number of mast cells in *Cpa3*^{hCD4/+} knockin mice

Skin, tongue, fat, stomach and peritoneal exudate cells from BALB/c *Cpa3*^{+/+}, BALB/c *Cpa3*^{hCD4/+}, C57BL/6 *Cpa3*^{+/+} and C57BL/6 *Cpa3*^{hCD4/+} mice were analysed by flow cytometry for the presence of CD45⁺ CD117⁺ IgE⁺ mast cells. Shown are the mean \pm SEM for three animals per genotype. (*p < 0.05, **p < 0.01).

In order to assess specificity and intensity of hCD4 expression, the mean fluorescence intensity (MFI) of the hCD4 staining was determined for different cell populations. By gating on live (Sytox blue⁻) CD45⁺ CD117⁺ IgE⁺ cells the hCD4 expression level of mast cells from different organs was compared. Specificity of hCD4 expression was determined by comparing the fluorescence intensity signals of different mast cell compartments to splenic B cells, T cells, basophils, eosinophils, neutrophils, and monocytes. We found hCD4 expression almost exclusively restricted to mast cells. All tested tissue mast cells in *Cpa3*^{hCD4} mice expressed hCD4 to a similar extent with the exception of peritoneal mast cells that displayed 3-4 fold higher MFI (Figure 5). Only basophils, which share a close lineage relationship with mast cells, stained weakly positive for hCD4.

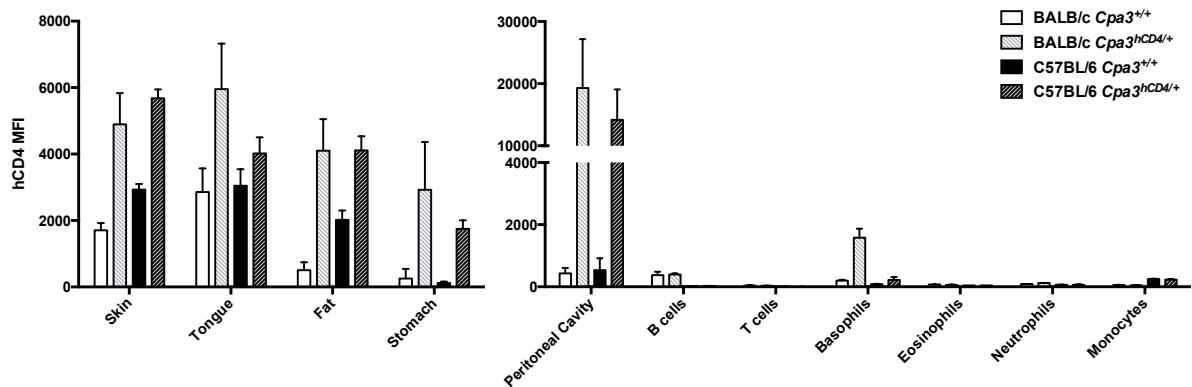


Figure 5: Mast cell specific cell surface expression of hCD4 in *Cpa3*^{hCD4/+} knockin mice
Mast cells (CD45⁺ CD117⁺ IgE⁺) from skin, tongue, fat and stomach cells were analysed by flow cytometry for intensity of hCD4 expression. Specificity was demonstrated by comparing peritoneal mast cells to B cells (CD19⁺), T cells (CD3⁺), basophils (CD49b⁺ IgE⁺), eosinophils (SSC^{hi} Siglec-F⁺), neutrophils (CD11b⁺ Gr-1⁺) and monocytes (CD11b⁺ F4/80⁺) from spleens of BALB/c *Cpa3*^{+/+}, BALB/c *Cpa3*^{hCD4/+}, C57BL/6 *Cpa3*^{+/+} and C57BL/6 *Cpa3*^{hCD4/+} mice. Shown are the mean \pm SEM of three animals per genotype pooled from 3 individual experiments.

Measurement of the hCD4 MFI implied differential expression levels of hCD4 on different peripheral mast cell compartments. More likely, however, would be the possibility of partial antigen loss during collagenase digestion for organ dissociation. To test the influence of collagenase treatment on hCD4 surface expression, I incubated peritoneal mast cells with and without 1 mg/ml Collagenase 8. hCD4 expression was approximately 10-fold lower on collagenase-treated peritoneal mast cells compared to untreated mast cells (Figure 6). In addition, it could be observed that CD117 cell surface expression was also reduced by collagenase digestion.

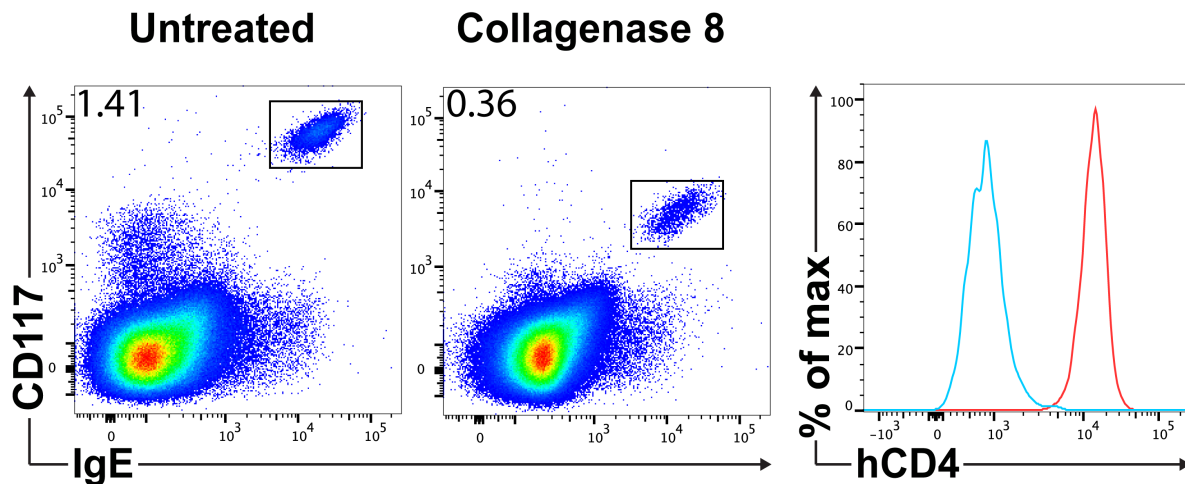


Figure 6: Receptor cleavage by collagenase treatment

Peritoneal cells from C57BL/6 *Cpa3^{hCD4/+}* mice were untreated (left) or incubated with 1 mg/ml collagenase 8 for 30 minutes at 37°C (middle). Cells were analysed by flow cytometry for binding of anti-hCD4 antibody (right). On the histograms, collagenase 8-treated mast cells are depicted in blue, untreated mast cells are depicted in red.

In summary, hCD4 is, with high specificity, strongly expressed in the mast cell lineage. Mast cell numbers are not affected by the gene knockin or transgene expression. Therefore the *Cpa3^{hCD4}* mouse is a suitable tool for establishing ADCC-mediated targeting protocols.

3.1.2. Characterisation of TNX355 (anti-hCD4) antibody

The TNX355 antibody (also known as Ibalizumab or TMB-355) is a monoclonal antibody against human CD4 with a mouse IgG2a isotype. The antibody was first developed by Tanox, now part of Genentech and was developed to inhibit cellular entry of HIV. Our collaborator Medimmune has generously provided it to us for experimental usage.

It has been shown by Nimmerjahn and colleagues that in mice the isotype IgG2a and the FcγRI and FcγRIV receptors are crucial for initiating antibody dependent cell-mediated cytotoxicity (ADCC). Moreover, binding strength between IgG2a and FcγRI or FcγRIV could strongly be enhanced by removal of the core fucose from the N-linked glycosylation of the IgG Fc portion (Nimmerjahn, 2005). In our experiments we also used an afucosylated TNX355 antibody (kindly provided by MedImmune) that was generated in a chinese hamster ovary cell line lacking the gene for the fucosyltransferase *Fut1*.

FACS analysis of peritoneal mast cells showed that both TNX355 and the afucosylated TNX355 variant bind to the hCD4 antigen on the surface of mast cells of C57BL/6 *Cpa3^{hCD4/+}* mice.

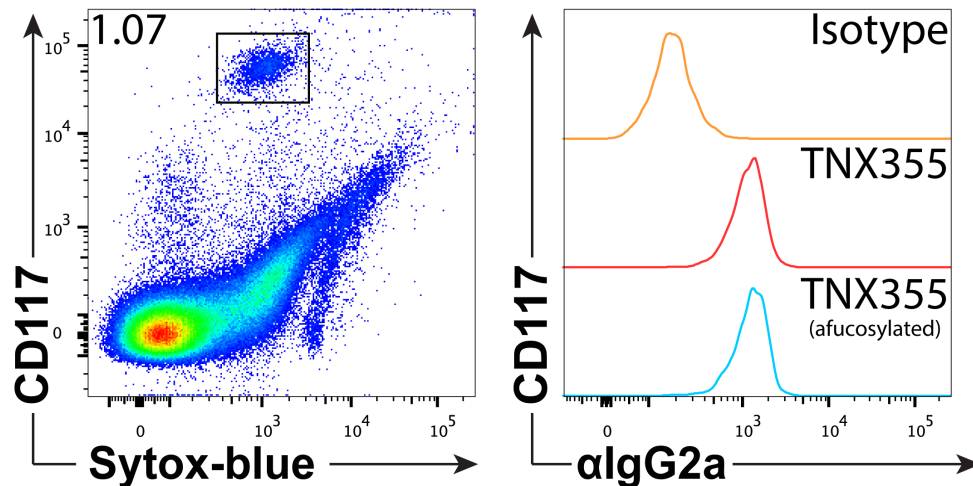


Figure 7: TNX355 binds hCD4 expressing mast cells in *Cpa3^{hCD4/+}* knockin mice
 Peritoneal exudate cells from C57BL/6 *Cpa3^{hCD4/+}* mice were stained with either isotype mouse antibody (IgG2a) or TNX355 or afucosylated TNX355 antibody. Cell surface bound mouse IgG2a antibody was detected by an anti-IgG2a secondary antibody. A representative FACS plot of live mast cells (Sytox-blue⁻ CD117⁺) (**left**) and anti-IgG2a staining is shown (**right**).

3.1.3. In vivo ablation of hCD4⁺ mast cells

Next, I wanted to investigate the in-vivo mast cell ablation capabilities of the TNX355 antibody in the *Cpa3^{hCD4}* mouse model. C57BL/6 *Cpa3^{hCD4/hCD4}* or BALB/c *Cpa3^{hCD4/+}* mice were treated intravenously with one dose of 300 µg TNX355 (Figure 8), 4 doses of 300 µg TNX355 (Figure 9), 3 doses of 900 µg TNX355 (Figure 10), or 3 doses of 900 µg afucosylated TNX355. Mice on C57BL/6 and BALB/c strain backgrounds were used interchangeably, due to availability. In experiments with multiple dosing, injections were performed on alternating days. Seven days after the last injection, mice were sacrificed and mast cell depletion was analysed by flow cytometry.

A single injection of 300 µg of TNX355 antibody resulted in a reduction of peritoneal mast cells to about 50% (Figure 8). However, no reduction could be observed for stomach, skin, fat and tongue tissue mast cells.

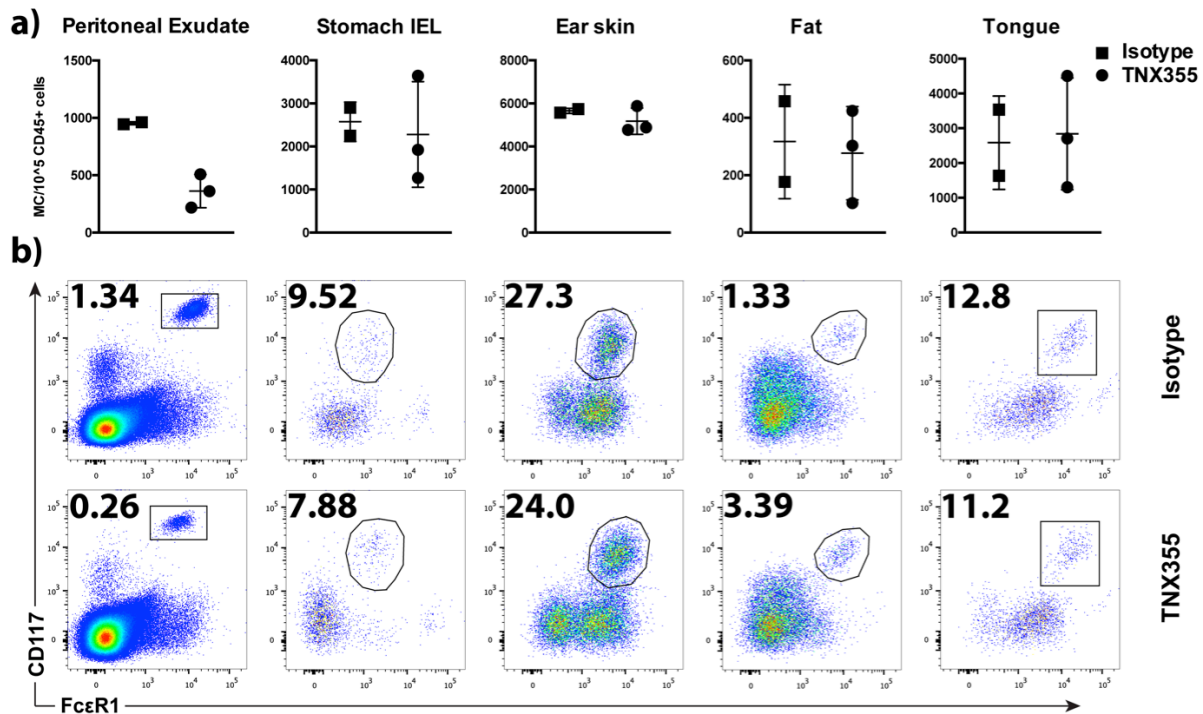


Figure 8: Mast cell depletion with a single dose of TNX355 treatment

C57BL/6 *Cpa3^{hCD4/hCD4}* mice were treated i.v. with 300 μ g of TNX355 or isotype control antibody. Seven days later, mice were sacrificed and organs were isolated for subsequent flow cytometric evaluation of mast cell ablation. **a)** The number of phenotypic mast cells per 10⁵ CD45⁺ cells in different organs is shown. The number of total CD45⁺ cells remained constant for each indicated organ. Mean \pm SEM for two to three animals per treatment group. **b)** Representative FACS plots of the different mast cell compartments. Numbers indicate percentages of mast cells within the live F4/80⁻ CD45⁺ gate.

Scholten and colleagues developed a mouse model of diphtheria toxin-dependent mast cell ablation by crossing their *Mcpt5-Cre* transgenic mouse strain to a floxed iDTR mouse strain. With this inducible model they observed that repetitive dosing of diphtheria toxin enhanced the depletion of mast cells in peripheral tissues (Julia Scholten, 2009). To test whether multiple doses of TNX355 antibody would also enhance ADCC-mediated mast cell ablation, we repetitively injected our mice in the following experiments. First we gave 4 x 300 μ g of TNX355 or isotype control antibody intravenously to BALB/c *Cpa3^{hCD4/+}* mice.

Four injections with a total dose of 1.2 mg of TNX355 antibody resulted in a strong peritoneal mast cell depletion. There was also depletion of stomach mast cells (Figure 9). However, no mast cell ablation could be detected in skin, fat and tongue tissue. In the isotype treated animals a marked influx of CD45⁺ cells into the tongue could be observed. This influx resulted in lower relative mast cell numbers (MC/10⁵

CD45⁺ cells), which accounts for the comparatively increased number of mast cells in tongue tissue (Figure 9a).

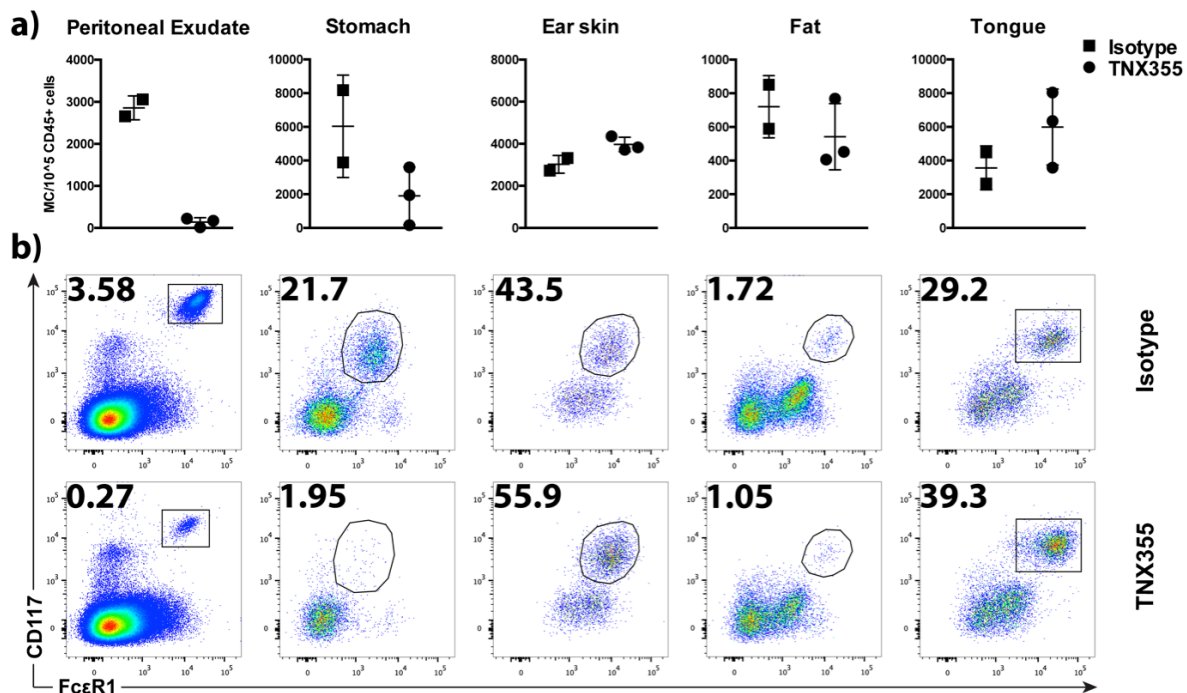


Figure 9: Mast cell depletion with multi-dose TNX355 treatment

BALB/c *Cpa3^{hCD4/+}* mice were treated with a maximum dose of 1.2 mg of TNX355 or isotype control antibody. Seven days after the last injection, mice were sacrificed and organs were isolated for subsequent flow cytometric evaluation of mast cell numbers. **a)** The number of phenotypic mast cells per 10⁵ CD45⁺ cells in different organs is shown. Mean ± SEM for two to three animals per treatment group. **b)** Representative FACS plots of the different mast cell compartments. Numbers indicate percentages of mast cells within the live F4/80⁺ CD45⁺ gate.

An adult C57BL/6 mouse of 25 g has approximately 1.6 ml blood and a haematocrit of 42% (GV-SOLAS). At an average IgG serum concentration of 2-5 mg/ml (Sigma-Aldrich) this translates into a total amount of circulating mouse IgG of 1.9 – 4.6 mg.

To determine the maximal feasible depletion efficacy in our experimental model we injected 3 x 900 µg of TNX355 or isotype control antibody intravenously into C57BL/6 *Cpa3^{hCD4/hCD4}* mice. This dose corresponds to half of the mouse's endogenous IgG.

Three injections with a total dose of 2.7 mg of TNX355 antibody resulted in near complete depletion of peritoneal and stomach mast cells (Figure 10). With this dose we were able to receive a small reduction in fat mast cells however no ablation of skin and tongue mast cells could be observed. As before, a marked influx of CD45⁺ cells into the tongue resulted in skewing of TNX355 treated tongue mast cell quantification (Figure 10a).

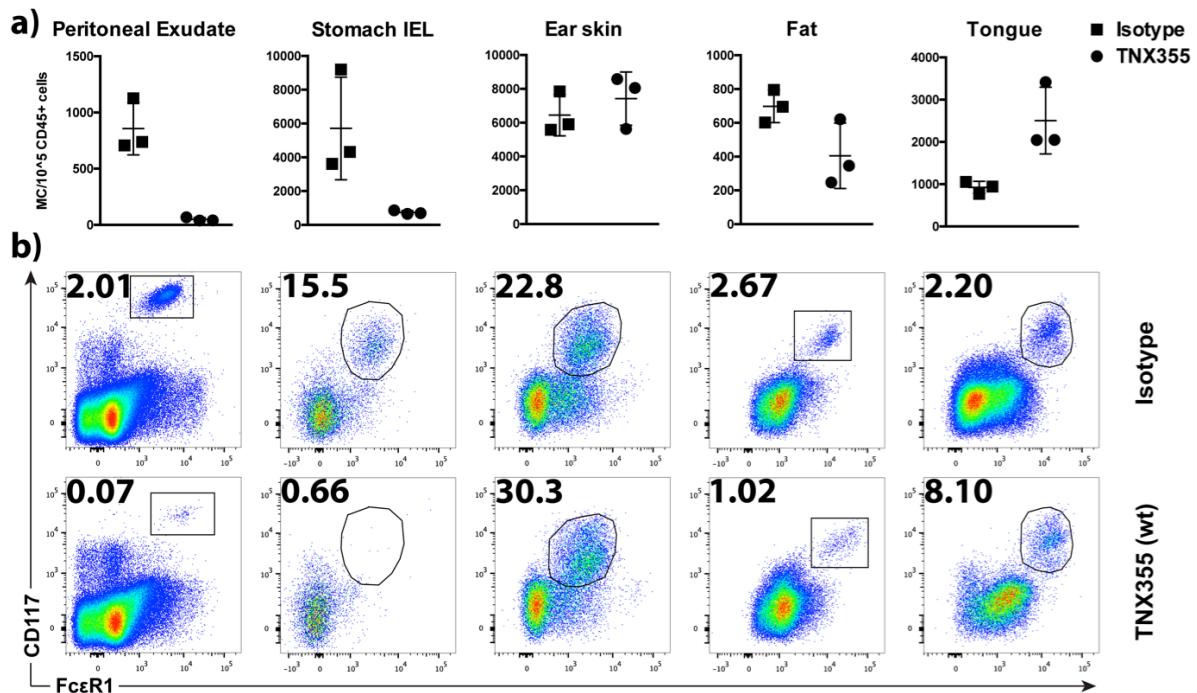


Figure 10: Mast cell depletion with maximal dose escalation

C57BL/6 *Cpa3^{hCD4/hCD4}* mice were treated with a total dose of 2.7 mg of TNX355 or isotype control antibody. 7 days after the last injection mice were sacrificed and organs were isolated for subsequent flow cytometric evaluation of mast cell ablation. **a)** The number of phenotypic mast cells per 10⁵ CD45⁺ cells in different organs is shown. Mean ± SEM for two to three animals per treatment group. **b)** Representative FACS plots of the different mast cell compartments. Numbers indicate percentages of mast cells within the live F4/80⁻ CD45⁺ gate.

To further increase the depletion efficiency without increasing the antibody dose, we investigated the depletion efficiency of the afucosylated TNX355 variant. Afucosylation has been previously shown to enhance ADCC in vivo (Nimmerjahn, 2005). In this experiment we injected 3 x 900 µg of afucosylated TNX355 or isotype control antibody intravenously into C57BL/6 *Cpa3^{hCD4/hCD4}* mice. A total dose of 2.7 mg of afucosylated TNX355 antibody resulted in near complete depletion of peritoneal and stomach mast cells (Figure 11). As in the previous experiments, a small reduction in fat mast cells, but no reduction in skin and tongue mast cells was observed.

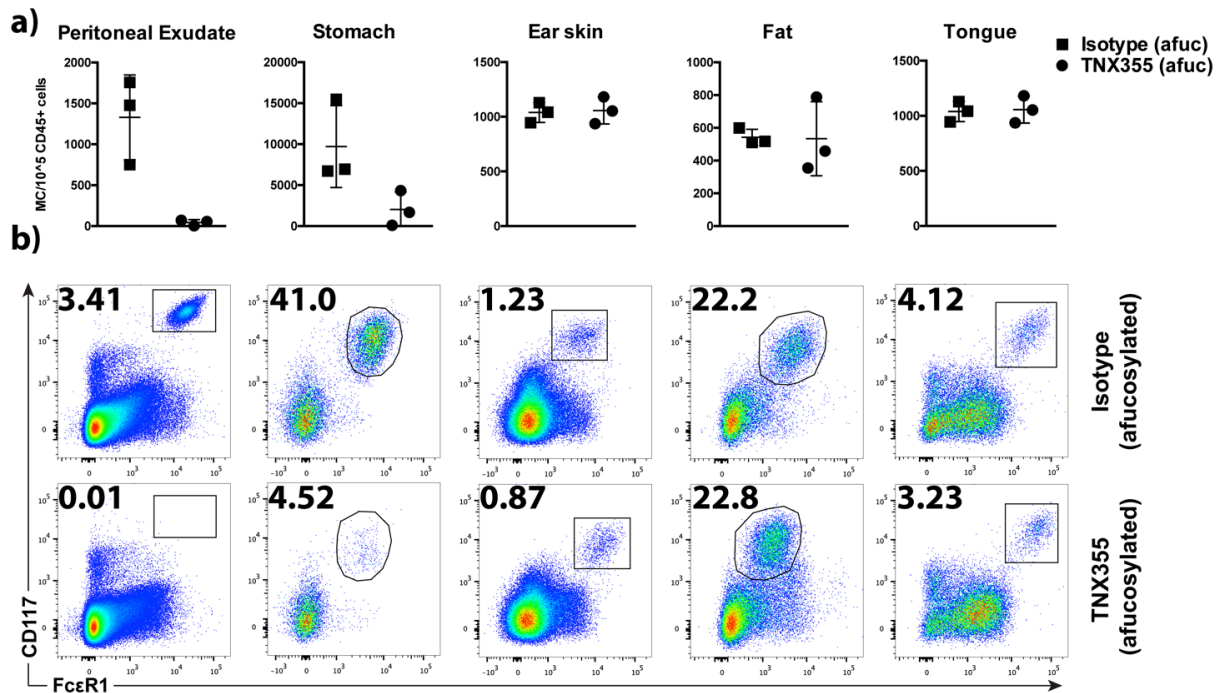


Figure 11: Mast cell depletion by treatment with afucosylated TNX355

C57BL/6 *Cpa3^{hCD4/hCD4}* mice were treated 3x on alternating days i.v. with 900 μ g of afucosylated TNX355 or afucosylated isotype control antibody in 200 μ l of PBS. 7 days after the last injection mice were sacrificed and organs were isolated for subsequent flow cytometric evaluation of mast cell ablation. **a)** The number of phenotypic mast cells per 10⁵ CD45⁺ cells in different organs is shown. Mean \pm SEM for two to three animals per treatment group. **b)** Representative FACS plots of the different mast cell compartments. Numbers indicate percentages of mast cells within the live, F4/80⁺, CD45⁺ gate.

In summary, we demonstrated that mast cells, in principle, can be depleted by an antibody dependent cytotoxicity mechanism. Mast cell ablation was different for individual organs. The degree of mast cell ablation in the *Cpa3^{hCD4}* model was correlated to the injected antibody dose. Mast cells of the peritoneal cavity and the stomach were most sensitive while mast cells from ear skin, fat, and tongue were refractory. In contrast to the literature, we were not able to further increase the ablation efficiency by using a glyco-engineered antibody.

3.1.4. Bio-distribution of TNX355 in vivo

Previously it has been shown that blood vessels form a semi-permeable barrier that, under non-inflammatory conditions, restricts the traffic across the endothelium for molecules larger than 70 kDa (Egawa et al., 2013). For monoclonal antibodies with sizes of \sim 150 kDa the main mechanism of transport from blood to the interstitium was shown to be convection (i.e. diffusion along a concentration gradient). The rate of

mAb convection is determined by the antibody concentration and by degree of endothelial fenestration (Wang et al., 2008).

To test whether insufficient transendothelial passage was responsible for the observed lack of mast cell depletion in the skin, tongue, and fat I labelled TNX355 and isotype control antibody with AlexaFluor-647 (A647). I intravenously injected 100 μ g of either of the two antibodies into C57BL/6 *Cpa3^{hCD4/hCD4}* mice. Mast cells were isolated 48 hours later from the different organs and tested for in situ bound antibody by flow cytometric analysis (Figure 12).

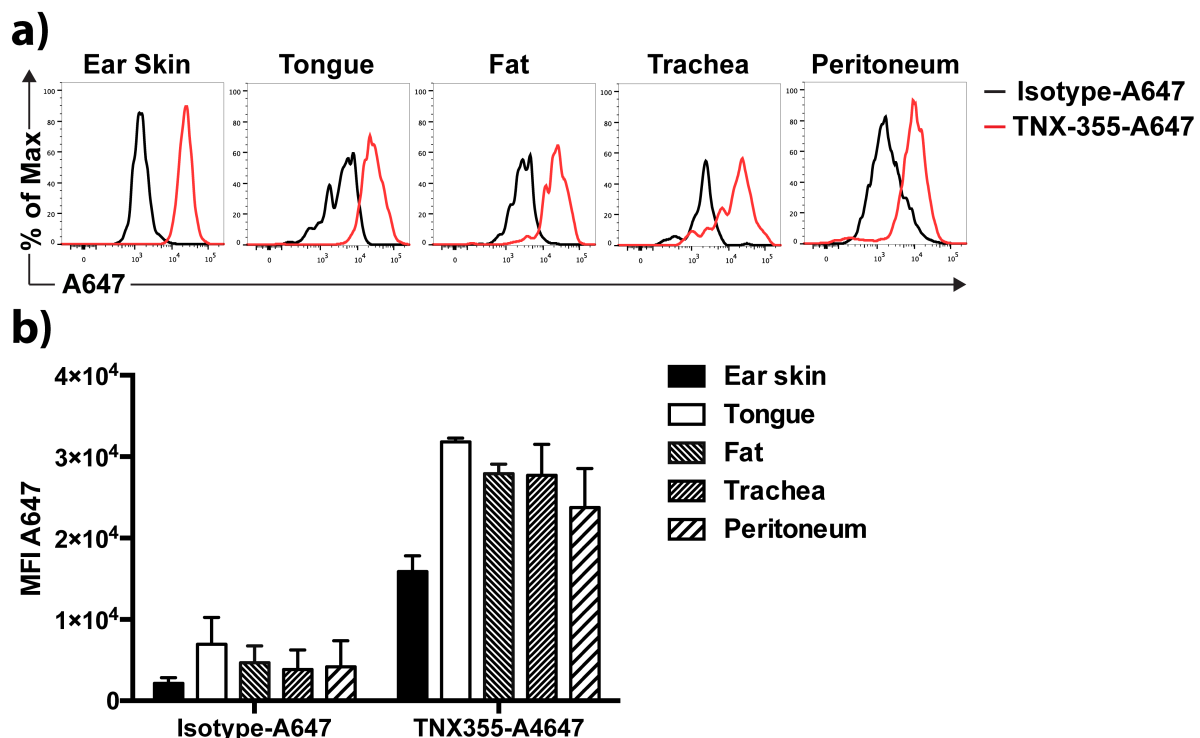


Figure 12: In situ labelling of mast cells by fluorescent coupled TNX355

C57BL/6 *Cpa3^{hCD4/hCD4}* mice were intravenously injected with 100 μ g of A647 labelled TNX355 or isotype control antibody. Mice were sacrificed 48 hours later and organs were isolated for subsequent flow cytometric evaluation of in vivo mast cell labelling. **a)** Histograms are pre-gated for mast cells (live, CD45⁺, F4/80⁻, CD117⁺ FcεRI⁺) and depict prior binding of the antibodies TNX355-A647 (red) or isotype control (black). **b)** The A647 mean fluorescence intensity of the different mast cell compartments is shown. Mean ± SEM for two animals per treatment group.

Interestingly, mast cells in all analysed tissues were labelled by TNX355 to similar extent. There was no difference in antibody binding between tissue mast cells and peritoneal mast cells. Therefore, mechanisms other than TNX355 antibody bioavailability or binding in tissues seem to account for the lack of ADCC-dependent mast cell depletion observed in the skin, tongue and fat tissue.

3.1.5. Passive systemic anaphylaxis assay

In order to test, whether the partial ablation of mast cells, i.e. their ablation in stomach and peritoneal cavity, already translates into a physiologically measurable phenotype, TNX355 treated mice were subjected to IgE-mediated anaphylaxis. The principle of this assay is to first passively load and sensitize mast cells with antigen-specific IgE, and then to induce mast cell degranulation via crosslinking of the FcεRI-bound IgE by injecting multivalent antigen. Subsequent release of bioactive amines, such as histamine and serotonin induces vascular permeabilization and smooth muscle contraction. Since both IgE and antigen are supplied systemically, mast cells throughout the body may respond, leading to systemic anaphylaxis. Subsequently, dramatic pathological reactions occur, e.g. the blood pressure, after a short transient raise, drops dramatically and hypothermia sets in. We used this decline of the body temperature to monitor anaphylaxis via mast cell activation.

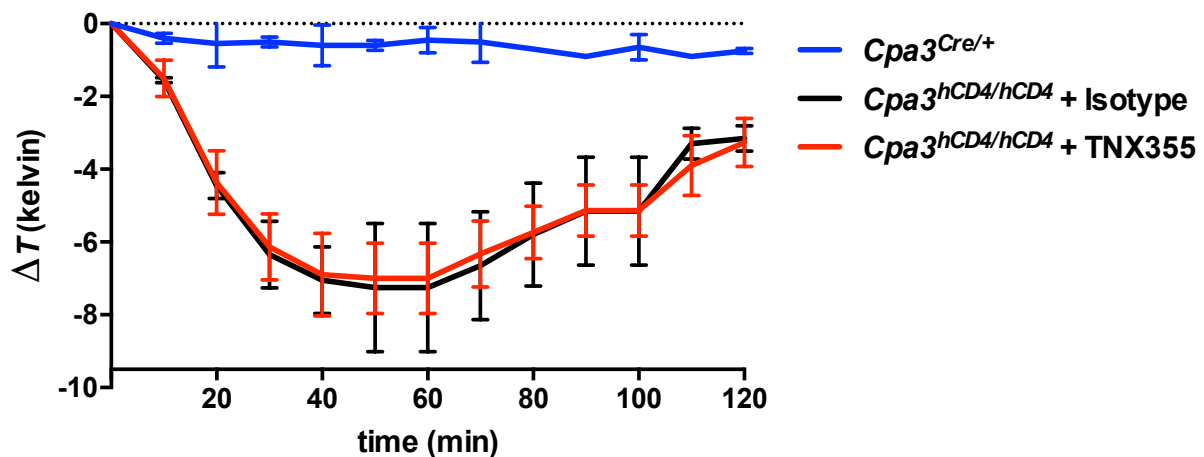


Figure 13: Passive systemic anaphylaxis in mast cell-depleted mice

C57BL/6 *Cpa3^{hCD4/hCD4}* mice that received 2.7mg of afucosylated TNX355 for mast cell depletion or that were injected with isotype antibody were subjected to passive systemic anaphylaxis. Genetically mast cell-deficient *Cpa3^{Cre/+}* mice were used as a positive control for the absence of mast cells. All mice were injected i.v. with 20 μ g anti-DNP IgE and challenged on the subsequent day by i.v. injection of 20 μ g DNP₁₅-Ovalbumin. The anaphylactic response was monitored by determining the change of body temperature. Rectal temperatures were measured in 10 min intervals and are expressed as temperature difference (ΔT) compared to baseline temperature. The mean \pm SEM for two to four animals per treatment group is shown.

As expected, strong hypothermia was observed in mice that were not mast cell depleted, but had received the isotype control antibody. Genetically mast cell-deficient *Cpa3^{Cre/+}* mice did not show any change in body temperature, thus were resistant to anaphylaxis (Feyerabend et al., 2011). However, mice that had received the TNX355 treatment displayed the same temperature drop seen in control depleted

and *Cpa3^{hCD4/hCD4}* mice. Hence, ablation of peritoneal and stomach mast cells is not sufficient to prevent anaphylaxis induced hypothermia.

3.2. Mast cell proteomics

To our knowledge there is currently no comprehensive mass-spectrometric (MS) dataset of primary mouse or human mast cells available. Such experiments however, would be very useful for the identification of key pathways and novel functions of mast cells, and the identification of novel mast cell-specific drug targets. Due to the very low abundance of mast cells in tissues, isolating large quantities of cells normally required for mass-spectrometry is difficult, and therefore most researchers instead focused on mRNA-expression analysis. However, for a functional analysis of mast cells the determination of protein expression on a global scale would be more meaningful.

The isolation of primary mouse mast cells is well established in our laboratory, and by using peritoneal cells as a source the need for enzymatic tissue digestion for mast cell isolation can be avoided. For these reasons, murine peritoneal mast cells are ideal starting material for the establishment of protein extraction and sample preparation for subsequent quantitative mass spectrometry.

3.2.1. Mouse peritoneal mast cell proteomics

Different strategies have been successfully employed to identify cell surface receptors of a variety of cells. To investigate the membrane proteome, and thereby cell surface receptors, researchers have relied on two main strategies. Traditionally, density gradient separation was used to separate the membrane fraction from the organelle and nuclear proteins. In the recent years, biotin or lectin labelling approaches have been successfully developed to label and capture cell surface proteins (Elia, 2008; Elschenbroich et al., 2010; Vuckovic et al., 2013). However, all of these biochemical approaches demand extremely large cell numbers, which is compatible with immortalized cell lines but often impossible with primary cells. Because numbers of primary mast cells remains limiting, we opted for whole proteome analysis without prior enrichment for membrane proteins.

As we are primarily interested in mast cell specific cell surface proteins, the isolation of mast cells from the peritoneal lavage, obtained without enzymatic tissue digestion

is advantageous. In this way, the extracellular domains of cell surface proteins are protected from cleavage by digestion enzymes.

The peritoneal lavage of C57BL/6 wild type mice contains about 2-4 mio. cells of which approximately 1-3% are mast cells. With positive magnetic bead selection for CD117⁺ cells, mast cells could be enrichment to 40 - 60 %. For purity of more than 96% cells were sorted on a BD FACSAria cell sorter (Figure 14). In our hands, approximately 5000-10000 peritoneal mast cells could be isolated from a single 6-8 week old C57BL/6 wild type mouse.

Apart from C57BL/6 wild type peritoneal cells and sorted mast cells we chose to include peritoneal cells from C57BL/6 *Cpa3*^{Cre/+} mice that are genetically mast cell-deficient and thus serve as an optimal negative control.

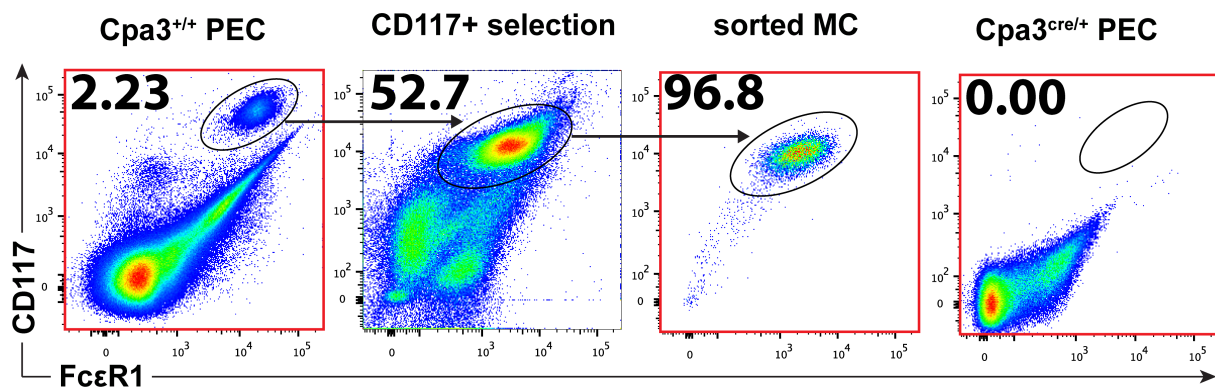


Figure 14: Isolation, enrichment and purification of mast cells for proteome analysis

Peritoneal cells of C57BL/6 *Cpa3*^{+/+} and C57BL/6 *Cpa3*^{Cre/+} mice were isolated by peritoneal lavage. Mast cells of C57BL/6 *Cpa3*^{+/+} were enriched by two-step purification. First, CD117⁺ cells were selected by magnetic beads and subsequently phenotypic mast cells (live, CD45⁺, F4/80⁻, CD117⁺ FcεR1⁺) were sorted on a BD FACSAria cell sorter. Representative FACS plots of the consecutive mast cell enrichment steps are shown. Samples used for proteomics are highlighted in red. Numbers indicate percentages of cells in each quadrant.

In collaboration with Mandy Rettel at the EMBL proteomics core facility we subjected three different cell populations (Figure 14) to quantitative mass spectrometry (MS). We chose total *Cpa3*^{+/+} peritoneal cells (including 1-3% mast cells), sorted mast cells (purities higher than 96%), and total *Cpa3*^{Cre/+} peritoneal cells (lacking mast cells). The three cell populations were digested with trypsin and then labelled with different, stable dimethyl isotopes. For each MS run, tryptic peptides from 50.000 cells of each population were mixed in a 1:1:1 ratio and run on a high pH HPLC. Subsequently, the collected fractions were analysed by low pH HPLC-coupled MS/MS. Because three

differentially labelled populations were analysed in parallel, the peptide intensities can be relatively quantified.

In collaboration with Dr. Bernd Fischer, from the computational genome biology group at Dkfz, we performed detailed bioinformatics analysis on the proteomic dataset. From the raw data, a total of 45396 peptides were identified. The peptides were then mapped to proteins in the uniprot database. Due to repetitive protein motives and sequence similarities, some peptides mapped to multiple proteins or splice variants. In order to quantify such peptides, protein groups were created to determine the coverage of a certain protein. Proteins were then mapped to genes in the Ensembl database. For each gene the highest-covered corresponding protein was chosen.

Some peptides could not be mapped to a unique protein group (non-unique protein group). Some peptides that mapped to a protein in the uniprot database could not be mapped because of missing entries in the Ensembl database (no gene). Some peptides mapped to a single protein and gene, however the peptide did not belong to the highest-covered protein (Not on largest group). Peptides that could not be mapped were excluded from further analysis. The unique peptides cover 5459 different genes (Figure 15).

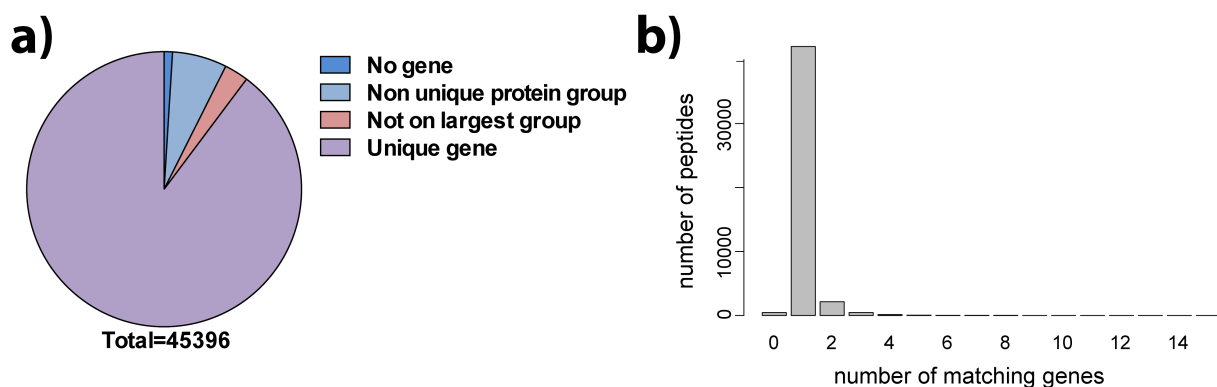


Figure 15: Mouse mast cell proteomics and peptide mapping

a) 45396 peptides were identified in three independent biological replicates (BR1-3). Peptides were mapped to the Uniprot protein database. 444 Proteins mapped to no gene. 2915 peptides mapped to non-unique protein group and 1289 peptides did not map to their highest-covered proteins. The remaining 40748 peptides were mapped to their corresponding genes.

b) The histogram depicts the uniqueness of the peptide mapping. The x-axis shows the number of genes a peptide maps to. The y-axis shows the number of peptides that map to as many genes.

The number of measured peptides and the number of identified proteins is within the range of a typical proteomics experiment. The correlation among the biological replicates exceeds 0.6 for all replicates, indicating a high quality of the dataset.

	Low 1% FDR	Low 10% FDR	unchanged	High 10% FDR	High 1% FDR
MC / <i>Cpa3</i> ^{Cre/+}	46	485	2717	408	98
MC / <i>Cpa3</i> ^{+/+}	32	419	2807	385	90

Table 2: Number of proteins differentially expressed in mouse mast cells compared to peritoneal exudate cells

Listed is the number of proteins being at least 2-fold higher (red) or lower (blue) expressed in mast cells compared to total peritoneal exudate cells with false discovery rate (FDR) of 1% or 10%. FDR is a statistical tool used for the analysis of large datasets to correct error from multiple testing. 1%/10% FDR introduces a threshold for normally distributed p-values in which either 99% or 90% of results are predicted to be correct (Benjamini and Hochberg, 1995).

The majority of proteins quantified in this proteomics screen (72%/75%) were unchanged in the comparison of sorted mast cells / *Cpa3*^{Cre/+} PEC as well as in the sorted mast cells / *Cpa3*^{+/+} PEC comparison. The number of proteins that are less expressed in mast cells is slightly higher than the proteins that are higher expressed.

Next, we looked closer at the data with the help of a volcano plot to display large magnitude changes (Figure 16).

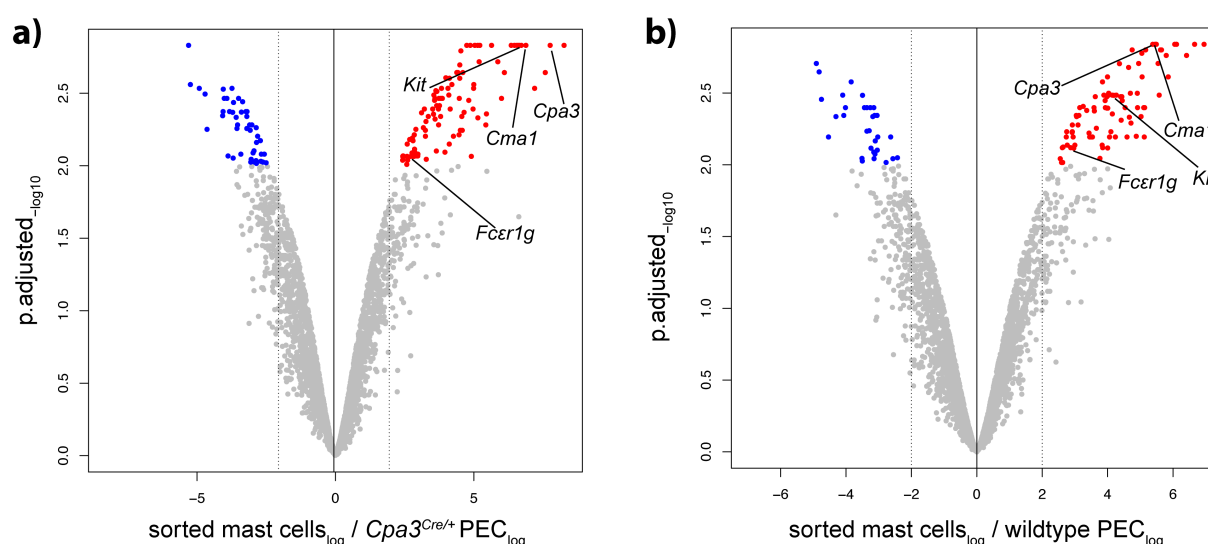


Figure 16: Depiction of differential protein expression of mouse mast cells versus peritoneal cells

Volcano plots presenting differential protein expression of sorted mast cells **a)** compared to *Cpa3*^{Cre/+} PEC and **b)** compared to wild type PEC (x-axis) and its respective significances (y-axis). Proteins with 2-fold expression change (employing 1% FDR) are either coloured in red (highly expressed) or blue (low expressed).

Typical mast cell markers identified with this screen are marked by arrows and indicated with their names.

The well-established mast cell markers Carboxypeptidase A3 (*Cpa3*), Chymase 1 (*Cma1*), and stem cell factor receptor Kit (*Kit*) were found among the proteins that were most strongly expressed in mast cells, which measures the validity of the dataset to identify mast cell specific proteins.

Previous studies have shown strong differences in mast cell related mRNA expression, when comparing whole tissue RNA preparations (skin) of mast cell sufficient *Cpa3*^{+/+} and mast cell deficient *Cpa3*^{Cre/+} mice (Feyerabend et al., 2011). However, the proteomic comparison of whole PEC of *Cpa3*^{+/+} and *Cpa3*^{Cre/+} mice in our experiment is not informative as the comparison shows minimal difference in mast cell specific protein expression. It is probable that this discrepancy results from the limit of detection in mass spectrometry experiments.

We therefore focussed our further analysis on the sorted MC vs. PEC comparisons. In that regard it appears that the MC / *Cpa3*^{Cre/+} comparison is more sensitive than the MC / *Cpa3*^{+/+} comparison in detecting mast cell specific proteins as there are more proteins detected (Table 2). For that reason, we are focussing on the comparison of sorted mast cells vs. *Cpa3*^{Cre/+} PEC for our subsequent analysis.

Having shown that the mast cell proteome dataset is valid to identify mast cell specific proteins, we sought to determine whether the dataset could also be used to identify mast cell specific functional pathways.

3.2.2. Gene ontology analysis of the mouse mast cell proteome

Gene ontology analysis enables the functional interpretation of experimental data by classification of genes into defined categories. Here, we performed gene ontology enrichment analysis to gain information about mast cell enriched processes and functions (Figure 17).

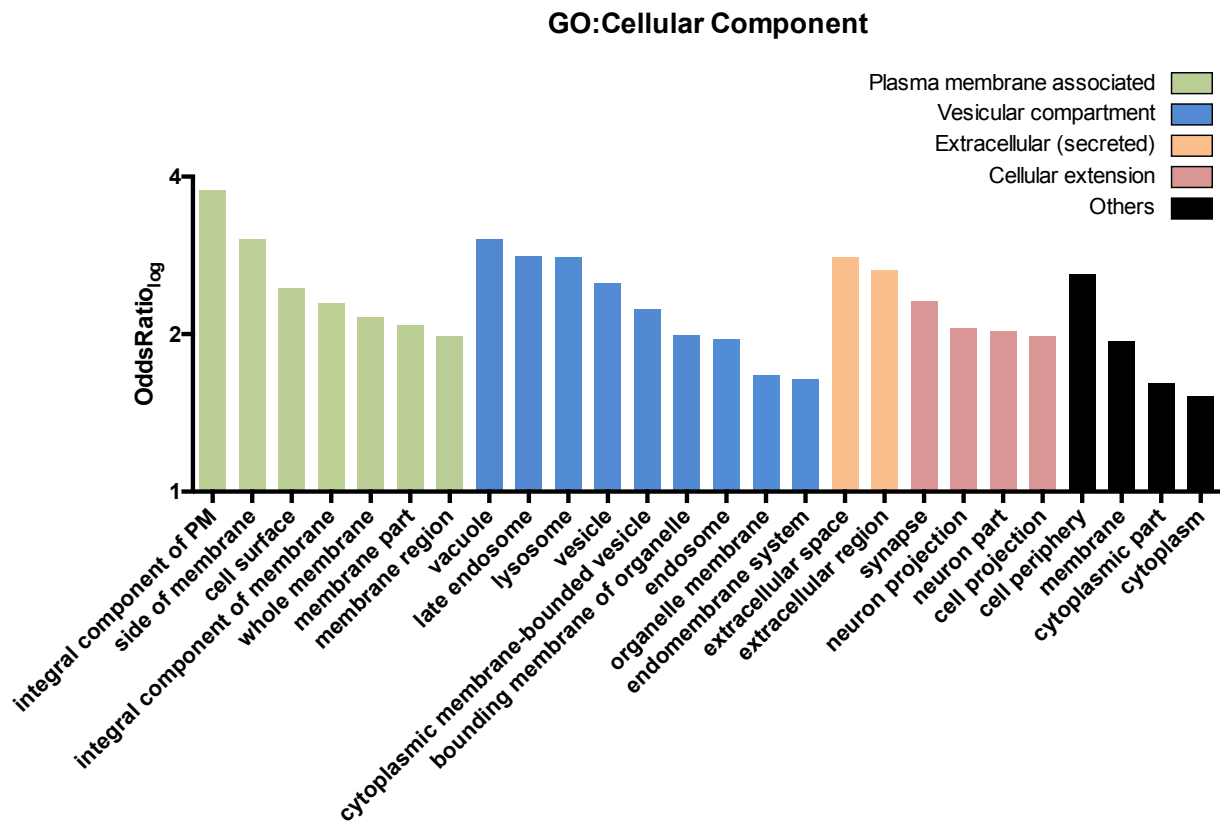


Figure 17: Proteome analysis based on mouse Gene Ontology (GO) analysis for the term ‘Cellular Component’

Shown are Gene Ontology terms for the category ‘Cellular Component’ based on mast cell enriched proteins depicted as OddsRatio in log scale.

The mast cell enriched GO terms in the category ‘Cellular Component’ can be divided into 5 groups. Plasma membrane associated (trans membrane, cell surface and membrane associated proteins); Vesicular compartment (vacuolar, lysosomal and granular proteins); Extracellular (secreted proteins); Cellular extension (synaptic, and membrane projection proteins); and Others.

The GO analysis of ‘Cellular Component’ reveals that the group Vesicular compartment is the biggest group represented, indicating that many vesicular proteins, likely also mast cell granule proteins, are enriched in this dataset.

Next, we were interested whether we can conclude unique mast cell functions based on the GO analysis of the term ‘Biological Process’ (Figure 18).

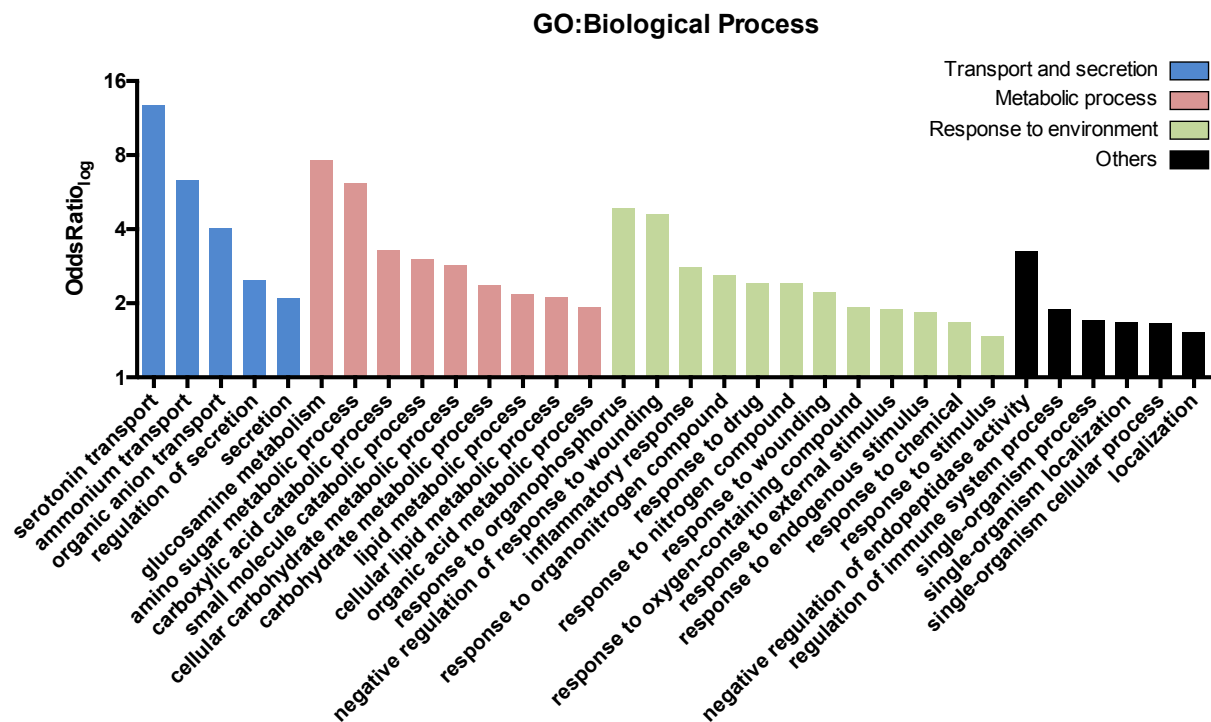


Figure 18: Proteome analysis based on mouse GO analysis for the term ‘Biological Process’

Shown are Gene-Ontology terms for the category ‘Biological Process’ based on mast cell enriched proteins depicted as OddsRatio (log scale).

The mast cell enriched GO terms in the category ‘Biological Process’ can be subdivided into 4 groups: transport and secretion; metabolic process; response to environment; and others. Interestingly, the two most prominent features that are highly enriched in this analysis are serotonin transport and glucosamine metabolism, both of which are known integral functions of mast cells. This analysis underscores the uniqueness of mast cells among hematopoietic cells to synthesize bioactive amines and proteoglycans.

3.2.3. The most abundant proteins of murine mast cells

In order to identify novel characteristic / unique mast cell marker proteins, proteomics data were listed by fold change and their p-values that were optimized for multiple testing (p.adjusted). All three populations were measured in parallel, thus the fold change describes the abundance of a certain protein in a sample over the abundance of the same protein in a second sample.

Below, I depict in detail the top 20 differentially expressed proteins with significant fold change in sorted mast cells over *Cpa3^{Cre/+}* PEC.

ProtID	Symbol	Protein name	log2FC	pvalue	padjusted	rep1	rep2	rep3
Q91XV3	Basp1	Brain acid soluble protein 1	8.260	1.37E-06	0.00148	8.387	9.110	7.282
P15089	Cpa3	Carboxypeptidase A3	7.756	3.37E-06	0.00148	8.065	8.663	6.541
P21812	Mcpt4	Mast cell protease 4	6.881	1.84E-06	0.00148	7.371	7.117	6.154
Q8CB87	Rab44	Ras-related protein Rab-44	6.717	3.43E-06	0.00148	6.338	7.648	6.165
Q8BW75	Maob	Monoamine oxidase type B	6.635	2.39E-06	0.00148	5.892	6.869	7.143
P21845	Tpsb2	Tryptase beta-2 (mMCP6)	6.619	9.38E-07	0.00148	6.708	6.771	6.377
P28293	Ctsg	Cathepsin-G	6.559	4.89E-06	0.00148	5.745	6.436	7.496
P41731	CD63	Tetraspanin	6.469	5.52E-06	0.00148	7.349	5.558	6.499
Q60963	Pla2g7	Platelet-activating factor acetylhydrolase	6.351	4.15E-06	0.00148	6.634	6.928	5.489
P14719	Il1rl1	IL-33 receptor	5.641	4.51E-06	0.00148	5.377	6.250	5.296
P70665	Siae	Sialate O-acetyltransferase	5.216	6.39E-06	0.00148	5.592	5.381	4.675
P07309	Ttr	Transthyretin	5.140	4.34E-06	0.00148	5.246	5.287	4.885
Q08642	Padi2	Protein-arginine deiminase type-2	5.038	5.80E-06	0.00148	5.066	5.356	4.693
Q9JIM1	Slc29a1	Equilibrative nucleoside transporter 1	5.033	6.78E-06	0.00148	4.745	4.852	5.503
Q9Z127	Slc7a5	Large neutral amino acids transporter small subunit 1	4.873	5.64E-06	0.00148	4.908	5.023	4.687
Q3UW53	Fam129a	Protein Niban	4.744	6.99E-06	0.00148	4.986	4.689	4.556
P51576	P2rx1	P2X purinoceptor 1	4.532	8.08E-06	0.00162	4.492	4.493	4.612
Q80UR4	Prss34	Mast cell protease-11	5.867	1.07E-05	0.00193	5.802	6.819	4.978
Q99M71	Epdrl	Mammalian ependymin-related protein 1	5.191	1.03E-05	0.00193	5.835	5.216	4.522
P29387	Gnb4	Guanine nucleotide-binding protein subunit beta-4	4.493	1.18E-05	0.00203	4.863	4.172	4.444

Table 3: Top 20 proteins (sorted mast cell vs. *Cpa3*^{Cre/+} PEC)

Shown are the top 20 protein expression values of sorted mast cells / *Cpa3*^{Cre/+} PEC. Log2FC is the fold change depicted as log 2; pvalue depicts the significance calculated by t-test; P.adjusted is the p-value corrected for multiple testing with a FDR of 0.05; rep stands for biological replicates.

Five of the 20 proteins most strongly expressed in mast cells are known mast cell proteases (*Cpa3*, *Mcpt4*, *Tpsb2*, *Ctsg* and *Prss34*). The top scored protein is brain acid soluble protein 1 (*Basp1*), which has not been described in mast cells before. *Basp1* is mainly known to contribute to arborisation in neurons and work from a single paper links *Basp1* expression to synapse formation in hematopoietic cells (Goodfellow et al., 2011). Mast cells have also been described to form degranulatory synapses with IgE opsonized target cells, which might be dependent on *Basp1* (Jouliia et al., 2015).

Second on the list of the top 20 mast cell proteins is the enzyme *Padi2* (protein-arginine deiminase type 2) that mediates the hydrolysis of arginine residues to citrulline. It has previously been shown that bone marrow derived mast cells express *Padi2*, which becomes activated after Purinoreceptor (*P2x7r*) ligation by extracellular ATP. *Padi2* and citrullinated proteins are implicated in mouse models of collagen induced arthritis, however mast cells could not clearly be linked as the source (Arandjelovic et al., 2012). To our knowledge this is the first description of *Padi2* to be highly expressed in primary mouse mast cells.

Apart from the mentioned proteins, we find several proteins related to known mast cell function among the top 20 such as *Maob* (metabolism of bioactive amines) and *Pla2g7* (PAF signalling).

With our proteomics screen we aimed to identify novel mast cell specific cell surface receptors that might be used as targets in an antibody-based ablation model. Therefore, the list of mast cell-enriched proteins was filtered for cell surface receptors. We found that automated bioinformatics-assisted annotation of cell surface expression was unreliable, most likely due to incomplete or erroneous annotation in online databases. Therefore, we sourced uniprot annotations and in conflicting cases conducted a literature search to manually annotate cell surface proteins (Table 4).

ProtID	Symbol	Protein name	log2FC	pvalue	padj.	rep1	rep2	rep3
P41731	CD63	Tetraspanin 30	6.469	5.52E-06	0.00148	7.349	5.558	6.499
P14719	Il1rl1	IL-33 receptor	5.641	4.51E-06	0.00148	5.377	6.250	5.296
P51576	P2rx1	P2X purinoceptor 1	4.532	8.08E-06	0.00162	4.492	4.493	4.612
Q60857	Slc6a4	Sodium-dependent serotonin transporter	6.104	1.60E-05	0.00229	4.875	7.123	6.313
P05532	CD117	Stem cell factor receptor	4.385	1.50E-05	0.00229	4.783	3.985	4.387
P97449	CD13	Aminopeptidase N	4.066	3.02E-05	0.00294	4.634	3.636	3.926
P10852	CD98hc	4F2 cell-surface antigen heavy chain	3.556	3.99E-05	0.00327	3.291	3.588	3.790
P13595	CD56	Ncam1	4.475	5.00E-05	0.00345	3.582	5.393	4.450
P15702	CD43	Leukosialin	3.811	4.49E-05	0.00345	3.209	4.130	4.093
P40237	CD82	CD82 antigen	3.271	1.14E-04	0.00498	2.939	3.899	2.976
P03958	Ada	Adenosine deaminase	3.727	1.27E-04	0.00525	4.401	2.755	4.026
Q5UKY4	CD200r3	Cell surface glycoprotein OX2 receptor 3	4.582	1.55E-04	0.00573	4.282		4.882
Q9D3P8	Plgrkt	Plasminogen receptor (KT)	4.467	1.69E-04	0.00615	5.320	2.932	5.148
Q08481	CD31	Platelet endothelial cell adhesion molecule	4.263	1.79E-04	0.00629	4.243	4.283	
P35762	CD81	Tetraspanin	2.683	1.93E-04	0.00662	2.644	2.488	2.917
P53986	Slc16a1	Monocarboxylate transporter 1	2.594	2.17E-04	0.00712	2.578	2.747	2.457
Q9QXW9	Slc7a8	Large neutral amino acids transporter small subunit 2	3.956	2.58E-04	0.00810		3.941	3.971
Q60870	Reep5	Receptor expression-enhancing protein 5	2.767	2.64E-04	0.00820	3.294	2.310	2.696
Q9Z1M0	P2rx7	P2X purinoceptor 7	2.830	3.06E-04	0.00866	2.165	3.370	2.956

Table 4: Top 20 mouse mast cell specific cell surface proteins

Shown are the cell surface protein expression values of sorted mast cells / *Cpa3*^{Cre/+} PEC. Only proteins with a p.adjusted > 0.01 are listed.

The top 20 mast cell-enriched cell surface proteins contain not only the previously mentioned typical mast cell markers *Il1rl1* and *Kit* (CD117) but also several novel mast cell specific markers. CD117, the most important growth factor receptor for mast cells, binds its ligand, SCF, to promote maturation, survival and activation (Kawakami, 2006). Interleukin-1 receptor-like 1 (*Il1rl1*) binds the alarmin IL-33, which is released after cellular injury e.g. from epithelia (Martin and Martin, 2016). In mast cells, IL-33 has been shown to induce leukotriene/prostaglandin synthesis and cytokine release (IL-6, IL-13, TNF and others), however, there appears to be

differences in the response to IL-33 depending on the mast cells' origin and species (Lunderius-Andersson et al., 2012).

The enriched surface proteins can be divided into functionally distinct groups. Adhesion molecules constitute the largest group. Among these are CD43, CD34, CD56 (Ncam1) and CD31 (Pecam1). Some of these proteins have been described to play a role in mast cell development (CD34) but the physiological role of others has been less well described (Gurish and Austen, 2012).

The group of solute carriers is the second largest group represented. Slc6a1, Slc16a1 and Slc7a8 (which associates with CD98) facilitate the transport of a wide array of substrates across the plasma membrane. Solute carriers play important roles in physiological processes such as nutrient, drug and xenobiotic uptake for downstream metabolism (Lin et al., 2015). So far, roles of these channel proteins in murine mast cells have not been described.

Another prominent group of surface proteins enriched in peritoneal mast cells are structural components associated with transmembrane signaling receptors. CD63, CD81 and CD82 are representatives of the tetraspanin family. Those molecules cluster together with transmembrane receptors and signalling coreceptors to form tetraspanin-enriched micro domains (TEM), thereby assisting in signal transmission across the plasma membrane (Köberle et al., 2012; Levy and Shoham, 2005). CD63 associates with Fc ϵ RI within TEMs and is required for efficient mast degranulation (Pols and Klumperman, 2009). CD13 (Aminopeptidase N) has only very recently been described to functionally interact with Fc ϵ RI and thereby to positively enhance degranulation (Zotz et al., 2016).

Another small group of proteins is functionally associated with ATP metabolism. Ada is a membrane bound deaminase that hydrolyses adenosine to inosine, and thereby limits extracellular ATP signalling (inferred from Uniprot). P2 purinoreceptors bind extracellular ATP or ADP and become activated to channel ions and larger metabolites across the membrane (Wareham et al., 2009). With our proteomics screen we could identify P2rx1, P2rx4 and P2rx7 of which only P2rx7 shows strong enrichment in mast cells. P2rx7 is of special interest as it has been shown to mediate mast cell-dependent colon inflammation (Kurashima et al., 2012). P2rx7 also activates the previously mentioned *Padi2* enzyme that most likely plays a role in arthritis development.

3.2.4. Verification of the most enriched mouse mast cell markers

Having identified a variety of differentially expressed cell surface proteins in the proteomics dataset of peritoneal mast cells, we wanted to verify their specific surface expression by antibody staining. For several of the listed proteins (Table 4) commercial monoclonal antibodies are available. We tested by flow cytometry the expression of Il-1r1, CD63, CD13 and CD98 on the different cell populations listed below. Antibodies against CD117 served as mast cell specific positive control (Fig. 19). Briefly, peritoneal mast cells (F4/80⁻ CD45⁺ CD117⁺ IgE⁺), macrophages (CD3⁻ CD19⁻ F4/80⁺), B cells (CD3⁻ CD19⁺), and T cells (CD19⁻ CD3⁺) as well as splenic basophils (CD45⁺ CD49b⁺ IgE⁺), eosinophils (CD45⁺ SSC^{hi} Siglec-F⁺), neutrophils (CD45⁺ Gr-1⁺), B cells (CD45⁺ CD3⁻ CD19⁺), and T cells (CD45⁺ CD3⁺) of C57BL/6 mice were stained with monoclonal antibodies, or isotype controls.

We calculated the staining index by subtracting the mean fluorescence intensity of the isotype control staining from its corresponding marker antibody staining, and divided the result by twice the robust standard deviation of the isotype control. The staining index has previously been shown to be a reliable method to normalize flow cytometry data across experiments (Maecker et al., 2004).

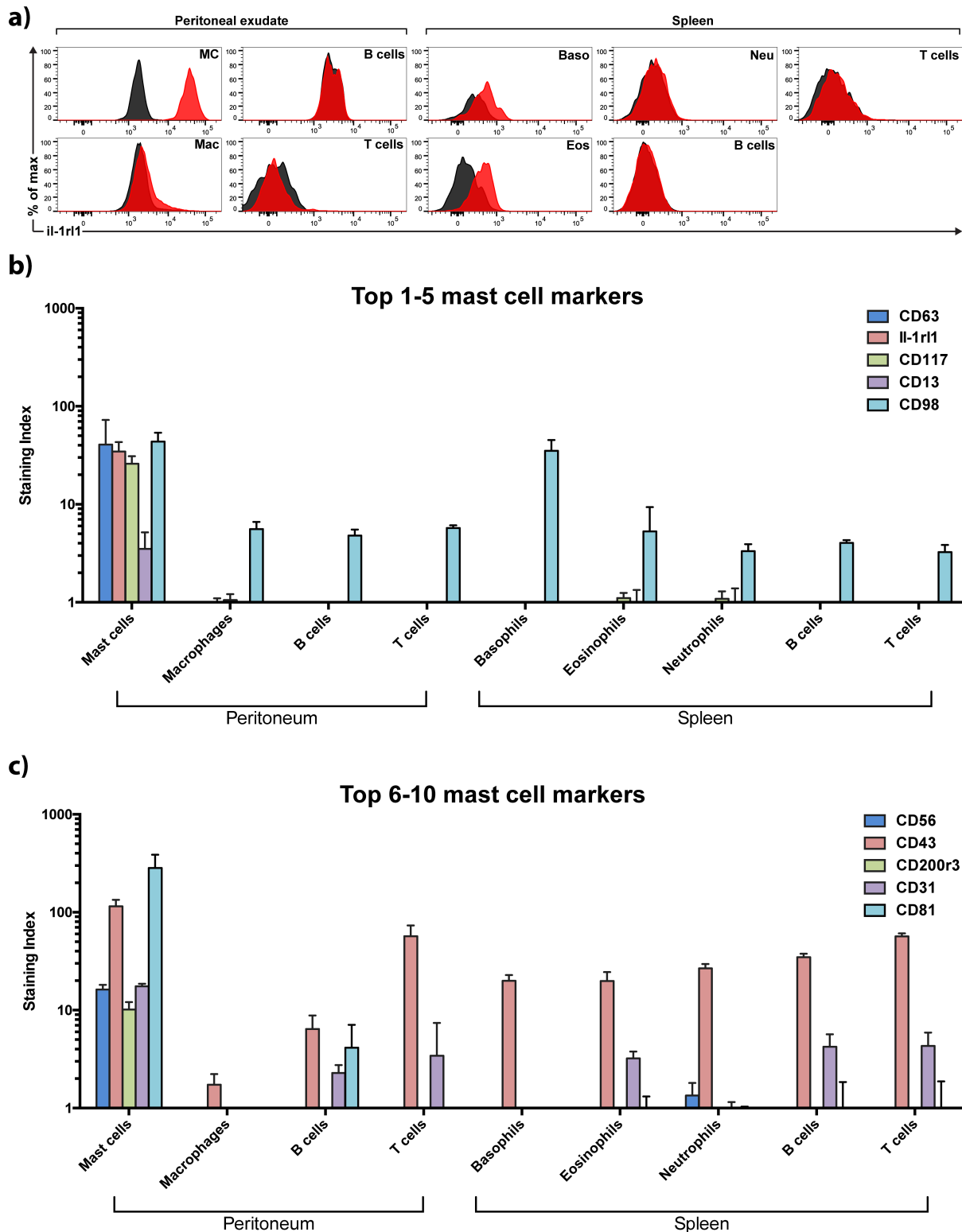


Figure 19: Flow cytometry of the 10 most enriched mast cell receptors

a) il-1r1 antibody staining of peritoneal mast cells, macrophages, B cells, and T cells as well as splenic basophils, eosinophils, neutrophils, B cells, and T cells of C57BL/6 mice analysed by flow cytometry. Shown are representative histogram plots of isotype (black) and il-1r1 antibody (red). **b,c)** Populations from (a) were tested for immunoreactivity against the mast cell enriched antigens il-1r1, CD63, CD117, CD13, CD98 (b) or CD56, CD43, CD200r3, CD31 and CD81 (c) by flow cytometry. Shown is the mean of the staining index \pm SEM of three animals per group.

When staining with specific antibodies, the antigens il-1r1, CD63, CD117, CD13, CD98, CD56, CD43, CD200r3, CD31 and CD81 were found to stain positive on peritoneal mast cells, thereby confirming the results obtained from the mass spectrometry based screening. While Il-1r1 does not stain macrophages, B- and T cells from the peritoneal cavity, low staining intensity could be observed on basophils and eosinophils, which are also important cells in type 2 immune responses.

CD63, CD117, CD13, CD200R3 and CD81 exhibited remarkable mast cell specificity, as negligible staining intensity could be detected on either hematopoietic cell type tested. While il-1r1, CD63, CD117 and CD98 all exhibited a very high staining index of 20-40 on mast cells, CD13 staining was considerably lower, which might reflect low protein abundance or weak antibody affinity.

CD98, CD43 and CD31 could also be detected on all other hematopoietic cell types tested albeit to a lower extent. Basophils exhibited the strongest staining for CD98, which was nearly identical to staining of mast cells. For the other hematopoietic subsets the staining intensity was approximately 10fold lower compared to mast cells.

Apart from the top 10 presented here this experiment was also performed for the mast cell-enriched markers: FcεRI, CD147, CD317, CD34, CD49b, CD171, CD107a, P2rx7, and β7-integrin (Supplement 2).

These results underscore the power and reliability of proteomics-assisted biomarker discovery, as all of the top markers tested could be indeed verified on the surface on mast cells by independent flow cytometric analysis.

3.2.5. Human mast cell proteomics

For the specific characterization of human mast cells we performed an analogous proteomic analysis as previously established for murine mast cell samples. Human mast cells were isolated and purified from skin and fat tissue obtained from patients undergoing aesthetic surgery.

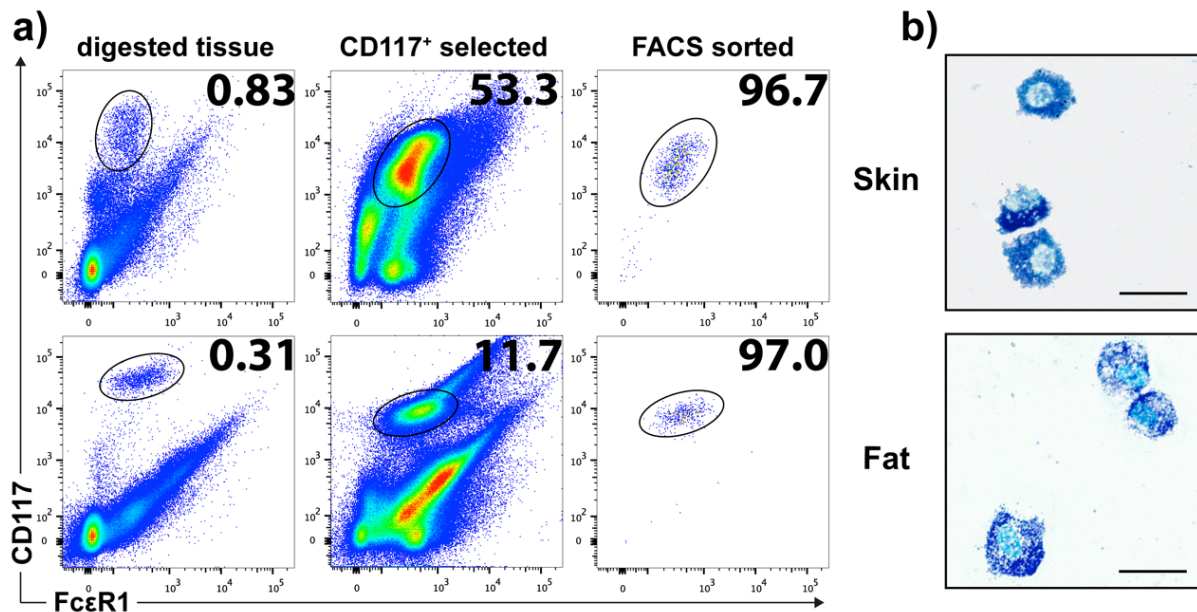


Figure 20: Purification of Human mast cells

Fat (upper row) and skin tissue (lower row) from patients undergoing cosmetic surgery was digested, and mast cells were enriched by two-step purification. **a)** FACS plots display the enrichment along the purification protocol. Numbers indicate percentages of gated cells. From total digested tissue (left), CD117⁺ cells were selected by magnetic beads (middle). Mast cells were sorted for live, CD45⁺, CD14⁻, CD117⁺ FcεRI⁺ on a BD FACSFusion cell sorter (right). **b)** Cytopspins of sort-purified mast cells were stained with toluidine blue.

For differential and quantitative comparison the following three different cell populations were isolated and labelled with stable dimethyl isotopes for subsequent mass spectrometric analyses: skin mast cells, mast cells from abdominal fat and peripheral blood mononuclear cells (PBMCs). PBMCs from healthy humans contain lymphocytes (T cells, B cells, and ILCs), monocytes, and dendritic cells and therefore represent a variety of immune cells but no mast cells. The frequency of those populations varies across individuals but is typically ~70 % T cells, ~15% B cells, ~5% ILCs (including NK cells); ~5% monocytes and ~1% dendritic cells (Murphy et al., 2012). Comparing purified mast cells to a mixture of peripheral blood leukocytes, devoid of mature mast cells, should provide information on mast cell specific protein expression, and provide information on relative expression levels of the detected proteins.

We performed three independent replicate experiments in which a total of 34483 peptides were identified. Peptides were mapped to proteins in the uniprot database and the corresponding genes via alignment to the Ensembl database. A total of 4452

unique genes were identified. From these we could identify up to 945 proteins that were at least 2 fold overexpressed in human mast cells relative to PBMC (Table 5).

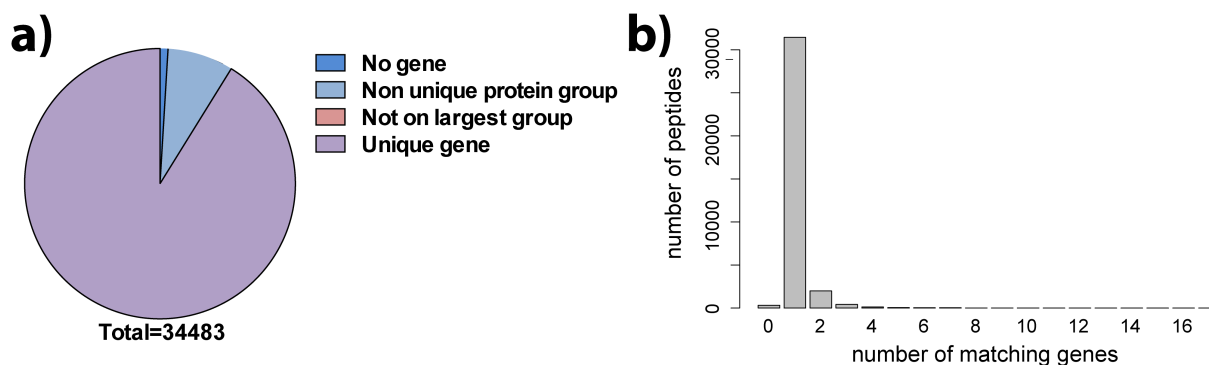


Figure 21: Human mast cell proteomics and peptide mapping

a) 34483 peptides were identified in three independent biological replicates (BR1-3). Peptides were mapped to the Uniprot protein database. 327 Proteins mapped to no gene. 2714 peptides mapped to non-unique protein group and 1 peptide did not map to its highest-covered protein. The remaining 31441 peptides were mapped to their corresponding 4452 genes.

b) The histograms depict the uniqueness of the peptide mapping. The x-axis shows the number of genes a peptide maps to. The y-axis shows the number of peptides that map to as many genes.

The measured peptide counts and the numbers of identified proteins in the human proteomics screen were in a comparable range, albeit slightly lower, as the data set obtained from murine mast cells and peritoneal cells. The frequency of peptide mapping to unique genes was approximately the same (90%) in both experiments.

	Low 1% FDR	Low 10% FDR	unchanged	High 10% FDR	High 1% FDR
Skin MC / PBMC	426	918	1375	945	468
Fat MC / PBMC	516	999	1313	938	515
Skin MC / Fat MC	1	4	3235	0	0

Table 5: Number of proteins differentially expressed in human mast cells compared to peripheral blood mononuclear cells

Listed is the number of proteins being at least 2-fold higher (red) or lower (blue) expressed in mast cells compared to total PBMC with false discovery rate of 1% or 10%.

Unlike the data obtained from mouse mast cells, the majority of proteins quantified in human mast cells were differentially expressed when comparing skin/fat mast cells to PBMC. The number of proteins being down regulated was similar to the number being up regulated.

In order to depict the statistically most significant differences in protein expression, we plotted the data of skin/fat mast cell proteome over PBMC on volcano plots (Figure 22). In this graph, significance is plotted against fold-change on the y and x axes, respectively.

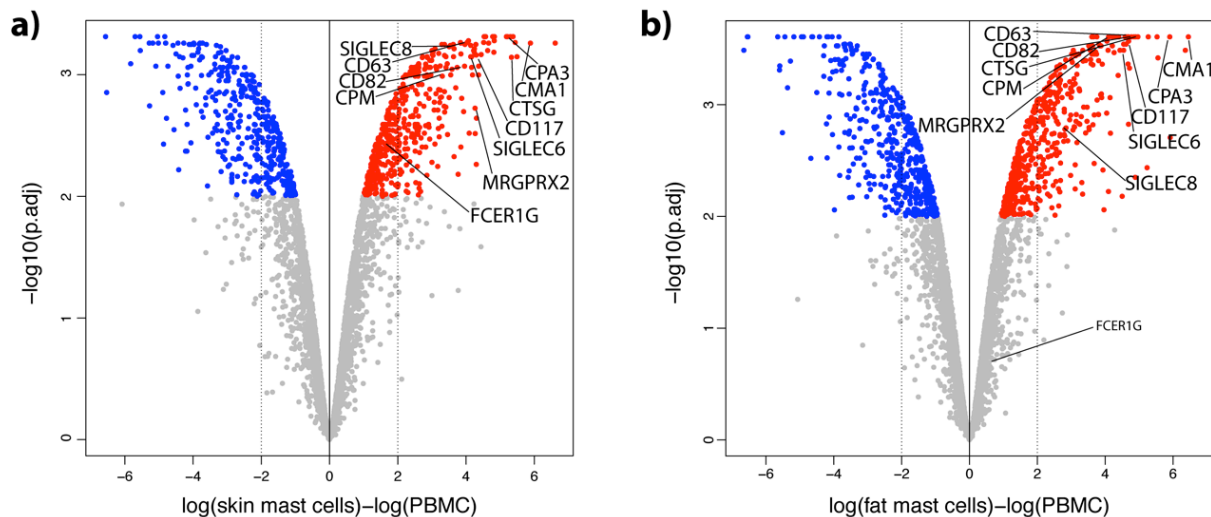


Figure 22: Depiction of differential protein expression of human mast cells and PBMC

Volcano plots presenting differential protein expression of **a)** sorted skin mast cells and **b)** sorted fat mast cells compared to PBMC (x-axis) and its respective significances (y-axis). Proteins with 2-fold expression change (1% FDR) are either coloured in red (higher expressed) or blue (lower expressed). Typical mast cell markers as well as novel mast cell markers, identified with this screen, are marked by arrows and indicated with their names.

Similar to mouse mast cells, proteases such as Carboxypeptidase A3 (*CPA3*), Carboxypeptidase M (*CPM*), Chymase 1 (*CMA1*), Cathepsin G (*CTSG*) and the prototypic mast cell markers stem cell factor receptor kit (*KIT*) and the Fc ϵ R1 γ chain (*FCER1G*) were found among the most up regulated proteins. We also found several, so far less studied, mast cell specific markers such as MAS Related GPR Family Member X2 (*MRGPRX2*), Sialic Acid Binding Ig Like Lectins 6 and 8 (*SIGLEC6/8*) and the Tetraspanins CD63 and CD82 among the highly enriched proteins.

Interestingly, we found two proteins discriminating between fat and skin mast cells; *FABP4*, which is involved in lipid transport across membranes and CD36, which is a glycoprotein receptor for lipids were both expressed on mast cells derived from fat but not on skin mast cells. On the other hand, no proteins were expressed on skin mast cells that were not also expressed by fat mast cells. Moreover, this result of only two tissue specific mast cell markers suggests that mast cells residing at

different connective tissues represent highly similar developmental and functional entities.

3.2.6. Gene ontology analysis of the human mast cell proteome

Gene ontology enrichment analysis was performed to decipher processes and functions specific to human mast cells (Figure 23).

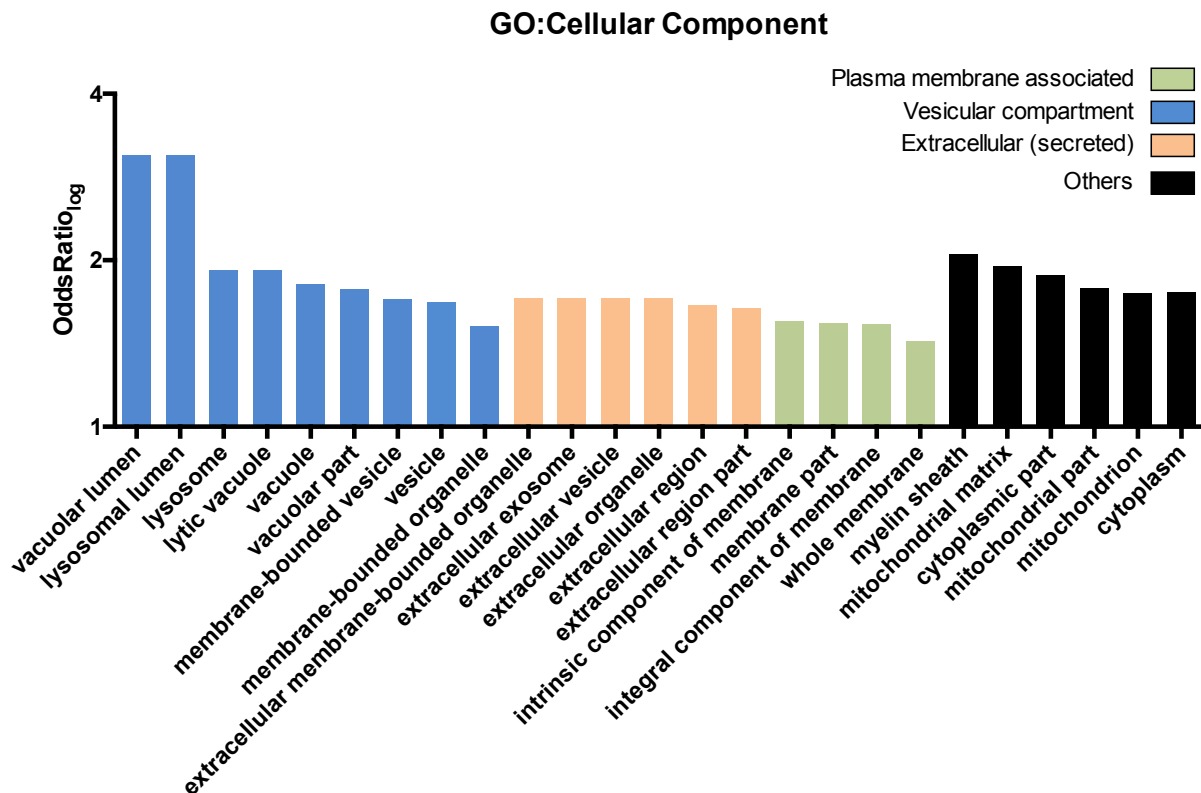


Figure 23: Proteome analysis based on human GO analysis for the term 'Cellular Component'

Shown are Gene-Ontology terms for the category 'Cellular Component' based on mast cell enriched proteins depicted as OddsRatio.

In agreement with the mouse mast cell proteome data, proteins belonging to the vesicular compartment, and thus falling into vesicle-associated GO:CC terms, were presented with the highest OddsRatio values also in human mast cells.

Gene ontology analysis for the term 'Biological Process' (Figure 24) revealed the strongest hit for genes categorized to glycosaminoglycan biosynthesis.

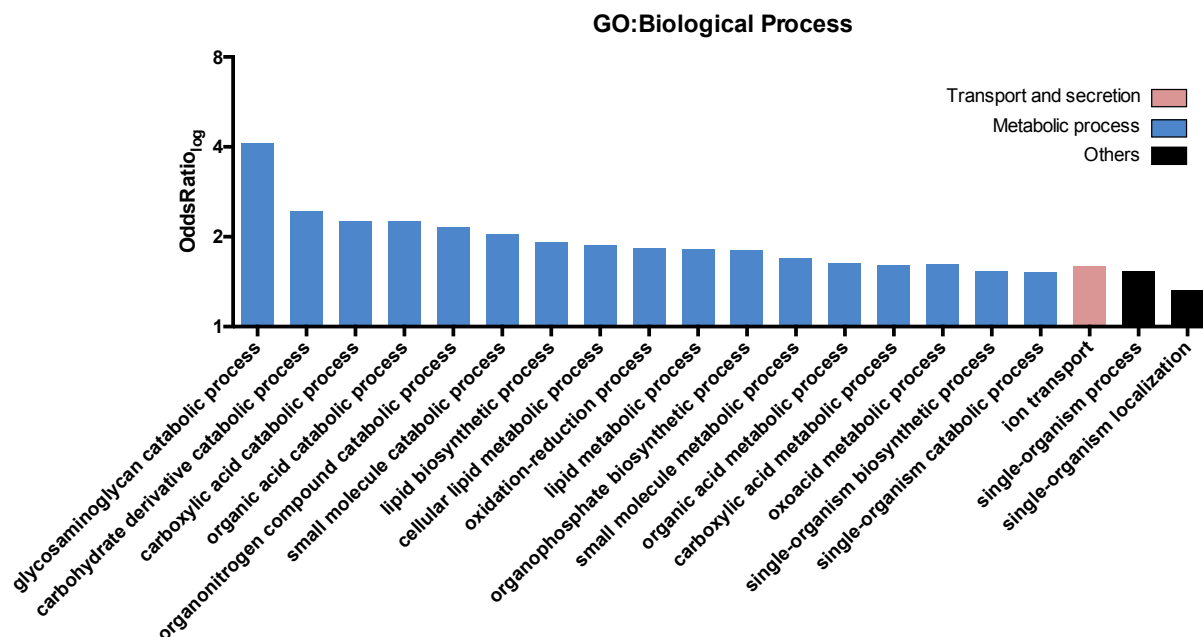


Figure 24: Proteome analysis based on human GO analysis for the term ‘Biological Process’

Shown are Gene-Ontology terms for the category ‘Biological Process’ based on mast cell enriched proteins depicted as OddsRatio.

Overall the human mast cell enriched GO terms in the category ‘Biological process’ display less diversity than the mouse GO:BP. Almost all enriched GO:BP terms in human mast cells belonged to ‘Metabolic processes’.

3.2.7. Human mast cell enriched proteins

In order to identify novel characteristic and in the best case even unique mast cell marker proteins, proteomics data were listed by fold change and their FDR optimized p-values (p.adjusted). The list of the top 20 differentially expressed proteins with significant fold change in sorted fat mast cells over PBMC is shown in the table below.

ProtID	Symbol	Protein name	log2FC	pvalue	padjusted	rep1	rep2	rep3
P23946	CMA1	Chymase	6.452	2.29E-06	0.00025	6.460	5.704	7.191
P15088	CPA3	Carboxypeptidase A3	5.902	2.54E-07	0.00025	5.957	5.704	6.047
Q6NZI2	PTRF	Polymerase I and transcript release factor	5.528	5.70E-07	0.00025	5.255	5.487	5.843
O00534	VWA5A	von Willebrand factor A domain-containing protein 5A	5.269	3.79E-07	0.00025	5.235	5.203	5.371
Q99536	VAT1	Synaptic vesicle membrane protein VAT-1 homolog	4.964	8.70E-07	0.00025	4.798	5.261	4.834
P08311	CTSG	Cathepsin G	4.898	1.36E-06	0.00025	4.668	4.734	5.292
P21266	GSTM3	Glutathione S-transferase Mu 3	4.847	1.26E-06	0.00025	5.208	4.645	4.687
P51688	SGSH	N-sulphoglucosamine sulphohydrolase	4.772	2.15E-06	0.00025	4.348	4.807	5.160
P27701	CD82	Tetraspanin-27	4.686	1.63E-06	0.00025	4.308	4.840	4.910
Q13237	PRKG2	cGMP-dependent protein kinase 2	4.675	2.58E-06	0.00025	4.802	5.019	4.204
P63096	GNAI1	Guanine nucleotide-binding protein G(i) subunit alpha-1	4.626	2.80E-06	0.00025	4.342	4.418	5.116
Q13277	STX3	Syntaxin-3	4.583	1.49E-06	0.00025	4.574	4.871	4.306
P54803	GALC	Galactocerebrosidase	4.400	2.55E-06	0.00025	4.464	4.717	4.020
Q96TA1	FAM129B	Niban-like protein 1	4.389	1.02E-06	0.00025	4.345	4.492	4.329
Q96N66	MBOAT7	Lysophospholipid acyltransferase 7	4.349	1.87E-06	0.00025	4.374	4.606	4.069
P08962	CD63	Surface	4.321	2.42E-06	0.00025	4.660	4.023	4.281
P02545	LMNA	Prelamin-A/C	4.278	1.25E-06	0.00025	4.192	4.414	4.227
P51606	RENBP	N-acylglucosamine 2-epimerase	4.216	2.07E-06	0.00025	4.453	3.950	4.245
Q96AC1	FERMT2	Fermitin family homolog 2	4.115	1.63E-06	0.00025	4.109	3.974	4.262

Table 6: Top 20 proteins enriched in fat mast cells

Shown are the top 20 protein expression values of fat mast cells compared to PBMC.

As for murine mast cells, we find several mast cell proteases (CPA3, CTSG, CPM and CMA1) among the most differential expressed proteins of human fat mast cells. Two proteins on top of this list (VWA5A and FAM129B) have not been described in mast cells before. In vitro studies suggest that VWA5A may act as a tumour suppressor whereas FAM129B has been described as an adherence junction-associated protein, which was able to suppress apoptosis (Chen et al., 2011). Mast cells are long-lived tissue resident cells and one might expect these proteins to regulate cell cycle and survival.

In our previous GO analysis we learned that several metabolic pathways were highly enriched in human mast cells. In line with this we find the enzymes MBOAT7 and GALC, which are involved in lipid metabolism, and RENBP, which is part of the amino-sugar metabolism, within the most enriched proteins in human fat mast cells. The enzyme SGSH, which is involved in heparan sulfate degradation, can be clearly linked to the core mast cell function of proteoglycan metabolism.

Mast cells contain large quantities of intracellular vesicles, thus it is not surprising to find proteins involved in endosome formation (PTRF) and synaptic docking (STX3) to be highly enriched. We have previously mentioned that mast cells are able to form degranulatory synapses. Interestingly, several proteins involved in cell shape and polarization were found preferentially expressed in human mast cells. FERMT2 is a scaffolding protein required for the assembly of focal adhesions and modulation of cell shape, and thus might also play a role in the site directed degranulation of mast cells.

With our proteomics screen we aimed to identify novel mast cell specific cell surface receptors that might be used as targets in an antibody-based ablation model.

Therefore, the list of mast cell enriched proteins was filtered for cell surface markers as described for the mouse proteome dataset (Table 7).

ProtID	Symbol	Protein name	log2FC	pvalue	padj.	rep1	rep2	rep3
P27701	CD82	Tetraspanin-27	4.686	1.63E-06	0.00025	4.308	4.840	4.910
P08962	CD63	Tetraspanin-30	4.321	2.42E-06	0.00025	4.660	4.023	4.281
P32004	CD171	Neural cell adhesion molecule L1	4.100	2.60E-06	0.00025	4.363	4.116	3.821
Q9UHX3	CD312	Adhesion G protein-coupled receptor E2	3.655	2.69E-06	0.00025	3.733	3.644	3.588
Q9P121	NTM	Neurotrimin	4.052	3.16E-06	0.00027	3.711	4.286	4.157
Q96LB1	MRGPRX2	Mas-related G-protein coupled receptor X2	3.816	3.65E-06	0.00029	3.730	3.611	4.108
P05026	ATP1B1	Sodium/potassium-transporting ATPase beta-1	3.627	5.03E-06	0.00030	3.803	3.314	3.763
P10721	CD117	Mast/stem cell growth factor receptor Kit	4.543	6.91E-06	0.00033	3.999	4.468	5.161
Q96QE2	SLC2A13	Proton myo-inositol cotransporter	3.030	1.34E-05	0.00042	3.208	2.715	3.167
O43699	SIGLEC6	Sialic acid-binding Ig-like lectin 6	4.673	1.41E-05	0.00043	3.813	5.252	4.955
P11279	CD107a	Lysosome-associated membrane glycoprotein 1	2.673	2.21E-05	0.00054	2.414	2.747	2.859
O14638	CD203c	Nucleotide pyrophosphatase 3	3.081	2.65E-05	0.00059	2.609	3.156	3.479
Q96GQ5	C16orf58	RUS1 family protein C16orf58	2.683	2.75E-05	0.00060	2.458	2.579	3.011
Q8WWI5	CD92	Choline transporter-like protein 1	2.653	2.77E-05	0.00060	2.786	2.839	2.333
P08582	CD228	Melanotransferrin	2.676	2.81E-05	0.00061	2.723	2.362	2.942
Q9Y5S1	TRPV2	Transient receptor potential cation channel V2	2.629	3.46E-05	0.00068	2.356	2.979	2.553
P19634	SLC9A1	Sodium/hydrogen exchanger 1	3.230	3.82E-05	0.00072	2.583	3.509	3.598
Q9NYZ4	SIGLEC8	Sialic acid-binding Ig-like lectin 8	3.233	4.03E-05	0.00073	2.855	3.894	2.952
P16070	CD44	Hyaluronate receptor	3.246	4.23E-05	0.00075	2.618	3.782	3.339

Table 7: Top 20 cell surface proteins enriched in fat mast cells

Shown are the cell surface protein expression values of sorted fat mast cells / PBMC PEC. Only proteins with a p.adjusted > 0.01 are listed.

In addition to the prototypic mast cell marker CD117, the top 20 mast cell enriched cell surface proteins contained several novel mast cell specific markers that could be functionally divided into distinct groups. Adhesion molecules, among which were CD171, CD312, NTM, SIGLEC6, SIGLEC8 and CD44, constituted the largest group. These molecules, might act in concert to mediate migration of mast cell precursors from the bone marrow into the periphery and regulate the maintenance of mast cells in their tissue niche. CD171 has recently been described as a marker for human skin

mast cells (Gschwandtner et al., 2017). Our proteomics screen found CD171 to be also specifically expressed on fat mast cells, suggesting that skin and fat mast cells have a similar phenotype. CD312 is a receptor for chondroitin sulfate and mediates adhesion to it (Stacey et al., 2003). It has been shown that in neutrophils CD312 ligation results in adhesion and migration, and augments superoxide production and degranulation (Yona et al., 2008). As neutrophils and mast cells have overlapping functions, CD312 might enhance mast cell degranulation and adhesion. Channel proteins were the second largest group represented on our list of mast cell specific surface proteins: ATP1B1, SLC2A13, CD92 and SLC9A1 transport ions and small metabolites across the plasma membrane.

The third group of receptors is involved in the transmission of signals from the environment across the plasma membrane. Analogous to mouse mast cells we found tetraspanins to be highly expressed in human mast cells. CD82 and CD63 are the most enriched proteins detected in mast cells and their mast cell specificity appears to be conserved across species. A high degree of homology between mouse and human (76,4% for CD82; 79.4% for CD63) suggests similar function, however whether they are truly functionally homologous remains to be determined. CD203c is involved in the hydrolysis of extracellular oligonucleotides, nucleoside phosphates, and NAD and thus contributes extracellular nucleotide signalling. MRGPRX2 is a G-protein coupled receptor that mediates mast cell degranulation by non-immunologic secretagogues, such as compound 48/80, and is able to bind cathelicidin (McNeil et al., 2015; Subramanian et al., 2016). TRPV2 is an ion channel that is activated by temperatures above 52°C. TRPV2 activation results in Ca²⁺ influx and degranulation (Zhang et al., 2012). The closest ortholog of C1orf58 has been described in the root of *Arabidopsis thaliana* and mediates the sensing of low energetic ultra-violet light during root development (Tong et al., 2008). Mast cell activation in response to UV-irradiation has been described in certain settings, however the precise mechanism of such cellular activation has not been elucidated (Hart et al., 2000).

3.2.8. Verification of novel human mast cell markers

Having identified a variety of differentially expressed cell surface proteins in the proteomics dataset of human fat and skin mast cells, we next analyzed their specific surface expression by antibody staining. In addition to fat and skin, we isolated lung and colon mast cells, and tested these for mast cell marker expression. For several

of the listed proteins (Table 7) monoclonal antibodies are commercially available. We tested by flow cytometry the expression of CD171, CD82, CD312, CD63, MRGPRX2 CD117, SIGLEC6, CD107a, CD203c and CD92 on the different cell populations listed below. Human fat, lung, colon and skin mast cells (CD14⁻ CD45⁺ CD117⁺ IgE⁺), as well as peripheral blood monocytes (CD45⁺ CD14⁺), basophils (CD45⁺ CD123⁺ FcεRI⁺), eosinophils (CD45⁺ SSC^{hi} CD193⁺), neutrophils (CD45⁺ CD16⁺), plasmacytoid dendritic cells (CD45⁺ CD123⁺ FcεRI⁻), B cells (CD45⁺ CD3⁻ CD19⁺), CD4 T cells (CD45⁺ CD3⁺ CD4⁺), and CD8 T cells (CD45⁺ CD3⁺ CD4⁻) were stained with these monoclonal antibodies, or isotype controls (Gating strategy in Supplement Figure 3).

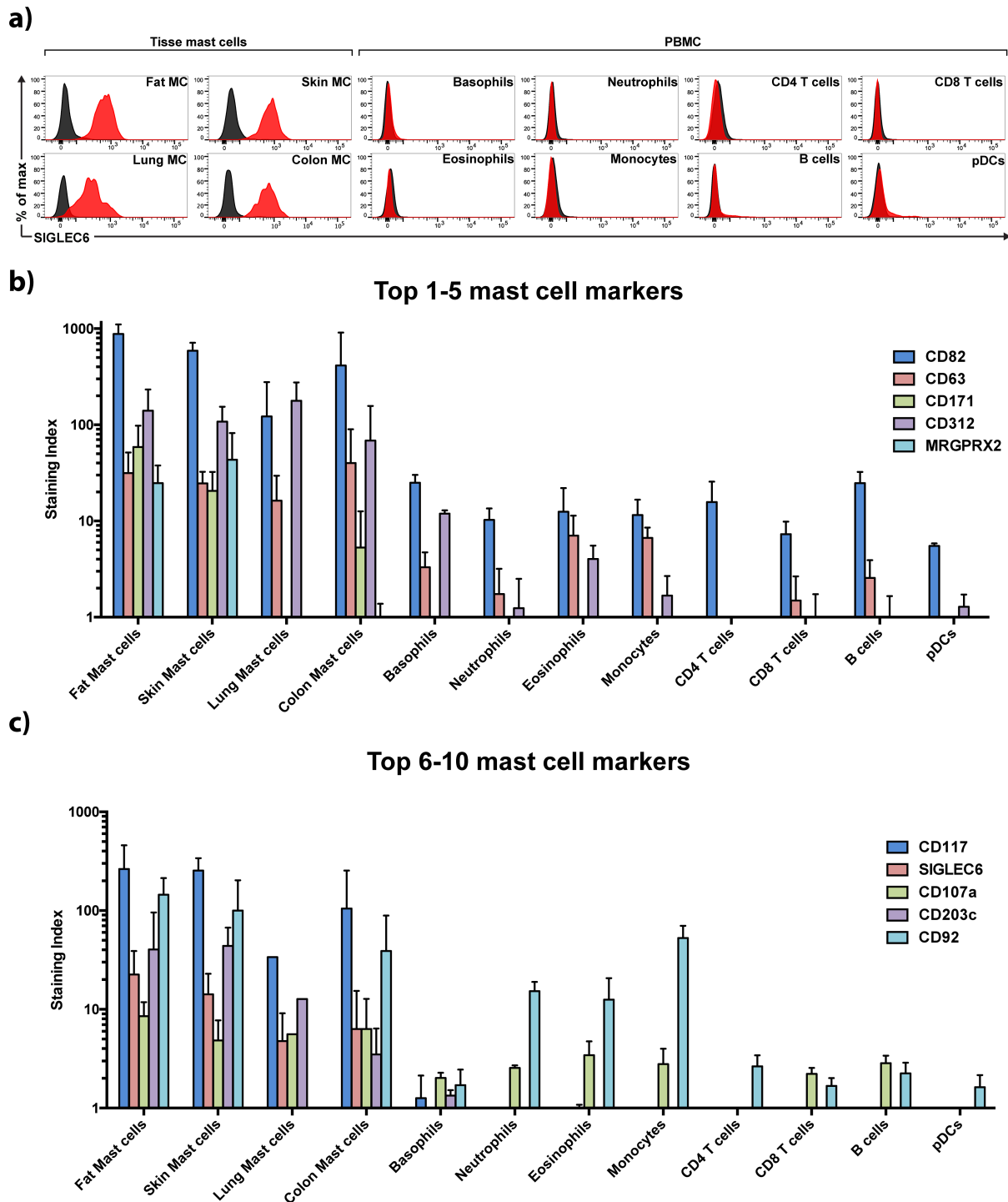


Figure 25: Flow cytometry of the 10 most enriched human mast cell surface proteins

a) Example for the tested antigens, histogram overlays are shown for SIGLEC6 antibody staining (red) and isotype control (black) on human fat, lung, colon and skin mast cells as well as peripheral blood monocytes, basophils, eosinophils, neutrophils, dendritic cells, B cells, CD4 T cells, and CD8 T cells.

b,c) The same 12 Populations depicted in (a) were tested for immunoreactivity against the antigens CD171, CD82, CD312, CD63, MRGPRX2 (b) or CD117, SIGLEC6, CD107a, CD203c and CD92 (c) by flow cytometry. Shown is the mean staining index \pm SEM of 1-6 samples per group.

All ten markers that were analysed by flow cytometry were found to be expressed on fat and skin mast cells, thereby confirming the results obtained from the mass spectrometry-based screening.

Interestingly, human lung and colon mast cells did not stain positive for MRGPRX2, which previously has been described to be predominantly expressed by the connective tissue type mast cells (MC_{TC}) but not by mucosal MC_T (Subramanian et al., 2016). CD171 might also be preferentially expressed on MC_{TC} as it was undetectable on lung mast cells and staining with anti-CD171 antibody revealed two populations of colon mast cells. In the colon, mucosal MC_T as well as connective tissue MC_{TC} are present, thus it is possible that CD171 discriminates between the two mast cell subtypes in the gut.

With respect to specificity, MRGPRX2, CD117, SIGLEC6 and CD203c were exclusively found on mast cells but not on other blood cell lineages. CD82 and CD92 were detected on both, mast cells and blood leukocytes, albeit with approximately 10 fold higher levels on mast cells.

The protein CD312 was found with similar staining intensities on mast cells from all analysed tissues and on the myeloid subsets as well as on plasmacytoid dendritic cells, but not on lymphocytes. This is in line with a previous report suggesting a role for CD312 in migration and adhesion of cells from the myeloid lineage (Chang et al., 2007a). CD63 and CD107a staining could be detected on all cell types, except CD4 T cells and pDCs. This expression pattern of human CD63 is therefore somewhat unexpected, as the homologous mouse protein showed extraordinary mast cell specificity. However, all mast cell subsets exhibit a 2-10 fold stronger staining intensity of CD63 and CD107a over other hematopoietic cells tested.

In addition to the top 5 enriched proteins this experiment was also performed for the markers: SIGLEC8, FcεRI, CD26, CD44, CD51, CD59 and CD54 (Supplement figure 4), all of which are mast cell enriched proteins .

3.2.9. Mapping of skin MC RNA-sequencing data to skin MC proteome

There has been a recent human transcriptome analysis by the FANTOM consortium for the identification of mast cell specific genes (Motakis et al., 2014). By comparing RNA expression of purified human skin mast cells to transcriptome data from a collection of 893 FANTOM5 samples, including various immune cells from peripheral blood, a list of 169 genes was generated (Supplement Motakis et al., 2014) which

were enriched by at least 10-fold in skin mast cells compared to the mean of all FANTOM5 samples.

To compare the mast cell specific genes identified from the FANTOM5 samples we mapped them onto our skin mast cell versus PBMC proteomic data (Figure 26). From the 169 genes we were able to map 51. The other 118 genes were not detected by the mass spectrometer, which might be a result of under sampling, but might also indicate that the protein expression level of such proteins is low in primary human mast cells. In addition, 30 genes that displayed strong mast cell-specificity in the FANTOM screen mapped to proteins that were not significantly upregulated in our proteome data. This discrepancy between RNA abundance and protein abundance might reflect gene regulatory differences on transcriptional and post-translational level. It has been estimated that mRNA levels only explain 40% of the variability observed on protein levels, and that protein abundance is predominantly regulated at the ribosome by means of translational control (Schwanhausser et al., 2011).

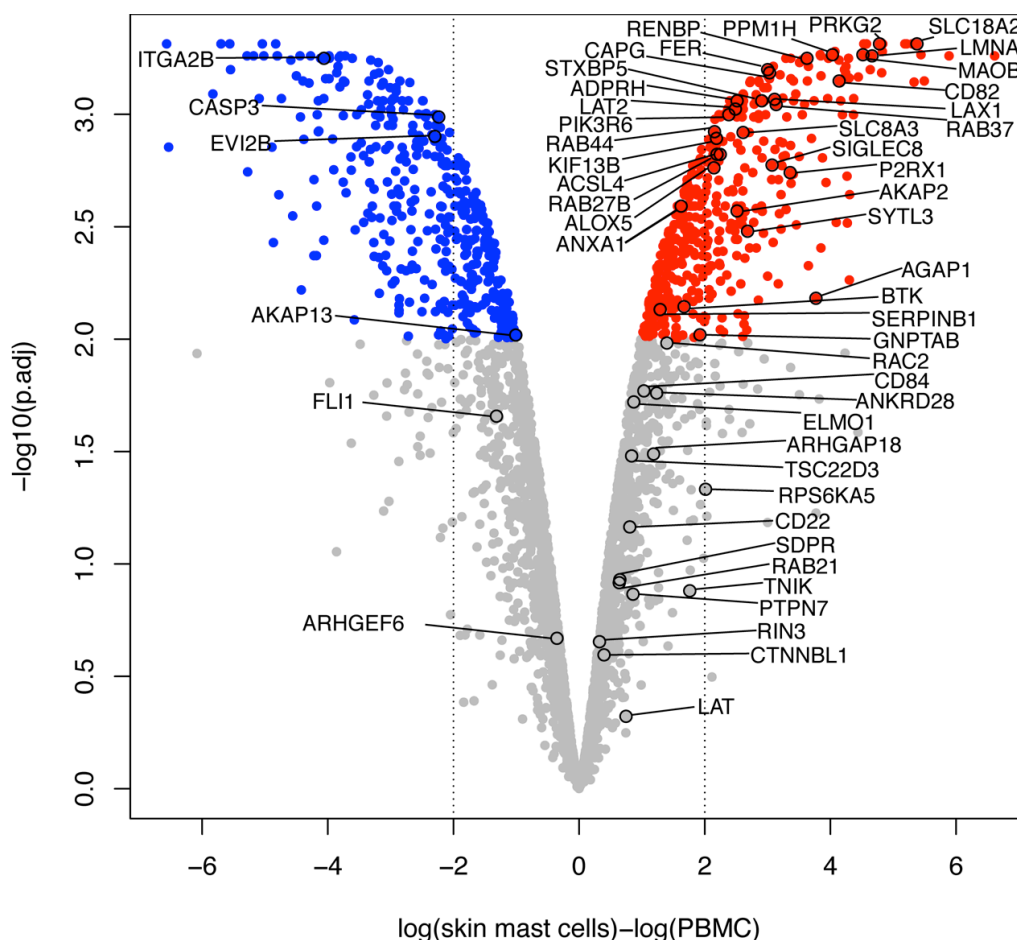


Figure 26: Comparison of RNA-sequencing to proteomics

Shown is the protein expression of sorted skin mast cells relative to PBMC versus the p.adjusted values. Proteins without significant change in expression are

displayed in grey. Proteins with 2-fold expression change are either coloured in red (higher expressed) or blue (lower expressed). Mast cell enriched genes identified by *Motakis et al.* are indicated with names and arrows.

As we were mainly interested in identifying mast cell enriched surface receptors we also compared the two data sets with focus on cell surface proteins. Of the 20 most enriched cell surface proteins, identified with our proteomics screen we only found CD82, SIGLEC8 and P2RX1 enriched on RNA as well as on protein level. This observation is not surprising as particularly for cell surface proteins the correlation of RNA and protein expression has been reported to be weak (Cox et al., 2009; Lundberg et al., 2010).

Therefore proteomic profiling is superior to RNA analysis in identifying novel mast cell enriched cell surface receptors.

3.2.10. Human – mouse mast cell comparison

The previous GO term analysis revealed an enrichment of comparable biochemical pathways in mouse and human mast cells. Such similarities suggest conserved functions of mast cells in mice and humans. To understand the molecular basis for these conserved functions, we performed an in-depth comparison of proteins enriched in mouse peritoneal mast cells (peritoneal mast cells / *Cpa3^{Cre/+}* PEC) and proteins enriched in human fat mast cells (fat mast cells / PBMC). Quantified proteins from the mouse and human datasets were compared, and based on their Ensembl annotation 378 proteins could be assigned to their homologs (Ensembl does not “know” all homologs). From these, 33 proteins were more expressed in mouse and human (Figure 27b), 4 were more expressed in mouse mast cells (Figure 27c), and 3 were more expressed in human mast cells (Figure 27d).

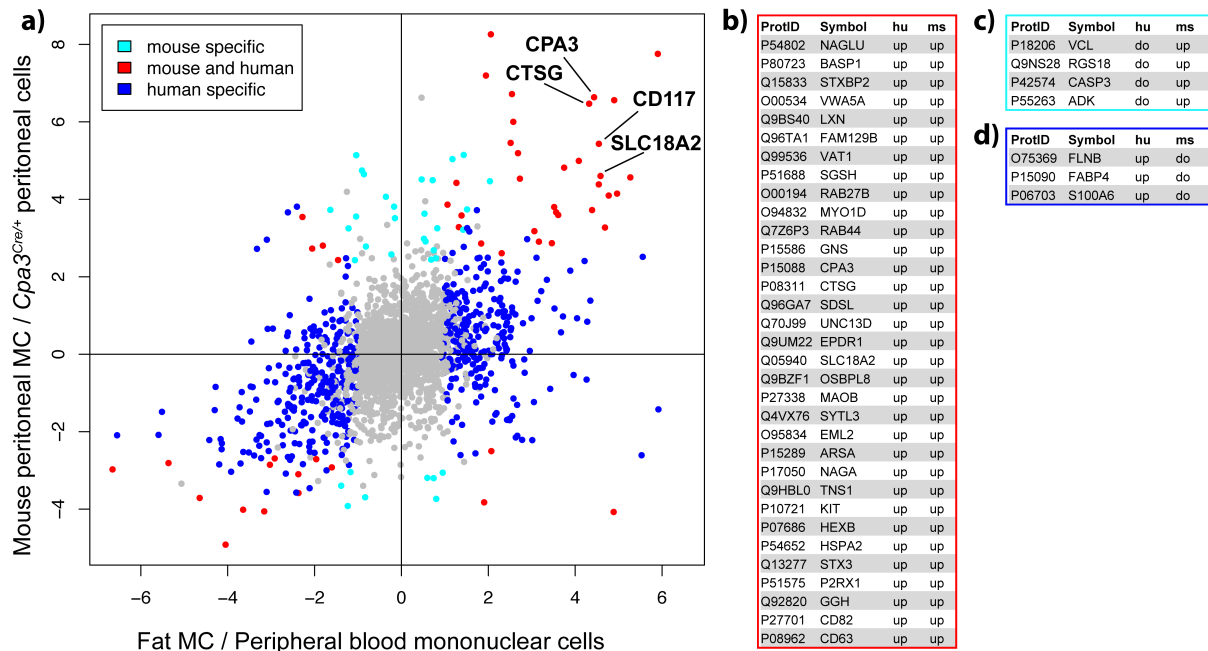


Figure 27: Cross-species conserved mast cell protein signature

a) Expression of mouse mast cell enriched proteins (vertical axis) versus human fat mast cell enriched proteins (horizontal axis) shown in log scale. Proteins significantly different in both mouse (ms) and humans (hu) are coloured in red; proteins significantly changed in mouse only are coloured turquoise and proteins significantly changed in human only are depicted as blue. **b)** The table shows the proteins that are specifically enriched in mast cells of both species ($p=0.01$). **c-d)** the tables show proteins solely enriched in mouse and humans respectively ($p=0.01$). Typical mast cell markers are marked by arrows and indicated with their names.

Based on this analysis we could identify a proteome signature for mast cells, which contains 33 proteins that were homologous between mouse and humans and were specifically and strongly expressed (upper right red dots and red box in Figure 27a and b, respectively). There are more blue dots visible as in the human dataset more proteins could be quantified in the Fat MC / PBMC comparison. The conserved genes can be grouped into six categories: proteases and protease inhibitors (CPA3, CTSG, LXN); bioactive amine metabolism (SLC18A2, MAOB); proteoglycan metabolism (NAGLU, SGSH, GNS, HEXB); granule machinery and cellular plasticity proteins (VAT1, BASP1, STXBP2, UNC13D, SYTL3, STX3); receptors for binding and responding to environment (FAM129b, CD117, P2RX1, CD63, CD82); and others (VWA5A, RAB27B, MYO1D, RAB44, SDSL, EPDR, OSBPL8, EML2, ARSA, NAGA, TNS1, HSPA2, GGH).

By comparing the mouse and human mast cell enriched proteins we detect core mast cell functions that are conserved across species suggesting that mast cells in both species are similar in function.

3.3. In vivo depletion of mast cells via targeting of the endogenous marker CD63

Next, we sought to investigate if the identified surface markers on mast cells would be suitable for antibody-mediated depletion. One of the most enriched mouse and human mast cell receptors identified is the tetraspanin CD63 (Figure 19b). CD63 is expressed not only in mast cells but also in granulated cells such as basophils, cytotoxic T cells, platelets and certain subsets of endothelial cells. However, due to a lysosomal targeting sequence, CD63 is thought to be retained within lysosomes, and only becomes exposed on the cell surface under conditions of granule exocytosis. This hypothesis is also supported by our flow cytometry data, which show specific cell surface staining of murine CD63 among the hematopoietic cell types tested. In addition, human and mouse mast cells of various origin have reportedly shown consistent cell surface expression of CD63 (Köberle et al., 2012).

Based on these considerations, CD63 may be a suitable target for antibody-mediated mast cell depletion.

3.3.1. ADCC-dependent depletion mechanism

According to the ADCC-dependent depletion of mast cells from huCD4-transgenic mice with TNX355 (anti-huCD4) antibodies, we tested the in-vivo mast cell depletion ability of the anti-CD63 antibody NVG-2 (rIgG2b). Therefore, C57BL/6 *Cpa3^{hCD4/hCD4}* mice were injected once i.p. with 500µg NVG-2. Control mice were treated with A161A1 (anti-hCD4, rIgG2b), TNX355 (anti-hCD4, mIgGa), or the respective isotype control antibodies (Figure 28). On day 7 after injection, mice were sacrificed and peritoneal mast cell depletion was measured by flow cytometry.

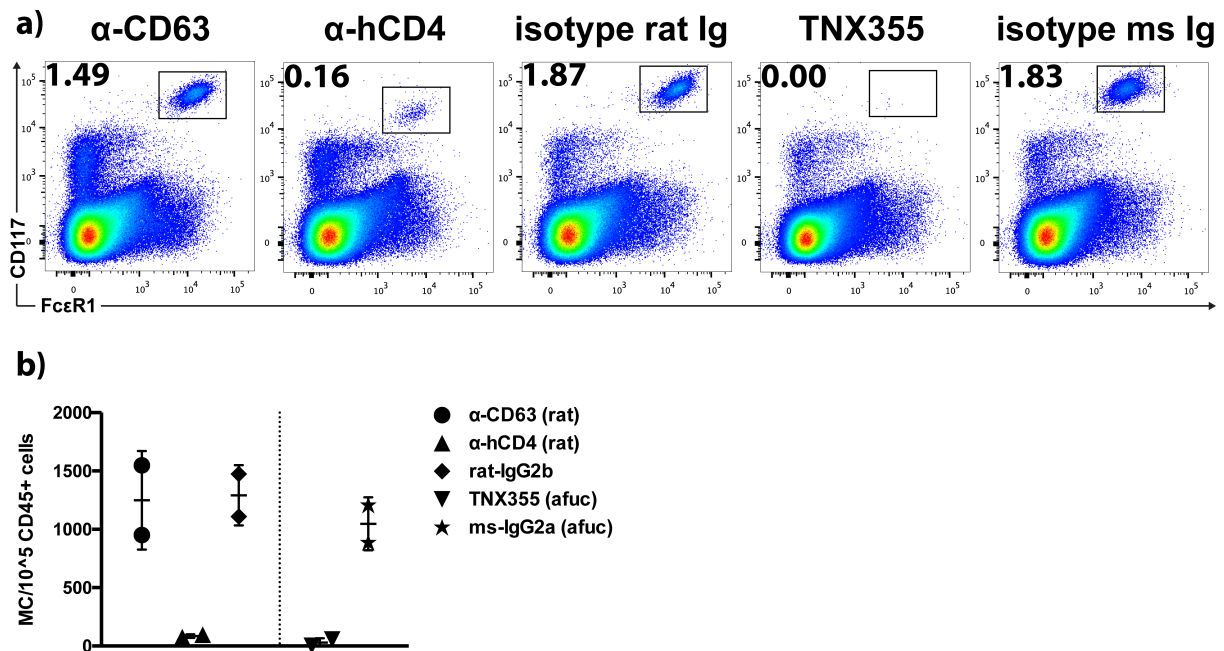


Figure 28: Anti-CD63 mediated mast cell ablation

C57BL/6 *Cpa3*^{hCD4/hCD4} mice were treated i.p. with 500 μ g of anti-CD63, anti-hCD4, TNX355 or isotype control antibodies in 200 μ l of PBS. 7 days later mice were sacrificed and peritoneal exudate was isolated for subsequent flow cytometric evaluation of mast cell ablation. **a)** Representative FACS plots of the different peritoneal exudate cells. Numbers indicate percentages of mast cells within the live, F4/80⁻, CD45⁺ gate. **b)** The number of phenotypic mast cells per 10^5 CD45⁺ cells is shown. Mean \pm SEM for two animals per treatment group.

A single intra-peritoneal injection of 500 μ g of anti-CD63 antibody did not result in any reduction of peritoneal mast cells (Figure 28). Treatment of mice with equal amounts of anti-hCD4 antibody (A161A1 or TNX355) resulted in near complete peritoneal mast cell depletion. Isotype control antibodies had no effect on mast cell numbers. Therefore, CD63 does not seem to be an effective target for ADCC-mediated mast cell depletion. This could be due to the fact that CD63 is more rapidly internalized upon antibody binding than the artificial hCD4 molecule and thus, in contrast to anti-hCD4 antibodies, NVG-2 may not efficiently activate a cellular cytotoxicity response.

3.3.2. Fluorimetric measurement of anti-CD63 internalization

To test whether bound antibody internalizes after binding with CD63, we coupled the pH sensitive reporter pHrodo to the anti-hCD63 antibody (C5H6). PHrodo is a fluorescent dye with excitation and emission maxima at 560 nm and 585 nm, respectively. Its fluorescent emission intensity is enhanced by orders of magnitude at acidic pH. We incubated primary human skin and fat mast cells on ice or at 37°C in the presence of anti-CD63-pHrodo or Isotype-pHrodo antibodies. Internalization into

acidic endosomal compartments was observed by measuring the increase of mean fluorescence intensity by flow cytometry at 37°C (Figure 29).

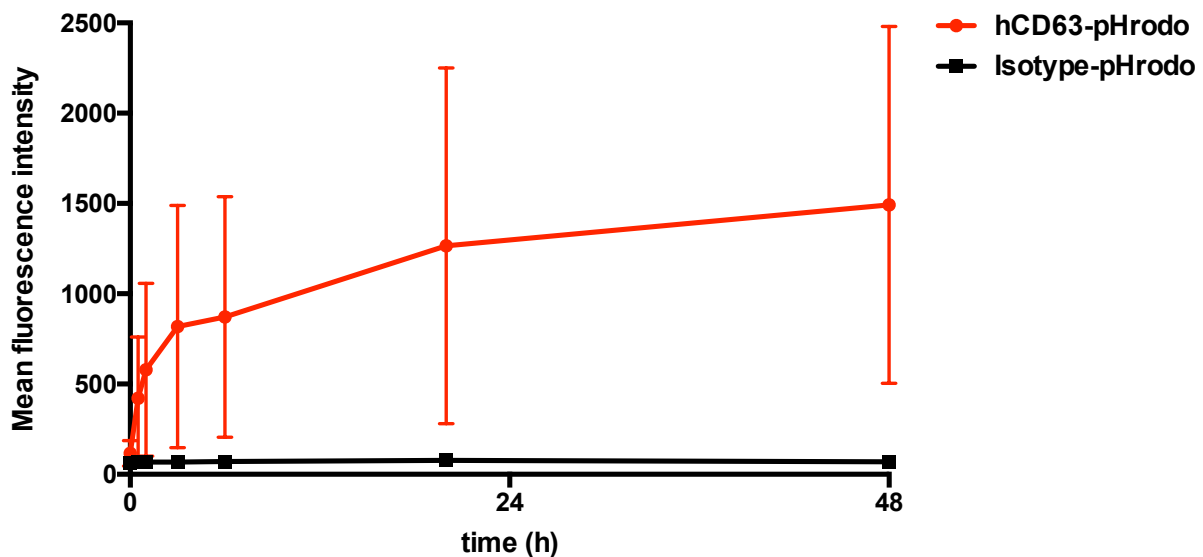


Figure 29: Anti-CD63 is internalized into primary human skin mast cells

Shown is the increase in mean fluorescence intensities of cultured human skin mast cells after incubation with anti-CD63-pHrodo or isotype-pHrodo antibodies at 37°C at the indicated time points.

Antibody binding to CD63 induced internalization in human skin mast cells. Internalization of bound antibody follows very rapid kinetics as fluorescent pHrodo can be detected as early as 1 minute after addition of the antibody to the culture medium.

These experiments with human mast cells suggest that CD63 is rapidly internalized and thus might not be available on the cell surface for effector cell binding. Alternative strategies for CD63-mediated cell depletion therefore are required, e.g. application of antibody-drug conjugates.

3.3.3. CD63 targeting by antibody-drug-conjugate

Antibody-drug conjugates (ADCs) usually follow a three-step mechanism of action. First the antibody, attached to the payload, binds its target on the cell surface. Secondly, the receptor-antibody complex is internalized. Next, within the endosome the cytotoxic drug is released from the antibody by endogenous peptidase cleavage. In a last step the toxin is transported to the cytosol where it interferes with essential cellular processes resulting in apoptotic cell death of the target cell.

Having shown that CD63 is rapidly internalized after antibody binding, we were interested whether it might be a suitable target for antibody-drug-conjugate-mediated mast cell ablation. The drug conjugate we chose was saporin. This is a ricin derivate that is able to enzymatically inactivate ribosomes resulting in a shut down of protein synthesis, eventually leading to apoptosis. Saporin is commercially available as an attachment to streptavidin and can therefore tightly be bound to biotinylated antibodies of interest.

To test whether a CD63-saporin conjugate may efficiently kill mast cells, we prepared an equimolar mixture of biotinylated anti-CD63 (clone NVG-2) and streptavidin-saporin (SAP) and incubated murine bone marrow-derived mast cells and mouse primary peritoneal mast cells with different amounts of that ADC-complex. Cell death was determined by measuring the decrease of viable cells, 72 hours after treatment, using the fluorescent redox viability assay CellTiter-blue (Promega) (Figure 30).

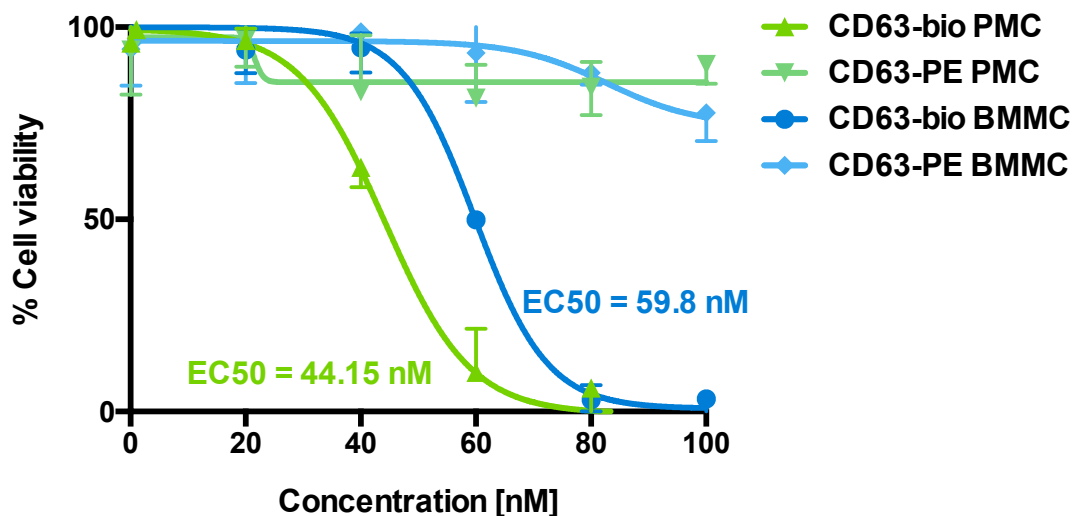


Figure 30: In vitro mast cell killing with CD63-saporin

C57BL/6 bone marrow-derived mast cells (BMMC) and peritoneal-exudate derived mast cells (PMC) were treated with different concentrations of CD63-saporin. After 72 hours the amount of viable cells was determined by CellTiter-Blue viability assay.

Internalization of CD63-saporin resulted in the specific cell death of both BMMC and PMC. Incubation of cells with a control mixture, (in which the Toxin is not specifically bound by the antibody) consisting of phycoerythrin-conjugated antibody (CD63-PE) and SA-Saporin, did not induce cell death. This experiment demonstrated that mast cells could specifically be killed with CD63-saporin, in vitro.

Next, I investigated the in-vivo mast cell ablation capability of CD63-SAP. C57BL/6 wild type mice were injected i.v. with 100 μ g CD63-SAP or the corresponding amount of 40 μ g SAP only. Animals were monitored daily for the occurrence of toxicities. Seven days after treatment, mice were sacrificed and mast cell depletion was quantified by flow cytometry.

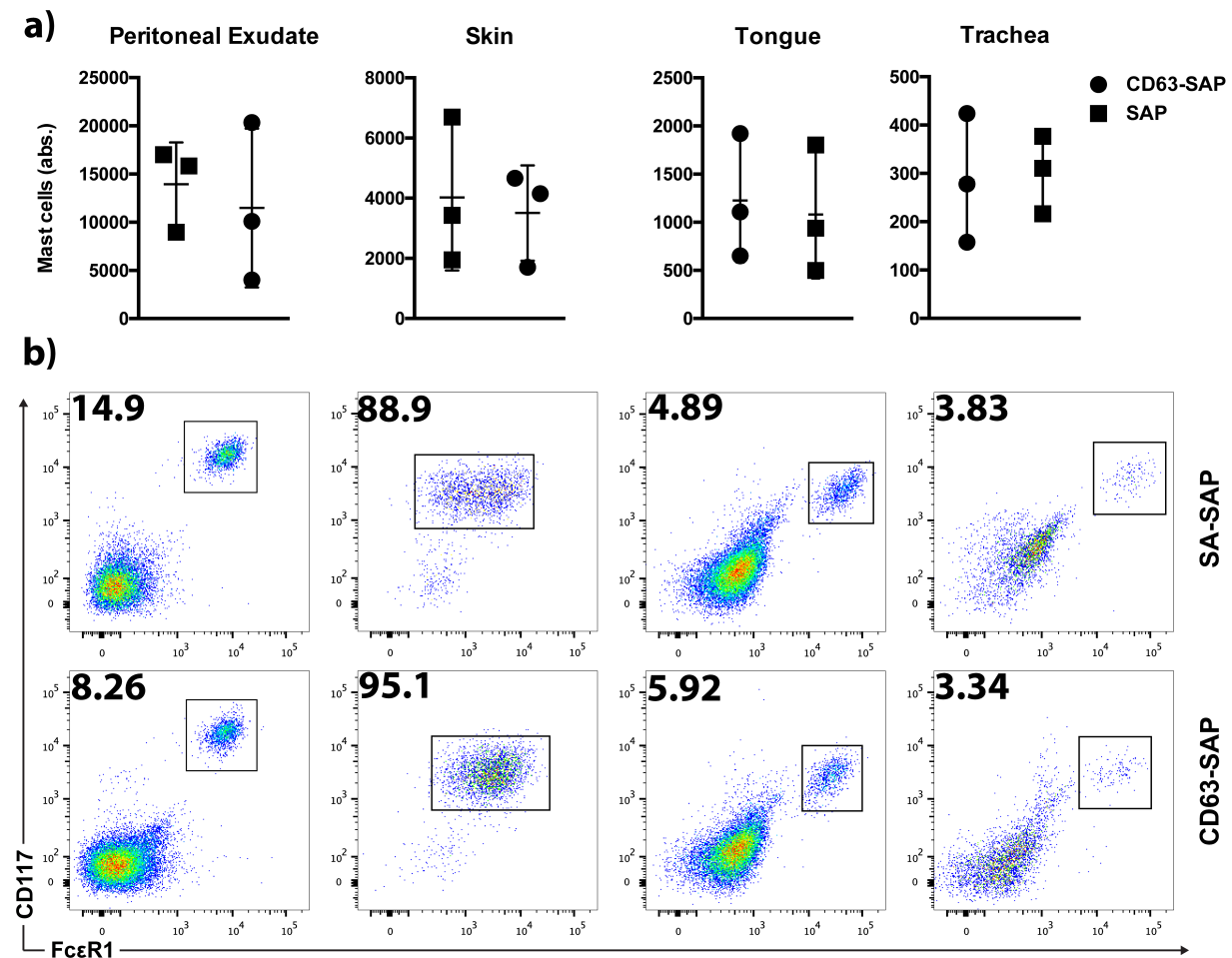


Figure 31: In vivo depletion of wild type mast cells with a CD63-saporin conjugate

C57BL/6 mice were treated i.v. with 100 μ g of CD63-SAP or naked SAP in 200 μ l of PBS. 7 days later mice were sacrificed and organs were isolated for subsequent flow cytometric evaluation of mast cell ablation. **a)** The absolute number of phenotypic mast in different organs is shown. Mean \pm SEM for three animals per treatment group. **b)** Representative FACS plots of the different mast cell compartments. Numbers indicate percentages of mast cells within the live, CD3⁻, CD19⁻, CD11b^{int}, CD45⁺ gate.

CD63-SAP did not exhibit anti-mast cell activity in vivo. From day 5 after treatment, two of the mice that received CD63-SAP displayed weight loss, hunch back, and impaired mobility. Upon necropsy, a shrunken stomach and vastly reduced epididymal fat could be observed in the CD63-SAP treated animals. Due to the

deterioration, it was not possible to perform flow cytometry on single cell suspensions from fat and stomach tissue. However, due to lack of mast cell ablation efficacy we did not further investigate the cause of the observed toxicities.

These results suggest that CD63 might not be a suitable target for in vivo ADCC- and ADC-mediated mast cell ablation due to its toxicity, possibly in the kidneys.

4. Discussion

Current therapeutics only target mast cells indirectly by neutralisation of secreted mediators or by reducing the activation capacity. In some patients symptomatic treatment strategies are often insufficient to control the very severe allergic diseases. In these instances, novel therapeutic agents are required, as affected patients depend on frequent, high dosed drugs to control their disease while sustaining a particular high risk of morbidity and mortality (Holgate and Polosa, 2008; Pakhale et al., 2011; Serra-Batlles et al., 1998). Monoclonal antibody therapy is successfully pursued in all current areas of drug development. Here, we present an experimental approach aimed at specifically eliminating mast cells by cell-depleting monoclonal antibodies.

4.1. Mouse mast cell proteomics

To identify physiologic mast cell antigens we established a mass-spectrometry assisted proteomics pipeline for primary mast cells. While, previous efforts of large-scale analysis of mast cells mostly focussed on the mast cell mRNA expression, we sought to analyse protein expression. RNA-based assays (microarray or RNA-sequencing) are useful to detect cell-type specific transcripts, however, protein abundance can be regulated at the ribosome. For cell surface proteins in particular the correlation of RNA presence and protein abundance may be poor (Cox et al., 2009; Lundberg et al., 2010). Moreover, many of the previously published transcriptome datasets relied on *in vitro* differentiated immature mast cells or immortalized mast cell lines (Jayapal et al., 2006; Nakajima et al., 2002; Sayama et al., 2002). *In vivo*, MCs develop from progenitors in the bone marrow and migrate as immature cells into the periphery (e.g. skin, lung, gut) where they complete their maturation (Gurish and Austen, 2012). Therefore, it is unclear to what extent mast cells generated by *in vitro* differentiation represent their mature tissue counterparts *in vivo*. In support of this note of caution, a recent report demonstrated that primary MCs undergo profound changes when placed into a cell culture environment (Motakis et al., 2014).

To decipher the proteome of mature tissue mast cells we isolated primary mast cells by FACS-sorting from the peritoneal cavity of C57BL/6 mice. Mast cells from the

peritoneal cavity are easily purified and minimize bias introduced by enzymatic tissue digestion. There are two main strategies for investigating the proteome of membrane proteins. Traditionally, density gradient separation was used to separate the membrane fraction from the organelle and nuclear proteins. In more recent years, biotin or lectin labelling approaches have been successfully developed to tag and capture cell surface proteins (Elschenbroich et al., 2010). The large quantities of cellular proteins required for such direct membrane fraction isolation procedures were impossible for primary mast cells in our hands. We therefore first determined the whole mast cell proteome without fraction pre-enrichment, and subsequently selected surface expressed proteins from this entire data set by bioinformatic criteria. For the quantification of proteins in a mass-spectrometry experiment it is required to, include an internal standard, or to measure differentially labelled protein samples side-by-side. For explorative mass spectrometry it is not possible to include a standard, as the composition of proteins in the experiment is unknown. For these experiments side-by-side comparisons are useful, which can be achieved in different ways. Typically the digested peptides are differentially labelled with stable isotopes. The basis for this strategy is the stable isotope dilution theory, which in principle states that a stable isotope-labelled peptide has the same physiochemical properties as its unlabelled counterpart, and thus will behave the same way during chromatographic separation and mass acquisition. The mass spectrometer can recognize these differentially labelled peptides and quantify them based on signal intensities (Bantscheff et al., 2007). In our experiments we used stable dimethyl labelling of trypsin-cleaved peptides (Boersema et al., 2009).

Previous studies from our laboratory analysed mRNA expression of skin whole tissue lysates (Feyerabend et al., 2011). In this study whole skin mRNA expression from mast cell-deficient *Cpa3^{Cre/+}* and mast cell-sufficient *Cpa3^{+/+}* mice were compared, and mast cell specific genes could be identified as differentially expressed mRNA without prior purification of mast cells.

Based on these findings, we reasoned that mast cell-specific proteins might easily be identified when comparing peritoneal cells of *Cpa3^{Cre/+}* and *Cpa3^{+/+}* mice. However, in contrast to the RNA-microarray of skin tissue, the proteomic comparison of *Cpa3^{+/+}* to *Cpa3^{Cre/+}* PEC displayed only minimal difference in detection of mast cell-specific markers. Unlike RNA-based screenings, the coverage of mass spectrometry-assisted proteomics experiments is estimated to be less than 10% of the genome, which

makes it difficult to detect rare proteins. Mast cells make up only 2-4% of all peritoneal cavity cells. Thus, the *Cpa3*^{+/+} and *Cpa3*^{Cre/+} PEC samples are too similar and the mast cell-specific proteins are too rare compared to all the proteins in the sample in order to be readily detected by the mass spectrometer.

To overcome this limitation (Bantscheff et al., 2007) we compared sorted mast cells vs. total peritoneal cells. This revealed abundant MC-specific proteins, as the mass spectrometer can detect sufficient proteins from the sorted mast cell sample. As expected, the MC / *Cpa3*^{Cre/+} comparison was more sensitive in detecting mast cell-specific proteins as there were more proteins significantly up- or down regulated in the MC vs. *Cpa3*^{Cre/+} dataset ($n=144$) than in the MC vs. *Cpa3*^{+/+} dataset ($n=122$).

We found several proteases (*Cpa3*, *Cma1*, *Tpsb2* and *Ctsg*) among the proteins that displayed the highest fold change comparing the proteomes of mast cells and the remaining peritoneal cells. Hence, proteases may be regarded as bona fide mast cell protein markers. Some of the mast cell enriched proteins are also abundantly expressed in brain tissue. Among these are: *Basp1*, *Slc29a1*, *CD56*, *Slc6a4* and *Slc16a1* that play roles in synapse formation and neurotransmitter release. Mast cells are well known for their role in histamine and serotonin release, which also have important function as neurotransmitters in the brain (Theoharides et al., 1982). We were also able to confirm this function of mouse mast cell proteins by gene set enrichment analysis, as the two most prominently enriched features in the GO category 'Biological process', are serotonin transport and glucosamine metabolism. With regard to synapse formation, it has only recently been shown that mast cells can form directional degranulatory synapses towards IgE coated cells and parasites in vitro (Joulia et al., 2015).

Among the top 20 candidate cell surface markers we find three groups of proteins that may be useful target proteins for cell ablation. The first group consists of receptors such as *Il-1r1*, *CD117* and *FcεRI*, which are well-known mouse mast cell specific markers. Cell surface proteins such as *CD63*, *CD81*, *CD82*, *CD43*, *CD34*, *Slc7a8* and *P2rx7* form the second group, which appear in several published high-throughput RNA or antibody binding screenings, but for which mast cell specificity has not been interrogated (Agis et al., 1996; Dwyer et al., 2016; Köberle et al., 2012; Saito, 2005; Valent et al., 2014). And lastly, a group of proteins such as *Slc6a1*, *Slc16a1*, *P2rx1*, *Ada* and *CD56* that are not well known as mast cell specific proteins.

While the mouse mast cell markers presented here are not novel in each case, this is the first report of a quantitative mass spectrometry-assisted assessment of mast cell-specific protein expression, and subsequent validation by flow cytometry. Thus, our data shall allow unprecedented conclusions about mouse mast cell-specific protein expression.

4.2. Human mast cell proteomics

The proteomics pipeline for detecting mast cell specific markers was established with murine mast cells. For human cells however, acquisition of sufficient amount of mast cells for mass spectrometry was a challenge. We decided to isolate primary mast cells from skin and fat tissue from patients undergoing voluntary cosmetic surgery. To overcome individual patient-derived variability of isolated human mast cells we chose to pool preparations of purified mast cells from three patients for each analysis. Purified skin mast cells, purified fat mast cells, and peripheral blood mononuclear cells (PBMCs) were differentially labeled and analysed. Technically, the experiment with human mast cells was very similar to the mouse mast cell proteomics. The measured peptide counts and numbers of identified proteins were in a similar range. However, in contrast to the data from mouse mast cells, the direct comparisons of human mast cells to non-mast cells (PBMCs) revealed considerably more differentially regulated proteins. The PBMC sample contains more diverse cell types than the peritoneal cells used for the mouse proteomics experiment the results most likely reflect a higher complexity proteins within PBMC. Skin and fat mast cells have very similar proteomes, as both belong to connective-tissue type mast cells (MC_{TC}). However, the MC_{TC} compartments in different tissues may be regulated or influenced by local microenvironmental factors (Moon et al., 2009). Indeed, we detected 5 proteins that were differentially expressed between fat and skin mast cells, suggestive of tissue-specific differences.

In line with the findings obtained from mouse mast cells, human mast cells specifically express characteristic proteases (CPA3, CTSG, CPM and CMA1). Apart from the proteases, the metabolic enzymes SGSH, GALC, RENBP and MBOAT7, as well as several other proteins, such as VWA5A and FAM129B with unknown function, were highly enriched in human mast cells. GO analysis revealed enrichment of glucosamine metabolism which is in agreement with well known functions of mast cells in heparin and chondroitin sulphate synthesis (Rönnberg et al., 2012).

Human mast cell specific antigens that we identified by our comparative proteomic screen may be divided into three main groups. The first group of proteins consists of receptors such as MRGPRX2, CD117, and FcεRI, which are well-known human mast cell specific markers. (Gurish et al., 1992; Kraft, 2005; McNeil et al., 2015). Cell surface proteins such as CD63, CD82, CD171, CD312, SIGLEC6, SIGLEC8, CD107a, CD203c, TRPV2, and CD44 form the second group, which appear in several published high-throughput RNA or antibody binding screenings, but for which mast cell specificity has not been interrogated (Florian et al., 2006; Ghannadan et al., 1998; Motakis et al., 2014; Valent et al., 2014), and for which a function in mast cells has been either shown or might be inferred from experiments with other cell types. The third group of proteins consists of NTM, ATP1B1, SLC2A13, C1ORF58, CD228, SLC9A1, and others, which are poorly recognised as mast cell specific proteins. Interestingly, we also found molecules related to the neuronal system enriched in human mast cells. Among these are CD171 (L1 neural cell adhesion molecule), NTM (Neurotrimin) and CADM1 (Cell adhesion molecule 1). Whether mast cells use these molecules to establish interactions with nerve cells is currently under debate (van Diest et al., 2012).

In general, human mast cells are characterised by the protease content of their granules into MC_T and MC_{TC} (Galli et al., 2011; Gurish and Austen, 2012). In addition to protease content, differential cell surface antigen expression has been postulated. The G-protein coupled receptor MRGPRX2, for example, was found to be selectively expressed on MC_{TC} but not MC_T (Subramanian et al., 2016). Our flow cytometry data confirmed the MC_{TC} specific expression of MRGPRX2 on skin and fat mast cells, while lung or intestinal mast cells did not stain for MRGPRX2. In addition, our data indicate that CD171 might be discriminative for MC_T from MC_{TC} as well. Skin and fat mast cells, which are thought to be exclusively MC_{TC}, stained uniformly for CD171, while alveolar mast cells, considered almost entirely of MC_T-type, stained negative for CD171. Mast cells staining positive or negative could be found in intestinal tissue, which is known to contain both subtypes of mast cells (Irani et al., 1986; Schwartz et al., 1987).

Given that RNA abundance may be a poor indicator of protein abundance (Cox et al., 2009; Lundberg et al., 2010), we were interested to compare the recently published

RNA-sequencing dataset of human skin mast cells with our proteomics data of human skin mast cells (Motakis et al., 2014). The FANTOM5 consortium generated RNA-sequencing datasets of more than 893 different human tissues and cell types. Motakis and colleagues generated a list of mast cell specific transcripts by comparing the RNA expression of purified skin mast cells to the 893 FANTOM5 samples. This list contains 169 genes that were at least 10-fold enriched on RNA level. However, when we probed these 169 genes to our skin mast cell proteome data set, only 30 of the 169 mast cell specific transcripts were significantly enriched on protein level. This result is particularly interesting as the FANTOM5 consortium included all major hematopoietic cell types in their search for mast cell specific transcripts, which is similar to the PBMC comparison we used. We conclude that there is poor overlap of RNA and proteome data in human mast cells. Thus, we conclude that mass spectrometry-based target discovery may be superior to RNA-based searches.

4.3. Evolutionary conserved mast cell proteome

By comparing the specifically enriched proteins of mouse peritoneal mast cells and human fat mast cells, we identified a common mast cell signature of 33 orthologous proteins. The similarity of mouse and human mast cell enriched proteins suggests a mast cell core functionality that has been evolutionary maintained. In depth analysis of the cross-species conserved proteins by grouping them into functional pathways revealed 5 clusters: proteases and protease-inhibitors, histamine/serotonin metabolism, proteoglycan metabolism, granule exocytosis machinery, and cell surface receptors for responding to environmental cues. All of these functions are already present in the so-called “test-cells”, from the urochordates, dating back over 500 million years ago (Cavalcante et al., 2002; de Barros et al., 2007). These ancient highly granulated cells have been found to associate with the ascidians’ oocytes. Upon stimulation, e.g. with compound 48/80, test cells release tryptase and have been postulated to be part of a rudimentary immune system, providing the oocyte protection against microbial infections (Cavalcante et al., 2002; Ribatti and Crivellato, 2014). In our proteomics screen we found the orthologous protein pair *Mrgprb2*/MRGPRX2 enriched in mouse and human mast cells. In 2011 it was shown that MRGRX2 (MRGPRX2), expressed on cultured human mast cells, may be activated by compound 48/80 (Kashem et al., 2011).

Altogether our data support the view that mast cell degranulation and the release of histamine, heparin and proteases have been conserved over 500 million years. While FcεRI was acquired in parallel to the appearance of IgE antibodies in mammals about 200 million years ago the mast cell proteases diversified and acquired different specializations, ranging from degradation of venoms to possibly, regulation of endogenous homeostasis (Pejler et al., 2007; Ribatti and Crivellato, 2014).

The evolutionary maintenance of mast cells, suggests important function. However, the most prominent function of mast cells, i.e. IgE-mediated immediate hypersensitivity reactions appears to mostly contribute to pathology. These functions of mast cells decrease the fitness of the host and hence would be negatively selected during evolution. This discrepancy suggests so far unknown beneficial mast cell functions, which may lie outside the classical field of immunology and allergy (Palm et al., 2012).

4.4. Anti-hCD4-mediated mast cell ablation

Successful cellular targeting by monoclonal antibodies depends on several factors. First, the molecule that is targeted needs to be accessible for antibodies, and thus to be exposed on the cell surface. Secondly, the expression of the molecule has to be mast cell specific in order to minimize side effects. The third requirement depends on the selected cell ablation mechanism. In the case of antibody dependent cellular cytotoxicity (ADCC), the targeted receptor should not be internalized, while for antibody-drug conjugates (ADC) the internalization of the targeted receptor is a prerequisite to deliver the toxin into the cell, its site of action. In ADCC, FcγR-bearing immune cells induce killing of the target cell, thus the antibody isotype is critical for effector cell binding, as well. For ADC, Fc-functions of the antibody are rather undesired as immune cell binding via FcγR may foster off target effects (Scott et al., 2012).

In order to explore antibody-mediated mast cell targeting we made use of the previously developed *Cpa3^{hCD4}* mouse model (Feyerabend et. al., unpublished). In this model, a chimeric hCD4 molecule, consisting of two Ig domains of human CD4 and the transmembrane region of haemagglutinin (influenza virus), was knocked into the *Cpa3* locus for mast cell-specific expression. In order to abrogate signalling

dependent receptor internalization, intracellular signalling chains of the hCD4 molecule were excluded.

To validate the model system for antibody-mediated mast cell depletion, we first demonstrated specific anti-hCD4 staining on mast cells from various tissues and no anti-hCD4 staining on circulating hematopoietic cells, with the exception of basophils. Differential intensity of hCD4 staining on mast cells from different tissues most likely reflects receptor cleavage by enzymatic treatment during tissue dissociation. Peritoneal mast cells harvested by peritoneal lavage display a 2-3 fold higher anti-hCD4 mean fluorescence than mast cells isolated by enzymatic tissue digestion from skin. Accordingly, incubation of peritoneal mast cells with collagenase reduced hCD4 staining intensity up to 10-fold. Gene expression data provided by the Immgen consortium indicate strong and highly similar levels of *Cpa3* mRNA expression in different mast cell populations (Dwyer et al., 2016). Taken together, all mast cell populations from *Cpa3^{hCD4}* mice that we analysed in our study stained positive for hCD4, and most likely express this knock-in allele at similar cell surface levels, hence, the *Cpa3^{hCD4}* mouse a suitable model for establishing antibody-mediated mast cell depletion conditions.

Previous studies have indicated that the antibody Fc-portion is paramount for the induction of specific effector functions. Main effector cells in ADCC are NK cells and phagocytic mononuclear cells, which are most efficiently activated by FcγRI and FcγRIV (Nimmerjahn and Ravetch, 2008). The antibody isotype with the highest affinity for these receptors is IgG2a (Nimmerjahn, 2005). We therefore chose TNX355, which is a mouse IgG2a monoclonal antibody recognizing human CD4. In our experiments, we compared two variants of TNX355, one with normal glycosylation and an afucosylated variant. Removal of the fucose from the Fc-fragment of IgG2a was reported to further enhance the cytotoxicity (Nimmerjahn, 2005).

Single dose intravenous treatment with TNX355 resulted in a reduction of peritoneal mast cells but had no effect on stomach, skin, fat or tongue mast cells. Scholten and colleagues, who developed the *Mcpt5-cre* iDTR mouse strain, showed that repetitive diphtheria toxin injections were required for skin mast cell ablation in their model (Julia Scholten, 2009). When we subjected mice to repetitive doses of TNX355 we

observed a dose-dependent depletion of peritoneal and stomach mast cells. At the highest dose tested, peritoneal and stomach mast cells were fully ablated, however the connective tissue embedded skin, tongue and fat mast cells could not be depleted by ADCC. Unexpectedly, injection of the afucosylated TNX355 antibody did not further enhance ADCC-mediated mast cell ablation in our model. Of note, injection of normally glycosylated isotype control antibody induced CD45⁺ immune cell infiltration into the tongue, which was absent in the afucosylated isotype control antibody. These results suggest that either the fucose chain of normally glycosylated mAbs has an effect on the immune system, as has been described for other glycans, such as sialic acid in IVIG preparations, or that the normal glycosylated isotype antibody was contaminated with endotoxin and therefore elicited an immune response (Abès and Teillaud, 2010).

We could not eliminate connective tissue mast cells. We therefore investigated whether antibodies can efficiently reach the tissue resident mast cells from the blood stream. Studies on antibody pharmacokinetics indicate diffusion along a concentration gradient as the major driver of mAb biodistribution in vivo (Tabrizi et al., 2009). Diffusion depends on the blood pressure, the capillary endothelium and the underlying basement membrane structure. In regard of the vessel structure, it has previously been reported that the vascular endothelium of the skin acts as a gatekeeper to proteins larger than 75 kDa, hence antibodies with sizes of more than 150 kDa should not cross the vascular bed (Egawa et al., 2013). In contrast, we observed positive staining of all skin resident mast cells after intravenous injection of a low dose (100 µg) of Alexa 647-labelled TNX355. Mast cells that are in vicinity of blood vessels may extend protrusions into the blood vessels e.g. to 'catch' IgE from the circulation (Cheng et al., 2013). It may be possible for circulating TNX355 to bind to the protrusions of blood vessel-associated mast cells. However, when we analysed several mast cell compartments of these mice, not all of which may be associated with the endothelium, we found homogenous A647 label on all mast cells suggesting that the antibody broadly entered tissues. We conclude that the absence of antibodies in the tissues is not responsible for lack of depletion of hCD4⁺ mast cells.

Efficient depletion of peritoneal mast cells by ADCC is most likely mediated by the large population of locally resident macrophages (15-30 times the number of mast cells), which can freely move around the serosal cavity (Davies et al., 2013). In the

skin, however, there are considerably lower number of macrophages (2-3 times the number of mast cells) and tight extracellular matrix of the connective tissue impairs free movement of cells (Tong et al., 2015). Thus, we propose that the lack of ADCC in skin, tongue and fat tissue may result from lack of effector cells and/or lack of functionality of the locally resident immune effector cells.

One of our aims was also to investigate the safety of mAb-dependent mast cell ablation in vivo. Sudden loss of mast cells likely leads to release of mast cell granules (Scholten et al., 2009). Instantaneous and massive release of mast cell granules could induce anaphylactic shock and thus limit the applicability of such a mast cell-directed targeting approach. In the *Mcpt5-cre* iDTR mouse model mast cell ablation by apoptosis resulted in morbidity of a small proportion of mice. The authors were able to rescue these mice by co-administration of H1-antagonists, and thus concluded that mast cell released histamine caused the observed morbidity (Scholten et al., 2009). In our ADCC-based mast cell ablation experiments we did not observe morbidity, which may result from our less efficient mast cell depletion, yet it might also indicate that mast cell ablation by phagocytosis follows slower kinetics.

4.5. Functional assessment of mast cell depletion

With the TNX355 antibody in our *Cpa3^{hCD4}* mouse model it was possible to induce complete elimination of mast cells in the peritoneal cavity and stomach. While the antibody reached other tissue-resident mast cells (skin, tongue, fat, trachea), no depletion occurred in these compartments. We tested whether mast cell depletion in peritoneal cavity and stomach may already have an impact on passive systemic anaphylaxis. This is one of the few in vivo assays that is mast cell specific (Feyerabend et al., 2011; Wershil et al., 1987). In this assay, mice are passively sensitized by injection of antigen specific IgE. Challenge of mice with antigen results in crosslinking of the FcεRI-bound IgE on the surface of mast cells. The degranulation of sensitized mast cells results in systemic release of histamine, leukotrienes and prostaglandins leading to vascular leakage, reduced blood pressure and hypothermia (Ogawa and Grant, 2007). The latter are key readout parameter in this in vivo model of mast cell activation. While complete mast cell deficiency protects *Cpa3^{Cre}* mice from IgE-mediated anaphylaxis (Feyerabend et al., 2011), partial TNX355-mediated ablation of peritoneal and stomach mast cells did not significantly

abolish the anaphylactic response, suggesting that mast cell activation in skin and other tissues is mainly responsible for the observed hypothermia.

4.6. CD63 as physiological target for mast cell ablation

The development of cell depleting biologicals is a relatively new field of treatment. For preclinical drug testing several different approaches have been used. We first aimed to evaluate the efficacy and safety of targeting physiological antigens that are conserved in mast cells across species. One of the molecules enriched in both mouse and human mast cells is CD63. We decided to use an anti-mouse CD63 antibody as our first candidate for antibody-mediated mast cell depletion. Binding of antibodies to the surface of mast cells may result in mast cell activation with potential lethal consequences for the host. In that regard, CD63 appears to be a reasonable target as, *in vivo* studies with mAbs directed at CD63 could show that antibody binding to the surface of mast cells attenuates mast cell activation, however does not induce cell death (Kraft, 2005; Kraft et al., 2013). However, apart from activating mast cells, the binding to- and depletion of CD63⁺ non-mast cells may induce side effects. This, so called, on target toxicity poses a serious risk, especially since human CD63 surface cell surface expression is not entirely restricted to mast cells (Fig. 24) and mouse CD63 is highly expressed in the kidneys (Pols and Klumperman, 2009). In our hCD4 system, peritoneal mast cells were safely and efficiently targeted presumably by Fc-mediated effector mechanisms, however, when we treated mice with anti-mouse CD63 antibodies there was no mast cell depletion. Given that anti-hCD4 of the same concentration and isotype was able to reduce the number of mast cells profoundly, we reasoned that intrinsic properties of CD63 were responsible for the lack of depletion. For efficient Fc-mediated effector engagement to occur, stable cell surface exposition of the target and antibody is required (Trail, 2013). When we tested hCD63 receptor internalization after antibody binding on human skin mast cells *in vitro*, we observed rapid internalization of anti-hCD63. These data suggest that antibody internalization limits efficacy of anti-mouse CD63 targeting *in vivo*. While internalization limits the efficacy of an ADCC-mediated mast cell depletion mechanism, it opens the possibility for antibody-drug-conjugate mediated mast cell depletion. In contrast to ADCC, ADC-cytotoxicity relies on target:toxin complex internalisation to be effective. Various antibody-drug conjugates have been used experimentally and in the clinics. Most molecules currently produced for the clinics

are fusion proteins of pseudomonas/diphtheria toxin and an antibody targeting moiety (Tabrizi et al., 2009; Trail, 2013). The production and purification of such targeted toxins is costly and only worthwhile once a suitable target is established. In order to circumvent the production of our own antibody-drug conjugates we chose to use the commercially available streptavidin-saporin conjugate. Saporin is a ricin derivate, devoid of the membrane translocation domain, and thus, by itself not toxic (Stirpe et al., 1992). Addition of this conjugate to biotinylated antibodies generates potent antibody drug conjugates, which have been used to target a variety of cells in vitro and in vivo (Cao et al., 2016; Ehrlich et al., 2014; Palchaudhuri et al., 2016).

The hCD4 molecule that was introduced into the *Cpa3* locus in our *Cpa3^{hCD4}* model was designed for persistent cell surface exposure for enhanced ADCC. For that reason it is unsuitable for ADC-mediated mast cell ablation that depends on target:toxin internalisation. To establish an ADC-mediated mast cell depletion, we chose the rapidly internalising physiological mast cell antigen CD63. Treatment of mouse peritoneal and bone-marrow derived mast cells with CD63-SAP resulted in specific dose dependent cell death in vitro.

In contrast to the encouraging results obtained in vitro, CD63-SAP did not induce mast cell depletion in vivo. 2 out of 3 mice displayed serious side effects, including weight loss, hunchback and impaired mobility. SAP-treated control animals did not display signs of disease, suggesting that the observed effect was due to binding of CD63 to its physiological target. Due to lack of mast cell ablation efficacy we did not further investigate the cause of the observed toxicities. However, we suspect that on-target toxicity, most likely, in the kidney contributed to the morbidity. Based on these results we conclude that systemic depletion of mast cells by anti-CD63 antibodies is not feasible. It might be possible to locally deplete tissue resident mast cells to circumvent systemic exposure of CD63-SAP or whether saporin might be used in combination with any of the other identified mast cell markers remains to be determined.

4.7. Summary and outlook

Even though mast cells have been discovered for over a century ago they are mostly known for their functions in IgE-mediated immediate hypersensitivity reactions, which in most cases contributes to pathology. To better understand the functions of mast

cells we performed quantitative mass spectrometry-assisted proteomic profiling of primary mouse and human mast cells. This analysis confirmed the expression of several well-known mast cell specific proteases as well as revealed several proteins that have previously not been described in mast cells. Comparison of the mouse and human mast cell proteome revealed that core functions of mast cells, such as the generation of granules and histamine synthesis, are conserved between species, and might have been evolutionary maintained in mast cells for over 500 million years.

Understanding the function of the mast cell specific proteins that we identified in our analysis will aid in deciphering new roles of the cells.

Mast cells are major players in asthma and allergic disease and their absence does not appear to cause immunodeficiency. Hence, mast cell ablation may become possible in the future. Our experiments with *Cpa3^{hCD4}* mice provide proof of principle that mast cell depletion by antibodies is safe and feasible, as we were able to completely eradicate peritoneal and stomach mast cells in vivo without apparent adverse effects. In most human allergic diseases, however, tissue-embedded mast cells, such as skin- or lung mast cells, are involved. These compartments appeared to be protected from antibody-dependent cell-mediated cytotoxicity, at least as far as we could test this in our model system.

In contrast to the generally accepted dogma, we could exclude that limited antibody availability in tissues is causative for the lack of tissue cell depletion. Instead, we argue that limited availability and activity of immune effector mechanisms results in the observed lack of anti-mast cell activity of the anti-hCD4 antibody. To bypass this immune-cell dependent limitation we explored the possibility of antibody drug conjugate-mediated mast cell depletion. Our proteomic profiling experiment revealed several physiologically expressed mast cell specific cell surface antigens that may allow for antibody-dependent cell ablation. One of these receptors is CD63, which we investigated as a target for saporin-coupled anti-CD63 antibodies. Incubation of mast cells with an anti-CD63 immunotoxin resulted in the efficient depletion of mast cell in vitro. Treatment of mice with this drug, however, resulted in severe side effects without mast cell depleting activity. From these experiments we conclude that CD63 may be unsuitable as a target for systemic delivery of anti-mast cell ADCs, however, local application of CD63 targeted immunotoxins, e.g. to the skin, might circumvent systemic side effects. In future studies aim at investigating such local application of

mast cell depleting agents, as well as use our newly identified physiological candidate receptors to deplete mast cells in vivo.

5. References

Abès, R., and Teillaud, J.-L. (2010). Impact of Glycosylation on Effector Functions of Therapeutic IgG. *Pharmaceuticals* 3, 146–157.

Agis, H., Füreder, W., Bankl, H.C., Kundi, M., Sperr, W.R., Willheim, M., Boltz-Nitulescu, G., Butterfield, J.H., Kishi, K., LECHNER, K., et al. (1996). Comparative immunophenotypic analysis of human mast cells, blood basophils and monocytes. *Immunology* 87, 535–543.

Arandjelovic, S., McKenney, K.R., Leming, S.S., and Mowen, K.A. (2012). ATP induces protein arginine deiminase 2-dependent citrullination in mast cells through the P2X7 purinergic receptor. *Journal of Immunology* (Baltimore, Md. : 1950) 189, 4112–4122.

Bankova, L.G., Dwyer, D.F., Liu, A.Y., Austen, K.F., and Gurish, M.F. (2015). Maturation of mast cell progenitors to mucosal mast cells during allergic pulmonary inflammation in mice. *Mucosal Immunol* 8, 596–606.

Bantscheff, M., Schirle, M., Sweetman, G., Rick, J., and Kuster, B. (2007). Quantitative mass spectrometry in proteomics: a critical review. *Analytical and Bioanalytical Chemistry* 389, 1017–1031.

Barnes, P.J., and Adcock, I.M. (1998). Transcription factors and asthma. *The European Respiratory Journal* 12, 221–234.

Benjamini, Y., and Hochberg, Y. (1995). Controlling the False Discovery Rate: A Practical and Powerful Approach to Multiple Testing. 57, 289–300.

Blank, U., Ra, C., Miller, L., White, K., Metzger, H., and Kinet, J.P. (1989). Complete structure and expression in transfected cells of high affinity IgE receptor. *Nature* 337, 187–189.

Boersema, P.J., Raijmakers, R., Lemeer, S., Mohammed, S., and Heck, A.J.R. (2009). Multiplex peptide stable isotope dimethyl labeling for quantitative proteomics. *Nature Protocols* 4, 484–494.

Brandt, E.B., Strait, R.T., Hershko, D., Wang, Q., Muntel, E.E., Scribner, T.A., Zimmermann, N., Finkelman, F.D., and Rothenberg, M.E. (2003). Mast cells are required for experimental oral allergen-induced diarrhea. *Journal of Clinical Investigation* 112, 1666–1677.

Brightbill, H.D., and Lin, Y.L. (2014). Quilizumab is an Afucosylated Humanized Anti-M1 Prime Therapeutic Antibody. 1–8.

Brightbill, H.D., Jeet, S., Lin, Z., Yan, D., Zhou, M., Tan, M., Nguyen, A., Yeh, S., Delarosa, D., Leong, S.R., et al. (2010). Antibodies specific for a segment of human membrane IgE deplete IgE-producing B cells in humanized mice. *Journal of Clinical Investigation* 120, 2218–2229.

Bussiere, J.L., Martin, P., Horner, M., Couch, J., Flaherty, M., Andrews, L., Beyer, J.,

- and Horvath, C. (2009). Alternative strategies for toxicity testing of species-specific biopharmaceuticals. *Int. J. Toxicol.* 28, 230–253.
- Cao, Q., Lu, J., Li, Q., Wang, C., Wang, X.M., Lee, V.W.S., Wang, C., Nguyen, H., Zheng, G., Zhao, Y., et al. (2016). CD103+ Dendritic Cells Elicit CD8+ T Cell Responses to Accelerate Kidney Injury in Adriamycin Nephropathy. *J Am Soc Nephrol* 27, 1344–1360.
- Casale, T.B., Wood, D., Richerson, H.B., Trapp, S., Metzger, W.J., Zavala, D., and Hunninghake, G.W. (1987). Elevated bronchoalveolar lavage fluid histamine levels in allergic asthmatics are associated with methacholine bronchial hyperresponsiveness. *J. Clin. Invest.* 79, 1197–1203.
- Cavalcante, M.C.M., de Andrade, L.R., Bocage Santos-Pinto, Du, C., Straus, A.H., Takahashi, H.K., Allodi, S., and Pavao, M.S.G. (2002). Colocalization of heparin and histamine in the intracellular granules of test cells from the invertebrate *Styela plicata* (Chordata-Tunicata). *J Struct Biol* 137, 313–321.
- Chang, G.-W., Davies, J.Q., Stacey, M., Yona, S., Bowdish, D.M.E., Hamann, J., Chen, T.-C., Lin, C.-Y., Gordon, S., and Lin, H.-H. (2007a). CD312, the human adhesion-PCR EMR2, is differentially expressed during differentiation, maturation, and activation of myeloid cells. *Biochemical and Biophysical Research Communications* 353, 133–138.
- Chang, T.W., Wu, P.C., Hsu, C.L., and Hung, A.F. (2007b). Anti-IgE Antibodies for the Treatment of IgE-Mediated Allergic Diseases. *Adv. Immunol.* 93 IS -, 63–119.
- Chen, S., Evans, H.G., and Evans, D.R. (2011). FAM129B/MINERVA, a novel adherens junction-associated protein, suppresses apoptosis in HeLa cells. *The Journal of Biological Chemistry* 286, 10201–10209.
- Cheng, L.E., Hartmann, K., Roers, A., Krummel, M.F., and Locksley, R.M. (2013). Perivascular Mast Cells Dynamically Probe Cutaneous Blood Vessels to Capture Immunoglobulin E. *Immunity* 38, 166–175.
- Cox, B., Kotlyar, M., Evangelou, A.I., Ignatchenko, V., Ignatchenko, A., Whiteley, K., Jurisica, I., Adamson, S.L., Rossant, J., and Kislinger, T. (2009). Comparative systems biology of human and mouse as a tool to guide the modeling of human placental pathology. *5*, 279.
- D Amato, G., Stanziola, A., Sanduzzi, A., Liccardi, G., Salzillo, A., Vitale, C., Molino, A., Vatrella, A., and D Amato, M. (2014). Treating severe allergic asthma with anti-IgE monoclonal antibody (omalizumab): a review. *Multidiscip Respir Med* 9, 23.
- Daëron, M., and Jönsson, F. (2012). Mast cells and company. *Frontiers in Immunology* 1–18.
- Dahlin, J.S., Heyman, B., and Hallgren, J. (2013). Committed mast cell progenitors in mouse blood differ in maturity between Th1 and Th2 strains. *Allergy* 68, 1333–1337.
- Davies, L.C., Jenkins, S.J., Allen, J.E., and Taylor, P.R. (2013). Tissue-resident macrophages. *Nature Immunology* 14, 986–995.

- de Barros, C.M., Andrade, L.R., Allodi, S., Viskov, C., Mourier, P.A., Cavalcante, M.C.M., Straus, A.H., Takahashi, H.K., Pomin, V.H., Carvalho, V.F., et al. (2007). The Hemolymph of the ascidian *Styela plicata* (Chordata-Tunicata) contains heparin inside basophil-like cells and a unique sulfated galactoglucan in the plasma. *The Journal of Biological Chemistry* 282, 1615–1626.
- Dudeck, A., Dudeck, J., Scholten, J., Petzold, A., Surianarayanan, S., Köhler, A., Peschke, K., Vöhringer, D., Waskow, C., Krieg, T., et al. (2011). Mast Cells Are Key Promoters of Contact Allergy that Mediate the Adjuvant Effects of Haptens. *Immunity* 34, 973–984.
- Dwyer, D.F., Barrett, N.A., and Austen, K.F. (2016). Expression profiling of constitutive mast cells reveals a unique identity within the immune system. *Nature Immunology* 17, 878–887.
- Egawa, G., Nakamizo, S., Natsuaki, Y., Doi, H., Miyachi, Y., and Kabashima, K. (2013). Intravital analysis of vascular permeability in mice using two-photon microscopy. *Sci Rep* 3, 1932.
- Ehrlich, D., Wang, B., Lu, W., Dowling, P., and Yuan, R. (2014). Intratumoral anti-HuD immunotoxin therapy for small cell lung cancer and neuroblastoma. *Journal of Hematology & Oncology* 7, 91.
- Ehrlich, P. (1878). *Beiträge für Theorie und Praxis der histologischen Färbung* (Leipzig.).
- Elia, G. (2008). Biotinylation reagents for the study of cell surface proteins. *Proteomics* 8, 4012–4024.
- Elschenbroich, S., Kim, Y., Medin, J.A., and Kislinger, T. (2010). Isolation of cell surface proteins for mass spectrometry-based proteomics. *Expert Rev Proteomics* 7, 141–154.
- Erjefalt, J.S. (2014). Mast cells in human airways: the culprit? *European Respiratory Review* 23, 299–307.
- Feyerabend, T.B., Hausser, H., Tietz, A., Blum, C., Hellman, L., Straus, A.H., Takahashi, H.K., Morgan, E.S., Dvorak, A.M., Fehling, H.J., et al. (2005). Loss of histochemical identity in mast cells lacking carboxypeptidase A. *25*, 6199–6210.
- Feyerabend, T.B., Weiser, A., Tietz, A., Stassen, M., Harris, N., Kopf, M., Radermacher, P., Möller, P., Benoist, C., Mathis, D., et al. (2011). Cre-Mediated Cell Ablation Contest Mast Cell Contribution in Models of Antibody- and T Cell-Mediated Autoimmunity. *Immunity* 35, 832–844.
- Florian, S., Sonneck, K., Czerny, M., Hennersdorf, F., Hauswirth, A.W., Bühring, H.-J., and VALENT, P. (2006). Detection of novel leukocyte differentiation antigens on basophils and mast cells by HLDA8 antibodies. *Allergy* 61, 1054–1062.
- Galli, S.J., Borregaard, N., and Wynn, T.A. (2011). Phenotypic and functional plasticity of cells of innate immunity: macrophages, mast cells and neutrophils. *Nature Publishing Group* 12, 1035–1044.

- Gauvreau, G.M., Harris, J.M., Boulet, L.-P., Scheerens, H., Fitzgerald, J.M., Putnam, W.S., Cockcroft, D.W., Davis, B.E., Leigh, R., Zheng, Y., et al. (2014). Targeting membrane-expressed IgE B cell receptor with an antibody to the M1 prime epitope reduces IgE production. *6*, 243ra85–243ra85.
- Ghannadan, M., Baghestanian, M., Wimazal, F., Eisenmenger, M., Latal, D., Kargul, G., Walchshofer, S., Sillaber, C., LECHNER, K., and VALENT, P. (1998). Phenotypic characterization of human skin mast cells by combined staining with toluidine blue and CD antibodies. *The Journal of Investigative Dermatology* *111*, 689–695.
- Goodfellow, S.J., Rebello, M.R., Toska, E., Zeef, L.A.H., Rudd, S.G., Medler, K.F., and Roberts, S.G.E. (2011). WT1 and its transcriptional cofactor BASP1 redirect the differentiation pathway of an established blood cell line. *435*, 113–125.
- Gschwandtner, M., Paulitschke, V., Mildner, M., Brunner, P.M., Hacker, S., Eisenwort, G., Sperr, W.R., VALENT, P., Gerner, C., and Tschachler, E. (2017). Proteome analysis identifies L1CAM/CD171 and DPP4/CD26 as novel markers of human skin mast cells. *Allergy* *72*, 85–97.
- Gurish, M.F., Ghildyal, N., McNeil, H.P., Austen, K.F., Gillis, S., and Stevens, R.L. (1992). Differential expression of secretory granule proteases in mouse mast cells exposed to interleukin 3 and c-kit ligand. *J. Exp. Med.* *175*, 1003–1012.
- Gurish, M.F., and Austen, K.F. (2012). Developmental Origin and Functional Specialization of Mast Cell Subsets. *Immunity* *37*, 25–33.
- Hochhaus, G., Brookman, L., Fox, H., Johnson, C., Matthews, J., Ren, S., and Deniz, Y. (2003). Pharmacodynamics of omalizumab: implications for optimised dosing strategies and clinical efficacy in the treatment of allergic asthma. *Curr Med Res Opin* *19*, 491–498.
- Holgate, S.T. (2014). New strategies with anti-IgE in allergic diseases. *World Allergy Organization Journal* *7*, 1–6.
- Holgate, S.T., and Polosa, R. (2008). Treatment strategies for allergy and asthma. *Nature Reviews Immunology* *8*, 218–230.
- Holmgren, H., and Wilander, O. (1937). Beitrag zur Kenntnis der Chemie und Funktion der Ehrlichschen Mastzellen (Leipzig: Akademische Verlagsgesellschaft).
- Huber, W., Heydebreck, von, A., Sultmann, H., Poustka, A., and Vingron, M. (2002). Variance stabilization applied to microarray data calibration and to the quantification of differential expression. *Bioinformatics* *18 Suppl 1*, S96–S104.
- Irani, A.A., Schechter, N.M., Craig, S.S., DeBlois, G., and Schwartz, L.B. (1986). Two types of human mast cells that have distinct neutral protease compositions. *Proc Natl Acad Sci U S A* *83*, 4464–4468.
- Ishizaka, K., and Ishizaka, T. (1966). Physicochemical properties of reaginic antibody. 1. Association of reaginic activity with an immunoglobulin other than gammaA- or gammaG-globulin. *J Allergy* *37*, 169–185.
- Jayapal, M., Tay, H.K., Reghunathan, R., Zhi, L., Chow, K.K., Rauff, M., and

- Melendez, A.J. (2006). Genome-wide gene expression profiling of human mast cells stimulated by IgE or FcεRI aggregation reveals a complex network of genes involved in inflammatory responses. *BMC Genomics* 7, 210.
- Johnson, A.R., Hugli, T.E., and Muller-Eberhard, H.J. (1975). Release of histamine from rat mast cells by the complement peptides C3a and C5a. *Immunology* 28, 1067–1080.
- Joulia, R., Gaudenzio, N., Rodrigues, M., Lopez, J., Blanchard, N., Valitutti, S., and Espinosa, E. (2015). Mast cells form antibody-dependent degranulatory synapse for dedicated secretion and defence. *Nat Commun* 6, 6174.
- Karasuyama, H., and Melchers, F. (1988). Establishment of mouse cell lines which constitutively secrete large quantities of interleukin 2, 3, 4 or 5, using modified cDNA expression vectors. *European Journal of Immunology* 18, 97–104.
- Kashem, S.W., Subramanian, H., Collington, S.J., Magotti, P., Lambris, J.D., and Ali, H. (2011). G protein coupled receptor specificity for C3a and compound 48/80-induced degranulation in human mast cells: roles of Mas-related genes MrgX1 and MrgX2. *Eur J Pharmacol* 668, 299–304.
- Kawakami, T. (2006). Development, Migration, and Survival of Mast Cells. *Immunologic Research* 1–19.
- Kawakami, T., Ando, T., Kimura, M., Wilson, B.S., and Kawakami, Y. (2009). Mast cells in atopic dermatitis. *Current Opinion in Immunology* 21, 666–678.
- Kitamura, Y. (1989). Heterogeneity of mast cells and phenotypic change between subpopulations. *Annu Rev Immunol* 7, 59–76.
- Kitamura, Y., Go, S., and Hatanaka, K. (1978). Decrease of mast cells in W/W^v mice and their increase by bone marrow transplantation. *52*, 447.
- Kitamura, Y., Shimada, M., Hatanaka, K., and Miyano, Y. (1977). Development of mast cells from grafted bone marrow cells in irradiated mice. *Nature* 268, 442–443.
- Kiwamoto, T., Kawasaki, N., Paulson, J.C., and Bochner, B.S. (2012). Siglec-8 as a drugable target to treat eosinophil and mast cell-associated conditions. *Pharmacol Ther* 135, 327–336.
- Köberle, M., Kaesler, S., Kempf, W., Wolbing, F., and Biedermann, T. (2012). Tetraspanins in Mast Cells. *Frontiers in Immunology* 3, 1–9.
- Kraft, S. (2005). Anti-CD63 antibodies suppress IgE-dependent allergic reactions in vitro and in vivo. *Journal of Experimental Medicine* 201, 385–396.
- Kraft, S., Jouvin, M.H., Kulkarni, N., Kissing, S., Morgan, E.S., Dvorak, A.M., Schroder, B., Saftig, P., and Kinet, J.P. (2013). The Tetraspanin CD63 Is Required for Efficient IgE-Mediated Mast Cell Degranulation and Anaphylaxis. *The Journal of Immunology* 191, 2871–2878.
- Krystel-Whittemore, M., Dileepan, K.N., and Wood, J.G. (2015). Mast Cell: A Multi-Functional Master Cell. *Frontiers in Immunology* 6, 620.

- Kubo, S., Matsuoka, K., Taya, C., Kitamura, F., Takai, T., Yonekawa, H., and Karasuyama, H. (2001). Drastic up-regulation of FcεRI on mast cells is induced by IgE binding through stabilization and accumulation of FcεRI on the cell surface. *Journal of Immunology (Baltimore, Md. : 1950)* *167*, 3427–3434.
- Kumar, R.K. (2012). Are mouse models of asthma appropriate for investigating the pathogenesis of airway hyper-responsiveness? 1–7.
- Kumar, V., and Sharma, A. (2010). Mast cells: emerging sentinel innate immune cells with diverse role in immunity. *Molecular Immunology* *48*, 14–25.
- Kurashima, Y., Amiya, T., Nochi, T., Fujisawa, K., Haraguchi, T., Iba, H., Tsutsui, H., Sato, S., Nakajima, S., Iijima, H., et al. (2012). Extracellular ATP mediates mast cell-dependent intestinal inflammation through P2X7 purinoceptors. *Nat Commun* *3*, 1034.
- Leung, D.Y.M., and Bieber, T. (2003). Atopic dermatitis. *Lancet (London, England)* *361*, 151–160.
- Levy, S., and Shoham, T. (2005). The tetraspanin web modulates immune-signalling complexes. *Nature Reviews Immunology* *5*, 136–148.
- Lin, L., Yee, S.W., Kim, R.B., and Giacomini, K.M. (2015). SLC transporters as therapeutic targets: emerging opportunities. *Nat Rev Drug Discov* *14*, 543–560.
- Lönnstedt, I., and Speed, T. Replicated Microarray Data. *Statistica Sinica* *12*, 31–46.
- Lundberg, E., Fagerberg, L., Klevebring, D., Matic, I., Geiger, T., Cox, J., Algenas, C., Lundberg, J., Mann, M., and Uhlen, M. (2010). Defining the transcriptome and proteome in three functionally different human cell lines. *Mol. Syst. Biol.* *6*, 450.
- Lunderius-Andersson, C., Enoksson, M., and Nilsson, G. (2012). Mast Cells Respond to Cell Injury through the Recognition of IL-33. *Frontiers in Immunology* *3*, 82.
- Maecker, H.T., Frey, T., Nomura, L.E., and Trotter, J. (2004). Selecting fluorochrome conjugates for maximum sensitivity. *Cytometry A* *62*, 169–173.
- Maity, H., Wei, A., Chen, E., Haidar, J.N., Srivastava, A., and Goldstein, J. (2015). Comparison of predicted extinction coefficients of monoclonal antibodies with experimental values as measured by the Edelhoch method. *Int. J. Biol. Macromol.* *77*, 260–265.
- Marshall, J.S. (2004). Mast-cell responses to pathogens. *Nature Reviews Immunology* *4*, 787–799.
- Martin, N.T., and Martin, M.U. (2016). Interleukin 33 is a guardian of barriers and a local alarmin. *Nature Immunology* *17*, 122–131.
- Matasar, M.J., and Neugut, A.I. (2003). Epidemiology of anaphylaxis in the United States. *Current Allergy and Asthma Reports* *3*, 30–35.
- Matsushima, H., Yamada, N., Matsue, H., and Shimada, S. (2004). TLR3-, TLR7-, and TLR9-mediated production of proinflammatory cytokines and chemokines from

- murine connective tissue type skin-derived mast cells but not from bone marrow-derived mast cells. *Journal of Immunology* (Baltimore, Md. : 1950) *173*, 531–541.
- McNeil, B.D., Pundir, P., Meeker, S., Han, L., Udem, B.J., Kulka, M., and Dong, X. (2015). Identification of a mast-cell-specific receptor crucial for pseudo-allergic drug reactions. *Nature* *519*, 237–241.
- Metcalfe, D.D., Baram, D., and Mekori, Y.A. (1997). Mast cells. *Physiol Rev* *77*, 1033–1079.
- Moon, T.C., St Laurent, C.D., Morris, K.E., Marcet, C., Yoshimura, T., Sekar, Y., and Befus, A.D. (2009). Advances in mast cell biology: new understanding of heterogeneity and function. *3*, 111–128.
- Mota, I., and Vugman, I. (1956). Effects of anaphylactic shock and compound 48/80 on the mast cells of the guinea pig lung. *Nature* *177*, 427–429.
- Motakis, E., Guhl, S., Ishizu, Y., Itoh, M., Kawaji, H., de Hoon, M., Lassmann, T., Carninci, P., Hayashizaki, Y., Zuberbier, T., et al. (2014). Redefinition of the human mast cell transcriptome by deep-CAGE sequencing. *Blood* *123*, e58–e67.
- Nakajima, T., Inagaki, N., Tanaka, H., Tanaka, A., Yoshikawa, M., Tamari, M., Hasegawa, K., Matsumoto, K., Tachimoto, H., Ebisawa, M., et al. (2002). Marked increase in CC chemokine gene expression in both human and mouse mast cell transcriptomes following Fcepsilon receptor I cross-linking: an interspecies comparison. *Blood* *100*, 3861–3868.
- Nesbitt, L.T. (1995). Minimizing complications from systemic glucocorticosteroid use. *Dermatol Clin* *13*, 925–939.
- Nigrovic, P.A., Gray, D.H.D., Jones, T., Hallgren, J., Kuo, F.C., Chaletzky, B., Gurish, M., Mathis, D., Benoist, C., and Lee, D.M. (2008). Genetic inversion in mast cell-deficient (*Wsh*) mice interrupts *corin* and manifests as hematopoietic and cardiac aberrancy. *Am. J. Pathol.* *173*, 1693–1701.
- Nimmerjahn, F. (2005). Divergent Immunoglobulin G Subclass Activity Through Selective Fc Receptor Binding. *Science* *310*, 1510–1512.
- Nimmerjahn, F., and Ravetch, J.V. (2008). Fcγ receptors as regulators of immune responses. *Nature Reviews Immunology* *8*, 34–47.
- Nimmerjahn, F., and Ravetch, J.V. (2011). Translating basic mechanisms of IgG effector activity into next generation cancer therapies. 1–7.
- Ogawa, Y., and Grant, J.A. (2007). Mediators of anaphylaxis. *Immunol Allergy Clin North Am* *27*, 249–60–vii.
- Paivandy, A., Calounova, G., Zarnegar, B., Ohrvik, H., Melo, F.R., and Pejler, G. (2014). Mefloquine, an anti-malaria agent, causes reactive oxygen species-dependent cell death in mast cells via a secretory granule-mediated pathway. *Pharmacol Res Perspect* *2*, e00066.
- Pakhale, S., Mulpuru, S., and Boyd, M. (2011). Optimal Management of

Severe/Refractory Asthma. *5*, 37–47.

Palchaudhuri, R., Saez, B., Hoggatt, J., Schajnovitz, A., Sykes, D.B., Tate, T.A., Czechowicz, A., Kfoury, Y., Ruchika, F., Rossi, D.J., et al. (2016). Non-genotoxic conditioning for hematopoietic stem cell transplantation using a hematopoietic-cell-specific internalizing immunotoxin. *Nature Biotechnology* *34*, 738–745.

Palm, N.W., Rosenstein, R.K., and Medzhitov, R. (2012). Allergic host defences. *Nature* *484*, 465–472.

Pejler, G., Åbrink, M., Ringvall, M., and Wernersson, S. (2007). Mast cell proteases. *Adv. Immunol.* *95*, 167–255.

Pennock, J.L., and Grecis, R.K. (2004). In vivo exit of c-kit⁺/CD49d(hi)/beta7⁺ mucosal mast cell precursors from the bone marrow following infection with the intestinal nematode *Trichinella spiralis*. *Blood* *103*, 2655–2660.

Pirquet, von, C. (1906). Allergie. *Münch Med Wochenschr* 1457–1458.

Pols, M.S., and Klumperman, J. (2009). Trafficking and function of the tetraspanin CD63. *Experimental Cell Research* *315*, 1584–1592.

Portier, P., and Richet, C. (1902). De l'action anaphylactique de certains vénins. *CR Soc Biol* 170–172.

Reber, L.L., and Frossard, N. (2014). Targeting mast cells in inflammatory diseases. *Pharmacol Ther* *142*, 416–435.

Ribatti, D., and Crivellato, E. (2014). Mast cell ontogeny: An historical overview. *Immunology Letters* *159*, 11–14.

Riley, J.F., and West, G.B. (1953). The presence of histamine in tissue mast cells. *J Physiol* *120*, 528–537.

Riley, J.F., and West, G.B. (1955). Tissue mast cells: studies with a histamine-liberator of low toxicity (compound 48/80). *J Pathol Bacteriol* *69*, 269–282.

Rocha e Silva, M., and Scroggie, A.E. (1947). Liberation of histamine and heparin by peptone from the isolated dog's liver. *Proc Soc Exp Biol Med* *64*, 141–146.

Rodewald, H.R., Dessing, M., Dvorak, A.M., and Galli, S.J. (1996). Identification of a committed precursor for the mast cell lineage. *Science* *271*, 818–822.

Rodewald, H.-R., and Feyerabend, T.B. (2012). Widespread Immunological Functions of Mast Cells: Fact or Fiction? *Immunity* *37*, 13–24.

Rönnerberg, E., Melo, F.R., and Pejler, G. (2012). Mast Cell Proteoglycans. *60*, 950–962.

Saito, H. (2005). Mast Cell-Specific Genes –New Drug Targets/Pathogenesis. *Chem Immunol Allergy* 1–15.

Sandig, H., and Bulfone-Paus, S. (2012). TLR signaling in mast cells: common and

unique features. *Frontiers in Immunology* 3, 185.

Sawaguchi, M., Tanaka, S., Nakatani, Y., Harada, Y., Mukai, K., Matsunaga, Y., Ishiwata, K., Oboki, K., Kambayashi, T., Watanabe, N., et al. (2012). Role of Mast Cells and Basophils in IgE Responses and in Allergic Airway Hyperresponsiveness. *188*, 1809–1818.

Sayama, K., Diehn, M., Matsuda, K., Lunderius, C., Tsai, M., Tam, S.-Y., Botstein, D., Brown, P.O., and Galli, S.J. (2002). Transcriptional response of human mast cells stimulated via the Fc(epsilon)RI and identification of mast cells as a source of IL-11. *BMC Immunology* 3, 5.

Scholten, Julia (2009). Novel tools for mast cell research: Mast cell-specific Cre-mediated gene inactivation and inducible ablation of mast cells. 1–104.

Schwanhausser, B., Busse, D., Li, N., Dittmar, G., Schuchhardt, J., Wolf, J., Chen, W., and Selbach, M. (2011). Global quantification of mammalian gene expression control. *Nature* 473, 337–342.

Schwartz, L.B., Irani, A.M., Roller, K., Castells, M.C., and Schechter, N.M. (1987). Quantitation of histamine, tryptase, and chymase in dispersed human T and TC mast cells. *138*, 2611.

Scott, A.M., Wolchok, J.D., and Old, L.J. (2012). Antibody therapy of cancer. *12*, 278–287.

Seale, J.P., and Compton, M.R. (1986). Side-effects of corticosteroid agents. *Med. J. Aust.* 144, 139–142.

Serra-Batlles, J., Plaza, V., Morejon, E., Comella, A., and Bruges, J. (1998). Costs of asthma according to the degree of severity. *The European Respiratory Journal* 12, 1322–1326.

Simons, F.E.R. (2010). Anaphylaxis. *J Allergy Clin Immunol* 125, S161–S181.

Smyth, G.K. (2004). Linear models and empirical bayes methods for assessing differential expression in microarray experiments. *Stat Appl Genet Mol Biol* 3, Article3–Article25.

Spiess, C., Zhai, Q., and Carter, P.J. (2015). Alternative molecular formats and therapeutic applications for bispecific antibodies. *Molecular Immunology* 1–12.

Stacey, M., Chang, G.-W., Davies, J.Q., Kwakkenbos, M.J., Sanderson, R.D., Hamann, J., Gordon, S., and Lin, H.-H. (2003). The epidermal growth factor-like domains of the human EMR2 receptor mediate cell attachment through chondroitin sulfate glycosaminoglycans. *Blood* 102, 2916–2924.

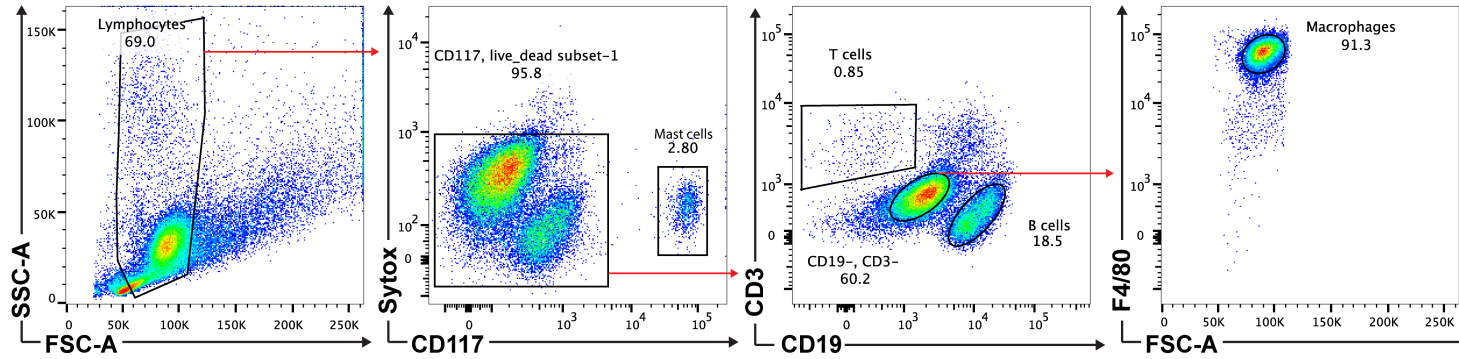
Stirpe, F., Barbieri, L., Battelli, M.G., Soria, M., and Lappi, D.A. (1992). Ribosome-inactivating proteins from plants: present status and future prospects. *Biotechnology (N Y)* 10, 405–412.

Subramanian, H., Gupta, K., and Ali, H. (2016). Roles of Mas-related G protein-coupled receptor X2 on mast cell-mediated host defense, pseudoallergic drug

- reactions, and chronic inflammatory diseases. *J Allergy Clin Immunol* 138, 700–710.
- Supajatura, V., Ushio, H., Nakao, A., Akira, S., Okumura, K., Ra, C., and Ogawa, H. (2002). Differential responses of mast cell Toll-like receptors 2 and 4 in allergy and innate immunity. *J. Clin. Invest.* 109, 1351–1359.
- Supek, F., Bošnjak, M., Škunca, N., and Šmuc, T. (2011). REVIGO Summarizes and Visualizes Long Lists of Gene Ontology Terms. 6, e21800.
- Tabrizi, M., Bornstein, G.G., and Suria, H. (2009). Biodistribution Mechanisms of Therapeutic Monoclonal Antibodies in Health and Disease. *The AAPS Journal* 12, 33–43.
- Theoharides, T.C., Bondy, P.K., Tsakalos, N.D., and Askenase, P.W. (1982). Differential release of serotonin and histamine from mast cells. *Nature* 297, 229–231.
- Tkaczyk, C., Okayama, Y., Metcalfe, D.D., and Gilfillan, A.M. (2004). Fcγ receptors on mast cells: activatory and inhibitory regulation of mediator release. *International Archives of Allergy and Immunology* 133, 305–315.
- Tong, P.L., Roediger, B., Kolesnikoff, N., Biro, M., Tay, S.S., Jain, R., Shaw, L.E., Grimbaldston, M.A., and Weninger, W. (2015). The skin immune atlas: three-dimensional analysis of cutaneous leukocyte subsets by multiphoton microscopy. *The Journal of Investigative Dermatology* 135, 84–93.
- Trail, P. (2013). Antibody Drug Conjugates as Cancer Therapeutics. *Antibodies* 2, 113–129.
- Tsai, M., Grimbaldston, M., and Galli, S.J. (2008). Immunomodulatory mast cells: negative, as well as positive, regulators of immunity. *Nature Reviews Immunology* 1–9.
- Valent, P., GH, S., WR, S., G, F., H, A., M, W., HJ, B., A, O., and L, E. (2014). Variable expression of activation-linked surface antigens on human mast cells in health and disease. *Immunological Reviews* 1–8.
- van Diest, S.A., Stanisor, O.I., Boeckxstaens, G.E., de Jonge, W.J., and van den Wijngaard, R.M. (2012). Relevance of mast cell-nerve interactions in intestinal nociception. *Biochim. Biophys. Acta* 1822, 74–84.
- Vichyanond, P. (2011). Omalizumab in allergic diseases, a recent review. *Asian Pac. J. Allergy Immunol.* 29, 209–219.
- Voehringer, D. (2013). Protective and pathological roles of mast cells and basophils. *Nature Reviews Immunology* 13, 362–375.
- Vuckovic, D., Dagley, L.F., Purcell, A.W., and Emili, A. (2013). Membrane proteomics by high performance liquid chromatography-tandem mass spectrometry: Analytical approaches and challenges. *Proteomics* 13, 404–423.
- Wang, W., Wang, E.Q., and Balthasar, J.P. (2008). Monoclonal antibody pharmacokinetics and pharmacodynamics. *Clin. Pharmacol. Ther.* 84, 548–558.

- Wardlaw, A.J., Dunnette, S., Gleich, G.J., Collins, J.V., and Kay, A.B. (1988). Eosinophils and mast cells in bronchoalveolar lavage in subjects with mild asthma. Relationship to bronchial hyperreactivity. *Am. Rev. Respir. Dis.* *137*, 62–69.
- Wareham, K., Vial, C., Wykes, R.C.E., BRADDING, P., and Seward, E.P. (2009). Functional evidence for the expression of P2X1, P2X4 and P2X7 receptors in human lung mast cells. *Br. J. Pharmacol.* *157*, 1215–1224.
- Weiner, L.M., Murray, J.C., and Shuptrine, C.W. (2012). Antibody-based immunotherapy of cancer. *Cell* *148*, 1081–1084.
- Weiner, L.M., Surana, R., and Wang, S. (2010). Monoclonal antibodies: versatile platforms for cancer immunotherapy. *Nature Reviews Immunology* *10*, 317–327.
- Wernersson, S., and Pejler, G. (2014). Mast cell secretory granules: armed for battle. *1–17*.
- Wershil, B.K., Mekori, Y.A., Murakami, T., and Galli, S.J. (1987). 125I-fibrin deposition in IgE-dependent immediate hypersensitivity reactions in mouse skin. Demonstration of the role of mast cells using genetically mast cell-deficient mice locally reconstituted with cultured mast cells. *139*, 2605.
- Wu, K., Bi, Y., Sun, K., and Wang, C. (2007). IL-10-producing type 1 regulatory T cells and allergy. *Cell Mol Immunol* *4*, 269–275.
- Yojiro Arinobu, H.I.M.F.G.S.-I.M.H.S.H.O.D.G.T.K.F.A.K.A. (2005). Developmental checkpoints of the basophil/mast cell lineages in adult murine hematopoiesis. *Proceedings of the National Academy of Sciences* *1–6*.
- Yona, S., Lin, H.-H., Dri, P., Davies, J.Q., Hayhoe, R.P.G., Lewis, S.M., Heinsbroek, S.E.M., Brown, K.A., Perretti, M., Hamann, J., et al. (2008). Ligation of the adhesion-GPCR EMR2 regulates human neutrophil function. *Faseb J.* *22*, 741–751.
- Zhang, D., Spielmann, A., Wang, L., Ding, G., Huang, F., Gu, Q., and Schwarz, W. (2012). Mast-cell degranulation induced by physical stimuli involves the activation of transient-receptor-potential channel TRPV2. *Physiol Res* *61*, 113–124.
- Zhang, M.-Q., and Timmerman, H. (1997). Mast cell tryptase and asthma. *Mediators of Inflammation* *6*, 311–317.
- Zotz, J.S., Wolbing, F., Lassnig, C., Kauffmann, M., Schulte, U., Kolb, A., Whitelaw, B., Muller, M., Biedermann, T., and Huber, M. (2016). CD13/aminopeptidase N is a negative regulator of mast cell activation. *Faseb J.* *30*, 2225–2235.

a) Mouse peritoneal exudate:



b) Mouse spleen:

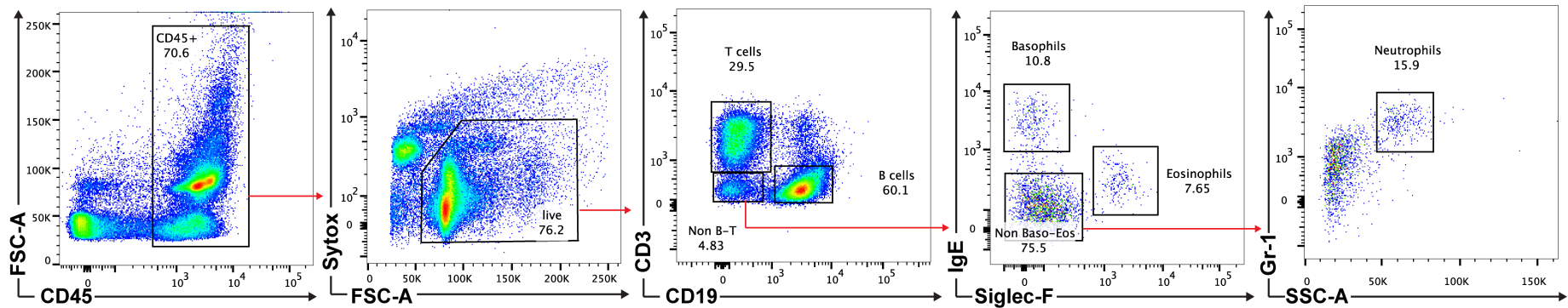


Figure S1: Flow cytometry-gating strategy for mouse peritoneal cells and splenocytes

a) Gating of peritoneal cells to identify mast cells (live CD117⁺), T cells (live CD3⁺), B cells (live CD19⁺) and macrophages (live F4/80⁺ CD3⁻ CD19⁻) by flow cytometry. **b)** Gating of spleen cells to identify T cells (live CD3⁺), B cells (live CD19⁺), basophils (live CD49b⁺ IgE⁺), eosinophils (live SSC^{hi} Siglec-F⁺), and neutrophils (live CD11b⁺ Gr-1⁺).

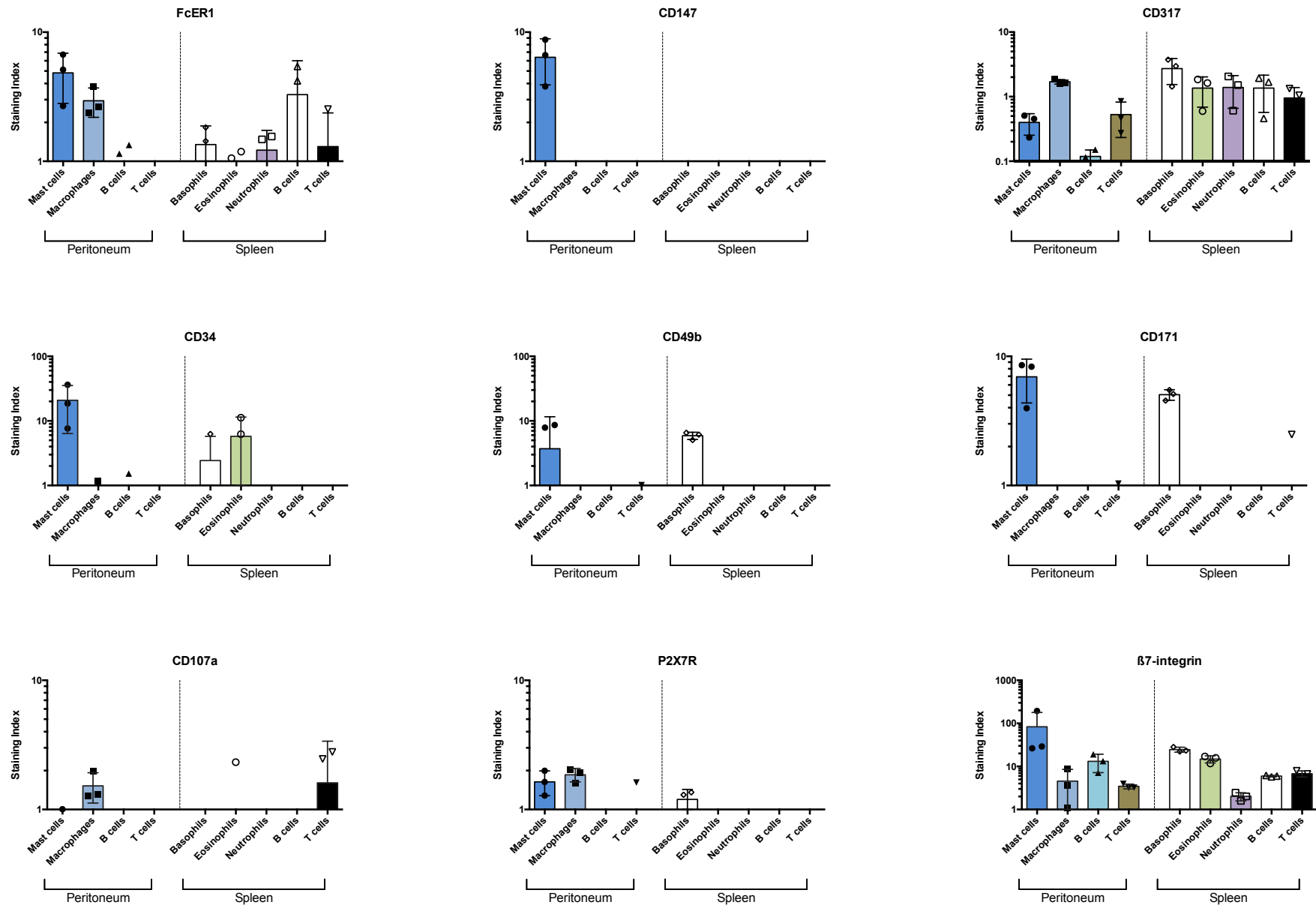


Figure S2: Flow cytometry of mouse mast cell enriched antigens

Populations from S1 were tested for immunoreactivity against the mast cell enriched antigens FcεRI, CD147, CD317, CD34, CD49b, CD171, CD107a, P2rx7, and β7-integrin by flow cytometry. Shown is the mean of the staining index ± SEM of three animals per group.

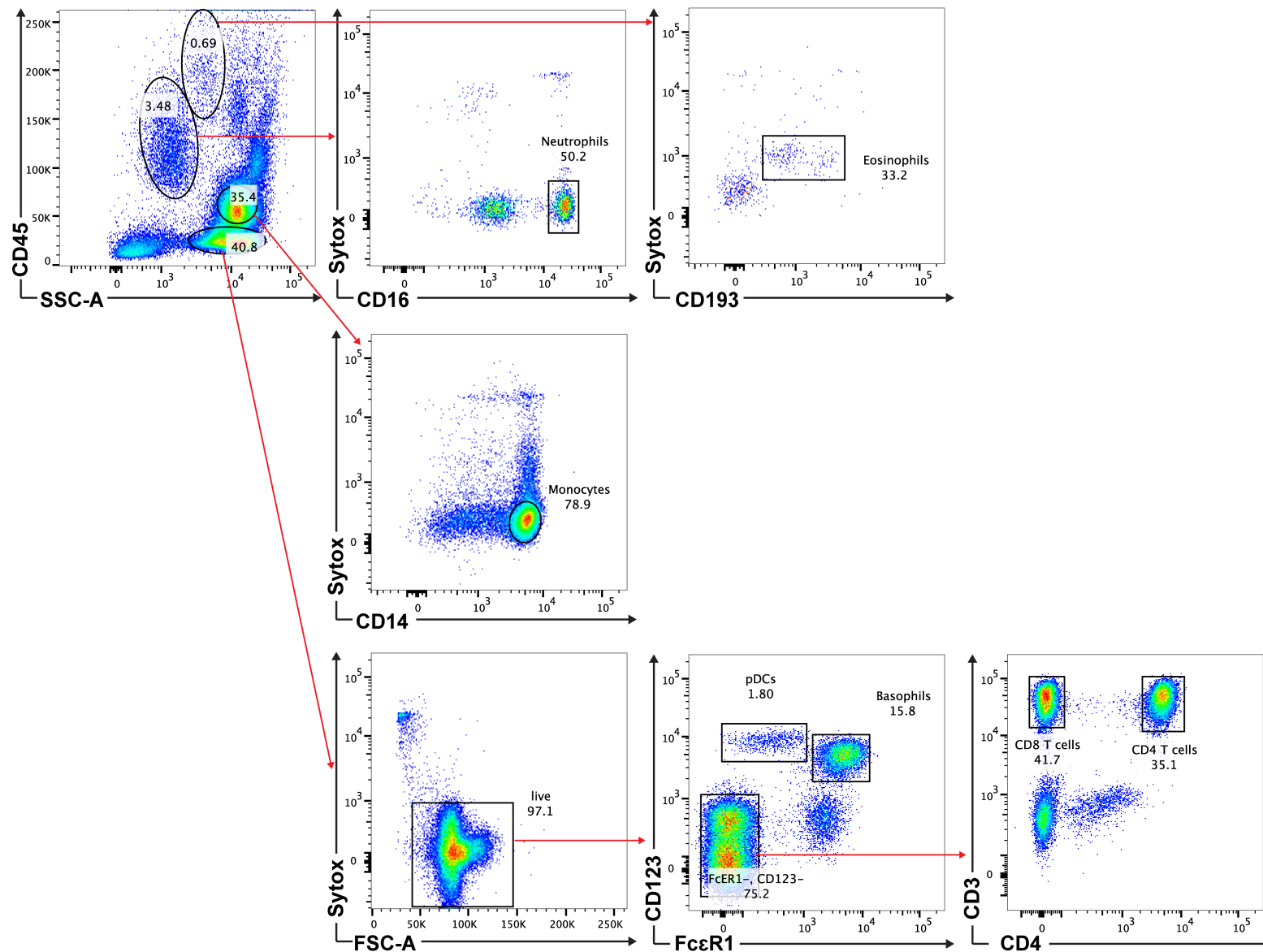


Figure S3: Flow cytometry-gating strategy for human PBMC

Gating of PBMC to identify neutrophils (SSC^{int} live $CD16^+$), eosinophils (SSC^{hi} high $CD193^+$), monocytes (live $CD14^+$), pDCs (live $CD123^+ Fc\epsilon R1^{low}$), basophils (live $CD123^+ Fc\epsilon R1^{hi}$), $CD4$ T cells (live $CD3^+ CD4^+$, and $CD8$ T cells (live $CD3^+$).

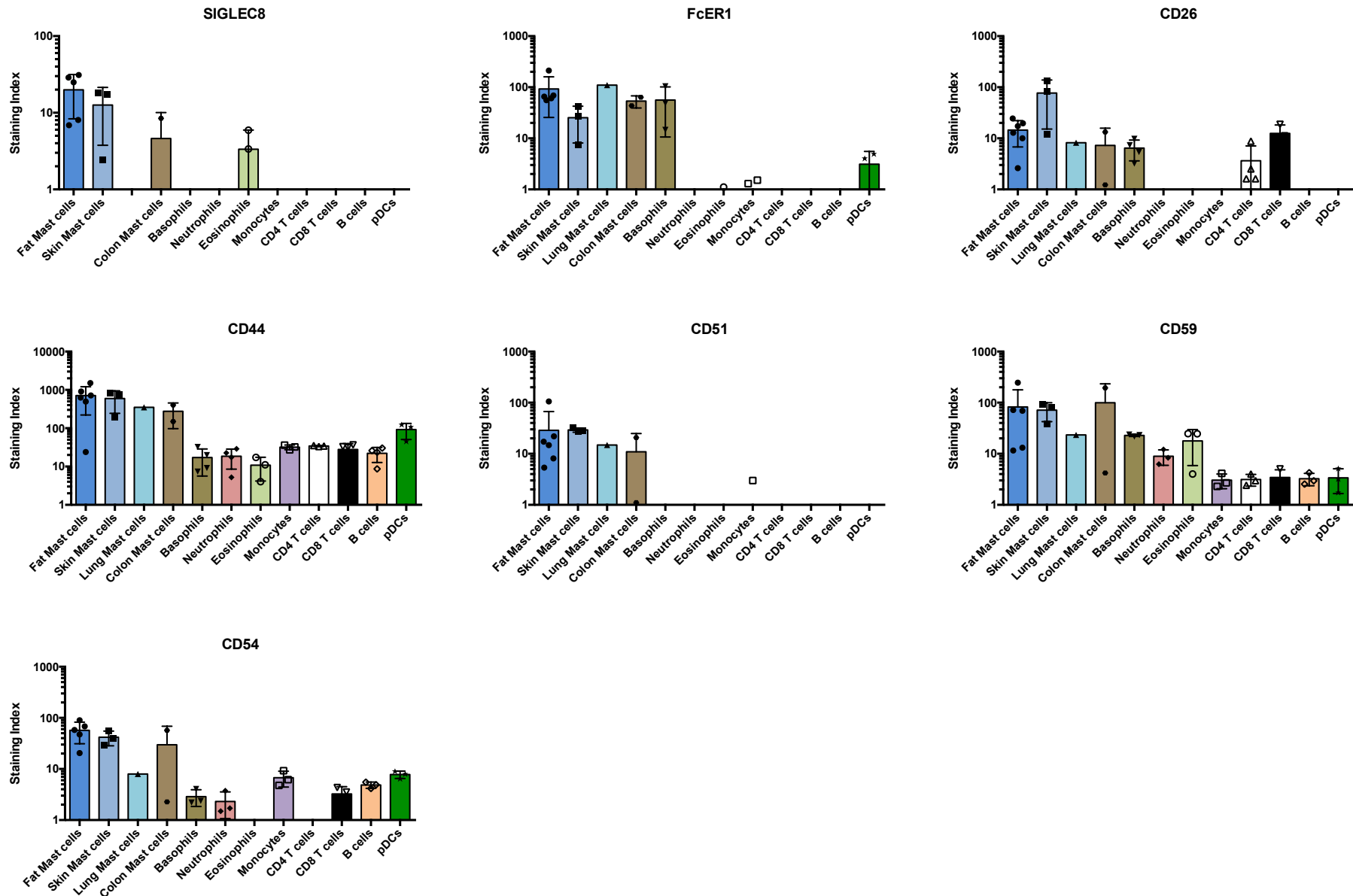


Figure S4: Flow cytometry of human mast cell enriched antigens

Populations from S3 were tested for immunoreactivity against the mast cell enriched antigens SIGLEC8, FcεRI, CD26, CD44, CD51, CD59 and CD54 by flow cytometry. Shown is the mean staining index ± SEM of 1-6 samples per group.

Acknowledgements

First of all I would like to express my sincere gratitude to my advisor Professor Hans-Reimer Rodewald for giving me the opportunity to work on this exciting project in his laboratory at the dkfz. His guidance and scientific expertise in times of need as well the freedom to pursue various side-projects independently made this PhD project an unforgettable experience.

I would like to thank Prof. Jochen Utikal and Prof. Jeroen Krijgsveld for providing useful guidance and their participation in my thesis advisory committee.

My sincere gratitude goes to Dr. Thorsten Feyerabend, who has supervised me, in the beginning with experimental advise, especially with cell biology methods, and later with scientific writing of regulatory permits and this thesis. I am grateful that I was able to use the hCD4 mouse model that he developed prior to me joining the lab. Without the hCD4 mouse model and the collaboration with Dr. Roland Kolbeck and Dr. Suzanne Cohen from MedImmune, who provided crucial input and reagents, the mast cell depletion project would have not been possible to realize.

I would like to thank Mandy Rettel and Dr. Bernd Fischer for their collaboration on the mast cell proteomics experiment.

I thank my friends and colleagues at the dkfz and in the Rodewald lab for the continuous support, stimulating discussions, and for all the fun we have had in the last four years.

Last but not least I would like to thank my family and in particular my parents who have always supported me.